AD_____

Award Number: DAMD17-98-1-8099

TITLE: Membrane-Bound Hyaluronidase in Breast Cancer Progression

PRINCIPAL INVESTIGATOR: Lurong Zhang, M.D., Ph.D.

CONTRACTING ORGANIZATION: Georgetown University
Washington, DC 20057

REPORT DATE: September 2002

TYPE OF REPORT: Final

PREPARED FOR: U.S. Army Medical Research and Materiel Command
Fort Detrick, Maryland 21702-5012

DISTRIBUTION STATEMENT: Approved for Public Release;
Distribution Unlimited

The views, opinions and/or findings contained in this report are those of the author(s) and should not be construed as an official Department of the Army position, policy or decision unless so designated by other documentation.

REPORT DOCUMENTATION PAGE

Form Approved
OMB No. 074-0188

1. AGENCY USE ONLY (Leave blank)	2. REPORT DATE	3. REPORT TYPE AND DATES COVERED
	September 2002	Final (1 Sep 98 -31 Aug 02)

4. TITLE AND SUBTITLE
Membrane-Bound Hyaluronidase in Breast Cancer Progression

5. FUNDING NUMBERS
DAMD17-98-1-8099

6. AUTHOR(S):
Lurong Zhang, M.D., Ph.D.

7. PERFORMING ORGANIZATION NAME(S) AND ADDRESS(ES)
Georgetown University
Washington, DC 20057

E-Mail: zhangl@georgetown.edu

8. PERFORMING ORGANIZATION REPORT NUMBER

9. SPONSORING / MONITORING AGENCY NAME(S) AND ADDRESS(ES)
U.S. Army Medical Research and Materiel Command
Fort Detrick, Maryland 21702-5012

10. SPONSORING / MONITORING AGENCY REPORT NUMBER

11. SUPPLEMENTARY NOTES
Original contains color plates: All DTIC reproductions will be in black and white.

12a. DISTRIBUTION / AVAILABILITY STATEMENT
Approved for Public Release; Distribution Unlimited

12b. DISTRIBUTION CODE

13. Abstract ***(Maximum 200 Words)*** *(abstract should contain no proprietary or confidential information)*
Using highly purified sperm hyaluronidase and PH-20 cDNA transfection approaches, we have demonstrated that: PH-20 HAase can release FGF2, stimulates the growth of both tumor cells in both anchorage -dependent and independent conditions. It can also stimulate the proliferation of endothelial cells and enhance the tumor angiogenesis. As the result of the dual effect, PH-20 HAase promotes the tumor growth *in vivo*. The results of in situ hybridization and immunohistochemistry staining indicate that both mRNA and protein of PH-20 HAase are expressed in breast cancer cells. While there is little staining in normal breast tissues, there is a strong staining in breast cancer cells. The expressing rate increases from primary breast tumors without metastasis (48.2%) to those with metastasis (70.8%) to those lymph node metastasis (83.3%), strongly suggesting that the PH-20 HAase is utilized by malignant breast cancer cells to promote their progression.The detection of the level of PH-20 HAase may serve as a poor prognosis index for human breast cancer. The reduction of the expression or the function of PH-20 HAase by genetic modification (anti-sense, ribozymes or siRNA) or small molecules may be an novel approach in anti-breast cancer.

14. SUBJECT TERMS	15. NUMBER OF PAGES
breast cancer	59
	16. PRICE CODE

17. SECURITY CLASSIFICATION OF REPORT	18. SECURITY CLASSIFICATION OF THIS PAGE	19. SECURITY CLASSIFICATION OF ABSTRACT	20. LIMITATION OF ABSTRACT
Unclassified	Unclassified	Unclassified	Unlimited

Table of Contents

INTRODUCTION

The interaction between malignant tumor cells and host extracellular matrix is a critical factor in regulating tumor progression. Tumor cells manage to utilize some powerful enzymes, such as MMPs (matrix metalloproteinase) and uPA (urokinase-type plasminogen activator, 1-3), to digest their surrounding matrix, which broken down the "restriction" and open a way for tumor cells to migrate to distant sites. However, a more important "benefit" of enzyme digestion is to release some factors that have a strong impact on growth of both tumor cells and tumor endothelial cells via an auto/paracrine effect and promote the tumor growth and metastasis (4-8).

A number of studies have suggested that after FGF-2 is produced and secreted from cells, it is initially immobilized in the extracellular matrix (ECM), binding to negatively-charged glycosaminoglycans (9). At certain critical times, some tumor-derived factors intervene to release it from the ECM to a free, active form (10). However, the nature of these release factors is not well characterized. Recently, Dr. Wellstein and coworkers have described that fibroblast growth factor binding protein (FGFBP) is involved in the release of FGF-2 (11, 12).

Alone this line of research, we believe that hyaluronan (HA), a highly negative-charged polysaccharide, might involve in the immobilization of growth factors. On the other hand, its enzyme, hyaluronidase (HAase) may serve as a "switch" to release growth factors, such as FGF2.

One special form of HAase, different from lysosomal HAase, is membrane bound HAase (PH-20) active at neutral pH (13), which is exclusively expressed by sperm cells and responsible for the penetration of sperm through the cumulus cells to the oocyte zone pellucida during the early stages of fertilization (14, 15). However, when some cells transform into malignant ones, this normally dormant gene is turn-on (16, 17).

Based on recent studies (17-25), we hypothesize that undifferentiated tumor cells utilize the sperm membrane-bound HAase to release growth factor and promote the tumor progression. This study is to test this hypothesis.

During the funding period, we were focused on two aims: 1) to examine the effect of human sperm-type membrane-bound hyaluronidase on tumor malignant phenotype; 2) to study the expression of membrane-bound HAase in human breast cancer tissues.

Our approaches were: 1) to use highly purified sperm hyaluronidase to determine its effects on release of growth factor and stimulation of colony formation of tumor cells; 2) to transfect tumor cells with cDNA of PH-20 (membrane-bound HAase) and examine the alteration of malignant phenotype; 3) to detect the expression of PH-20 in human breast cancer tissues using our generated anti-human PH-20 antibody and cDNA probe specific for mRNA of PH-20.

Our results indicate that PH-20 can release FGF2, stimulates the growth of both tumor cells and endothelial cells, promotes the tumorigenicity and angiogenesis. The expression of PH-20 can be detected in malignant breast cancer cells, especially metastatic cell, strongly suggest that the breast cancer cells indeed utilize this enzyme to promote their progression.

BODY

Aim 1. To examine the effect of human sperm-type membrane-bound hyaluronidase on tumor malignant phenotype.

There are two ways to obtain a high level of HAase in tumor cells. One is to directly add exogenous HAase to the tumor cells, and the other is to transfect the cDNA of HAase into tumor cells.

I. Effect of exogenous membrane-bound HAase on the growth of tumor cells.

The first study that we carried out was to add highly purified bovine testicular HAase to the MDA468 breast cancer cells and SW13 adenocarcinoma cells cultured in soft agar, since these two cell lines express a high level of both FGFs and FGF receptors. To our amazement, the colony formation in soft agar was greatly stimulated (**Fig 1A and B**) and this phenomenon was dose-dependent and heat-sensitive (**Fig 1 C and D**), indicating that the HAase strongly stimulates the tumor colony formation.

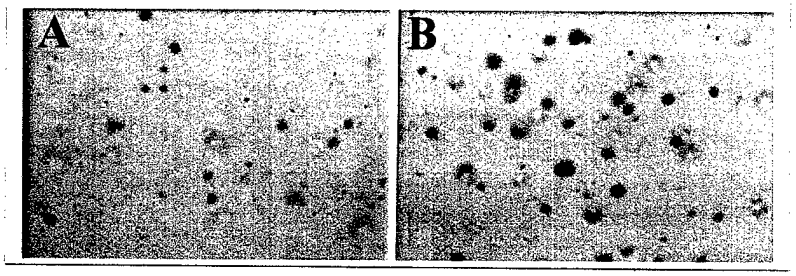

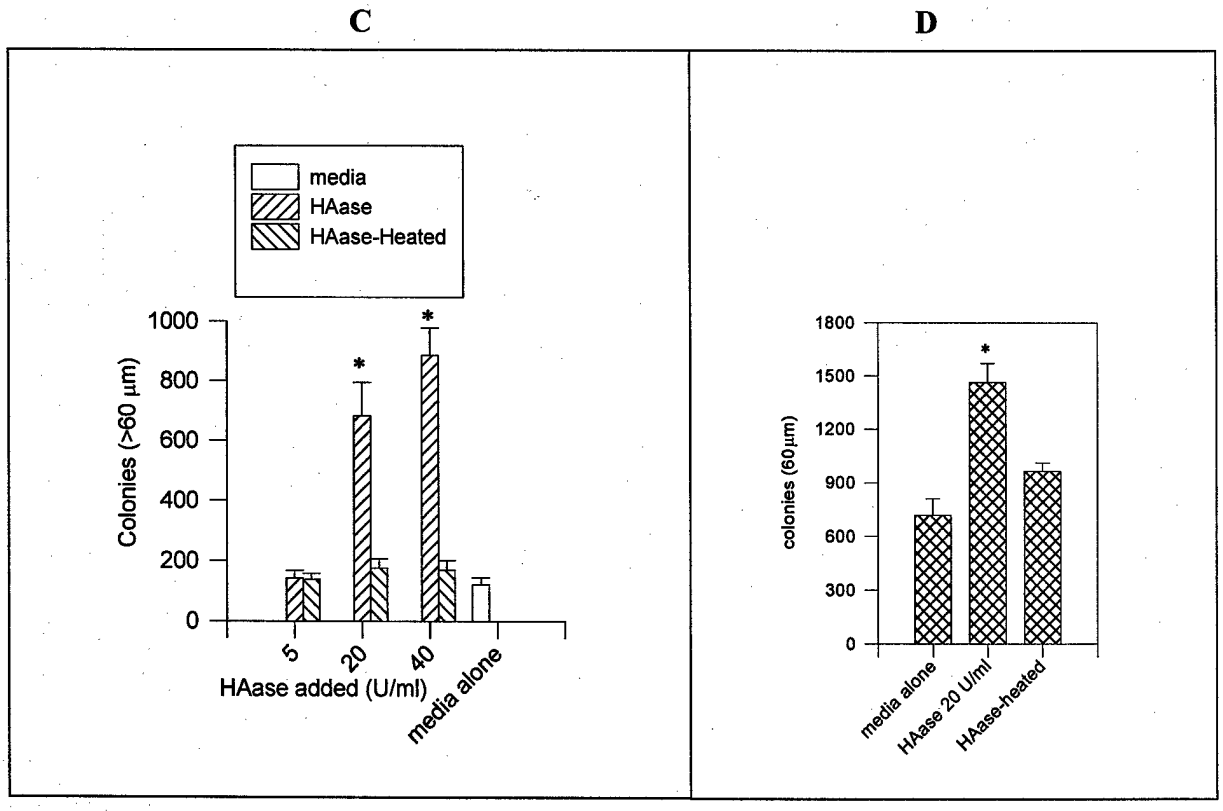

Figure 1. Effect of exogenous bovine testicular hyaluronidase on colony formation of tumor cells. Colony formation in soft agar. Twenty thousands of tumor cells were growth in 0.36% of soft agar and two weeks later the numbers of colony >60 µM were counted using Omnicon Image Analysis system. **A**: Vehicle control; **B**: treated with 20 U/ml of HAase. **C:** The colony formation of SW13 cells treated without or with different amount of HAase or HAase-heated. **D**. The colony formation of MDA468 cells treated without or with HAase or HAase-heated.

Then, what is the underlying mechanism of this phenomenon?

Considering that the HA is a major component of ECM, we speculated that the stimulatory effect on colony formation by HAase might be mediated by the release of growth factors by HAase. If this is the case, then we should be able to see a shift of growth factors from an immobilized form (normally in cell lysate proportion) to a free form (in conditioned media, CM). To test if is true, the MDA468 and SW13 tumor cells were treated with HAase. After 48 to 72 hours, the cell lysate and CM were harvested and subjected to quantitative analysis for FGF-2 and VEGF using sensitive ELISA. As shown in **Fig. 2**, there was high level of FGF-2 in lysate portion, however this shifted from cell lysate to CM when treated with HAase, indicating that the immobilized FGF2 is released by HAase. This was in a dose-dependent manner (**Fig. 3**).

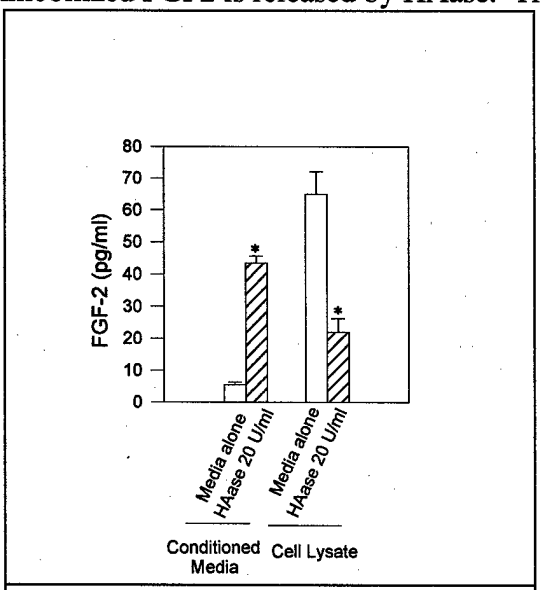

Figure 2. The shift of FGF2 from an immobilized form (in cell lysate) to a free form (in conditioned media, CM). The MDA 468 cells were cultured in 60 well plate and treated with or without 20 U/ml of HAase. After 48 hours, the cell lysate and CM were harvested and subjected to quantitative analysis for FGF-2 using ELISA.

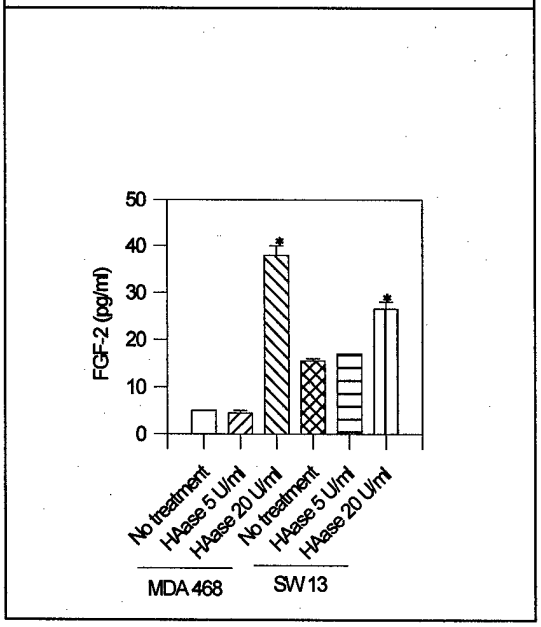

Figure 3. The release of FGF2 by HAase was in a dose-dependent manner. The MDA 468 and SW13 cells were cultured in 60 well plate and treated with or without different doses of HAase. After 48 hours, the cell lysate and CM were harvested and subjected to ELISA for FGF-2.

To confirm the specificity of HAase effect, the apigerin, a HAase specific inhibitor, was used to see if the release of FGF2 by HAase could be blocked by its inhibitor. Indeed, the result (**Fig. 4**) showed that the release of FGF2 by HAase was inhibited, indicating that the release of growth factor is a special function of HAase, which can enhance the tumor growth via autocrine / paracrine effect.

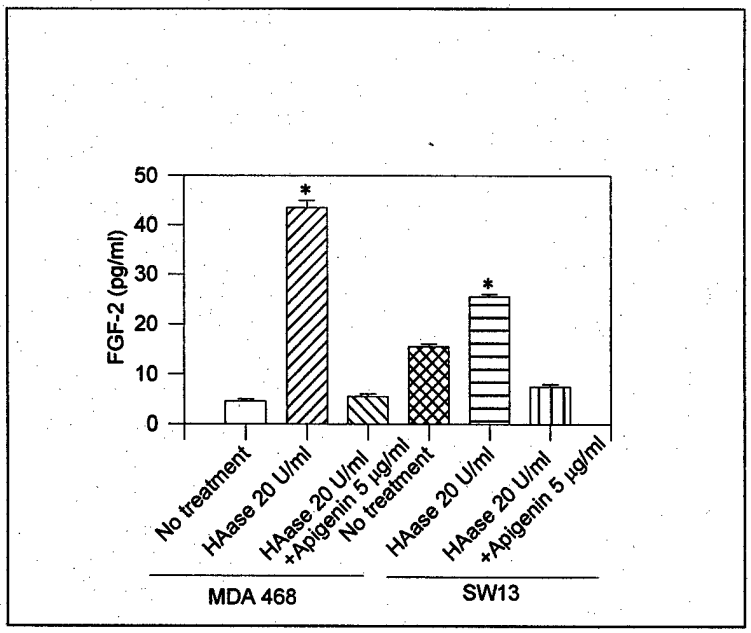

Figure 4. The release of FGF2 by HAase was inhibited by apigerin. The ML20, MDA468 and SW13 cells were cultured in 60 well plate and treated with or without 20 U/ml of HAase or 5 µM of apigerin. After 48 hours, the cell lysate and CM were harvested and subjected to ELISA for FGF-2.

However, when we analyzed the alteration of the other growth factor, VEGF (vascular endothelium growth factor), we did not see the increase of VEGF in CM, rather than a decrease (**Fig. 5**). At this time point, we do not have a good explanation for this phenomenon, but speculated that this might due to: 1) free VEGF may be rapidly immobilized again by sticking to the plastic plate; 2) The vacated binding FGF-2 sites were taken by VEGF; and 3) HAase prevents the recognition of VEGF by antibodies through some unknown mechanism.

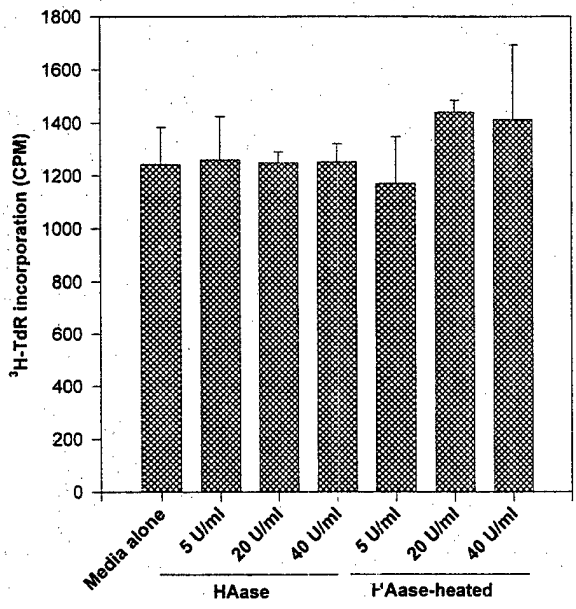

Figure 5. No change of VEGF in CM treated with HAase. The MDA468 and SW13 cells were cultured in 60 well plate and treated with 0, 5, 20 U/ml of HAase. After 48 hours, the cell lysate and CM were harvested and subjected to ELISA for VEGF.

We also examine the effect of exogenous HAase on tumor cells growing in an anchorage-dependent condition. The SW13 tumor cells were cultured in 96 well plate and treated with different doses of HAase or heat-inactive HAase as control. The result (**Fig. 6**) showed that there was no effect of HAase on the proliferation of SW 13 cultured in anchorage-dependent condition. It seems that the effect of released growth factor that can stimulate the cells to form more colonies is overridden by the tight cell-cell contact and the cell-plastic contact. The underlying mechanism of this phenomenon is worth to be further investigated. However, we believe that the three-dimensional growth condition (in soft agar) mimics tumor growth condition *in vivo* better than anchorage-dependent culture condition. The stimulatory effect of HAase on colony formation is significant.

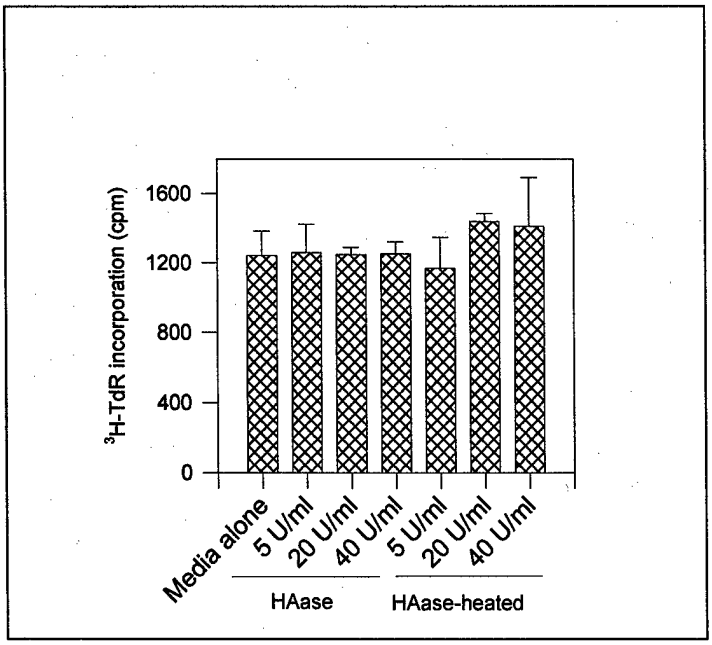

Figure 6. No change of cell proliferation by HAase under anchorage-dependent culture condition. The SW13 cells were cultured in 96 well plate and treated with 0, 5, 20, 40 U/ml of HAase or heat-inactive HAase. After 24 hours, 0.3 μCi/well of ^{3}H-TdR was added and 8 hours later the cells were harvested. The incorporated ^{3}H-TdR was counted.

Taken together, the *in vitro* addition of HAase into cultured tumor cells implies that the HAase may play an important role in tumor progression via release of FGF-2.

II. Effect of over-expression of PH-20 on malignant phenotype of breast cancer cells.

To see if HAase is, indeed, related with the malignancy of tumor cells, the **best way is to transfect the gene of Haase (PH-20) into tumor cells and examine the alteration of resulting cells.** This way will yield a clear-cut "cause and effect" result, since the comparison between mock transfectants and PH-20 transfectants will based on same background, except that PH-20 is over-expressed on test group.

The MDA 231 breast cancer cell line was transfected with cDNA of PH-20. The successful transfection was examined by the Western blotting. The result (**Fig 7**) showed that while there was no band can be detected with anti-HAase in the cell lysate of vector alone transfectants, there was a strong band appeared in the PH-20 transfectants.

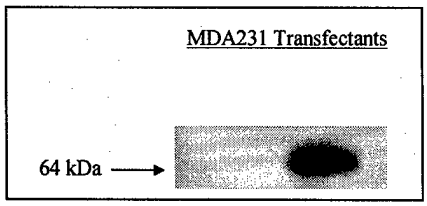

Fig 7. Detection of PH-20 expression in MDA231 transfectants by Western bolt. Thirty μg of cell lysate was electrophoreszed on 8% SDS-PAGE, transferred to a nitrocellulose membrane and incubated with rabbit anti-bovine testicular HAase (1:1000), HRP-anti-rabbit (1:4000) followed by ECL.

To see if this immuno-reactive PH-20 does have its bioactivity, a HAase ELISA-like assay was conducted. With the increased addition of lysate from PH-20 transfectants, an increased amount of coated HA was digested and the less of bound HA could be detected by biotinylated HA binding (**Fig 8**). This indicates that the HAase produced by PH-20 transfectants possesses the ability to digest HA.

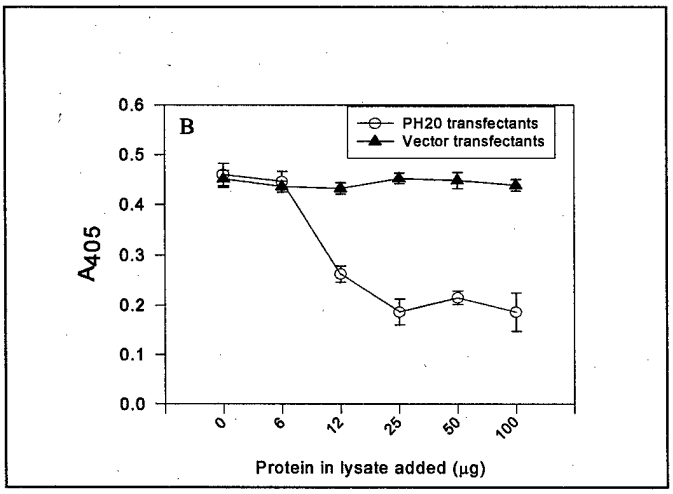

Fig 8. ELISA for activity of PH-20 in cell lysate of MDA231 transfectants. Different amounts of cell lysate were added to the HA coated ELISA plate and incubated at 37°C overnight. The digested HA were washed away, and the HA remained in the plate was detected by biotinylated HA binding protein followed by HRP streptavidin and substrate.

In previous study, we demonstrated that when exogenous HAase was added to culture media of SW13 and MDA468 cells, the FGF-2 was released from the immobilized portion to the free media portion. To see if this holds-up in cells expressing high level of HAase, the conditioned media from PH-20 transfectants was examined for FGF-2 by enrichment with heparin-affinity column followed by Western blotting. The result (**Fig 9**) showed that FGF-2 was significantly increased in the media of PH-20 transfectants compared to the control, indicating that endogenously expressed HAase indeed can shift the immobilized FGF-2 to the free portion, which is required for its activity.

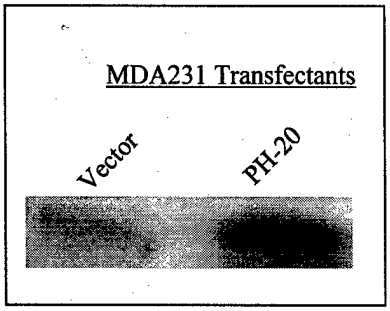

Fig 9. FGF2 was released by PH-20 in conditioned media of MDA231 transfectants. Six ml of conditioned media harvested from some density of MDA231 transfectants was mixed with heparin-Sepharose 4B at 4°C overnight. After washed with 0.3 M NaCl, 30 µl of loading buffer were added to the beads, boiled and electrophoresed on 8% SDS-PAGE. The Western bolt was carried out with anti-FGF2 (1:1000).

We then wanted to see if the released FGF-2 could exert its biofunction. Four isoforms of FGF receptors are expressed by MDA231 cells and can tranduce the signal via tyrosine kinase and MAPK pathway. The lysate from the transfectants were examined for phosphorylation of tyrosine and MAPK. The results of Western blotting (**Fig 10**) showed that the phosphorylated tyrosine and MAPK were increased in the PH-20 transfectants, suggesting that the HAase released FGF-2 could trigger the MAPK signal pathway via the paracrine effect.

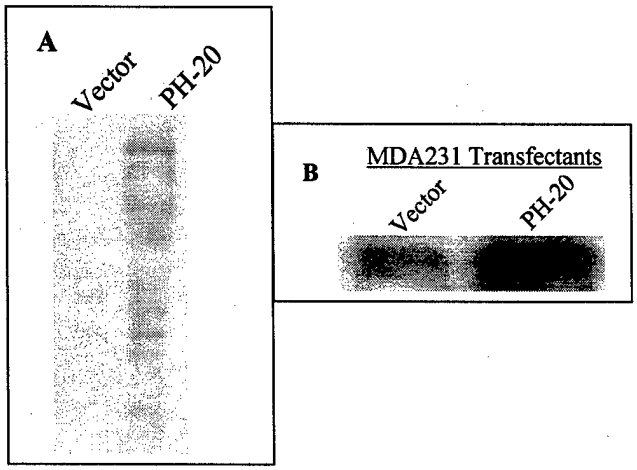

Fig 10. Increased phosphorylation of tyrosine and MAPK in PH-20 transfectants. Thirty µg of cell lysate was electrophoreszed on 8% SDS-PAGE, transferred to a nitrocellulose membrane and incubated with rabbit anti-phosphorylated tyrosine and MAPK (1:1000), HRP-anti-rabbit (1:4000) followed by ECL. There was an increased phosphorylation of tyrosine (**A**) and MAPK (**B**) in PH-20 transfectants.

If the paracrine effect is true in the HAase high expression condition, then the cell growth is likely to be stimulated. To check this out, an anchorage-dependent growth assay was performed. The result (**Fig 11**) showed when cultured in the 24 well plate, the PH-20 transfectants grew faster than the vector alone transfectants, especially in later stage of culture (day 4 and 5), indicating that there may be a accumulation effect of both HAase and FGF-2. This phenomenon caused by endogenously over-expressing of HAase differs from that caused by exogenous addition of HAase to cells, indicating that the endogenously over-expressing of HAase could be more profoundly influence the behavior of breast cancer cells.

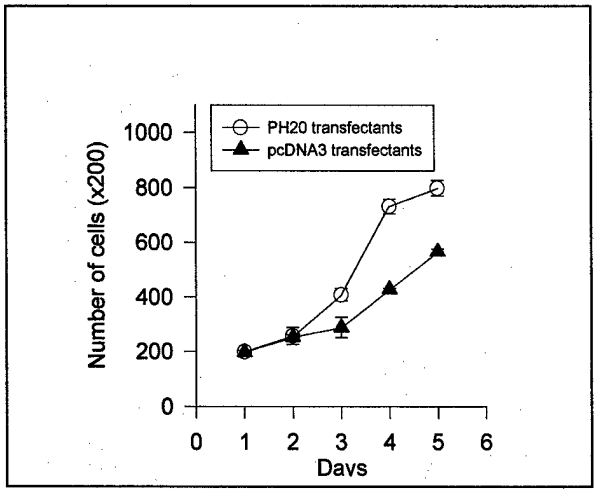

Fig 11. Effect of PH-20 on anchorage-dependent growth of transfectants. The cells were seeded in 24 well plate, harvested on indicated day and counted with Coulter counter. The PH-20 stimulated the growth of transfected cells compared to vector control ($P<0.05$).

Colony formation is one of the characteristics of malignancy tumor cells. To see if this is enhanced, a colony formation assay was conducted in soft agar. The results showed that the PH-20 transfectants formed much bigger colony than vector alone control cells (**Fig 12 A**) and the number of colonies bigger than 60 μm in diameter was double in PH-20 cells compared to the vector alone transfectants (**Fig 12 B**). The pattern was similar to the exogenous addition of HAase (**Fig 1**). Again, it further proved that HAase released FGF-2 could enhance the anchorage-independent growth of tumor cells.

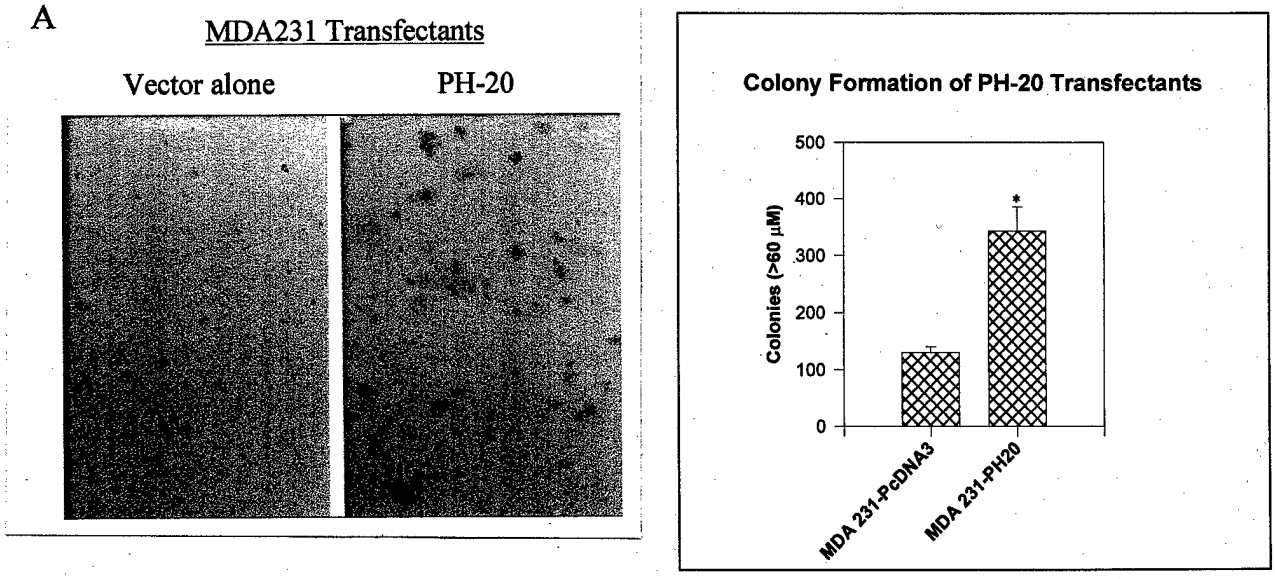

Fig 12. Effect of PH-20 on anchorage-dependent growth of transfectants. Twenty thousand transfected cells will be mixed with 0.18% of agarose in 10% FBS-DMEM and then placed on top of 0.36% agarose. Two to three weeks later, the colonies (>60 μm) were pictured (**A**) and quantified (**B**) using an Omnicon Image Analysis system. PH-20 transfectants formed much more big colonies than mock controls ($P<0.01$).

To see the HAase enhanced malignant phenotype *in vitro* can be translated *in vivo*, the tumor growth on CAM and in nude mice model was examined. When one million of PH-20 cells were placed on the top of 10 days chicken embryo, they formed bigger tumors than vector control cells (**Fig 14**).

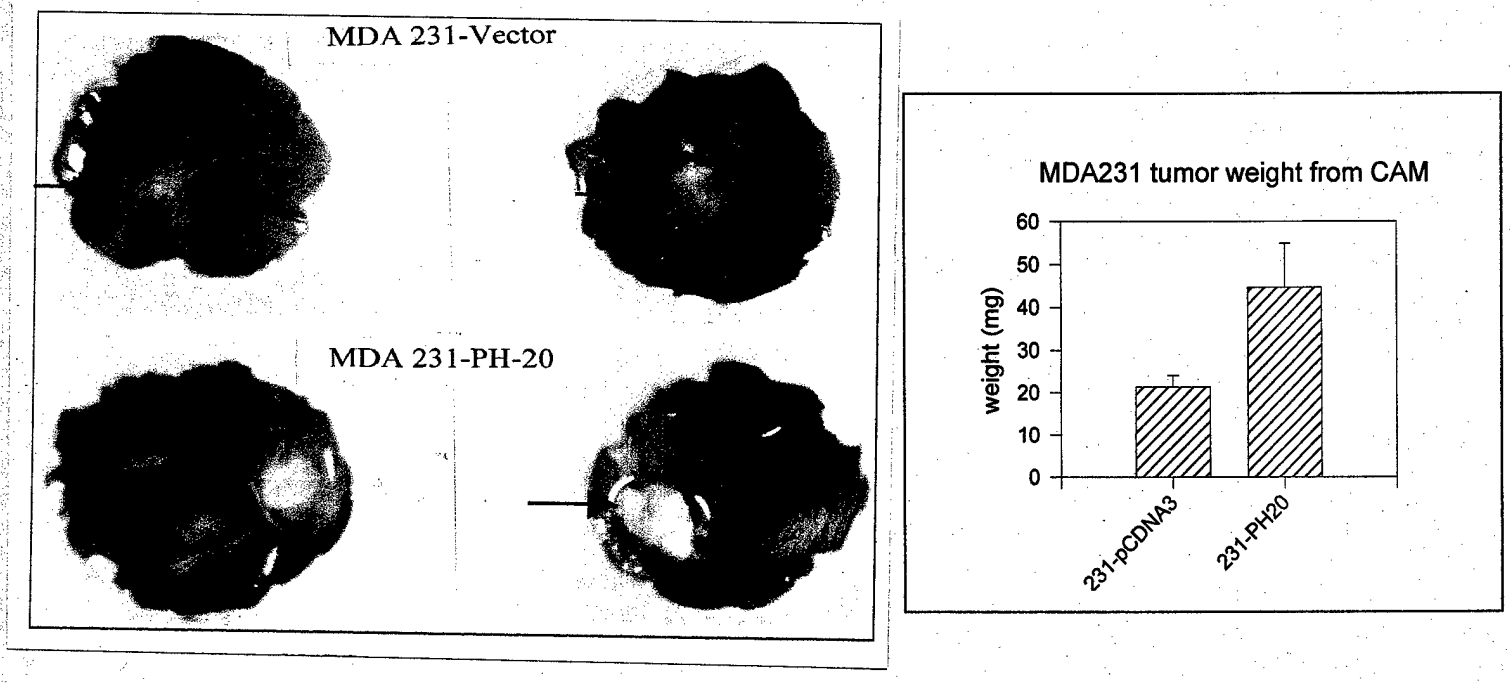

Fig 14. Effect of PH-20 on tumor growth on CAM. The vector or PH-20 transfectants (1 x 10^6) were placed on the top of CAM of 10 days old chicken embryo (15eggs/group) and four days later, the tumors formed on CAM were photographed (**A**), harvested and weighted (**B**). The PH-20 transfectants formed bigger tumor than vector transfectants.

This was further confirmed by nude mice model. Two millions of MDA 231 cells transfected with either vector alone or PH-20 were subcutaneously injected into 5 weeks-old nude mice (5 /group). Four weeks later, the mice were photographed, and the tumors were harvested and weighted. The results (**Fig 15**) showed that the tumors formed by PH-20 transfectants were much bigger than that formed by control vector transfectants, indicating that the HAase could enhance the breast cancer growth *in vivo*.

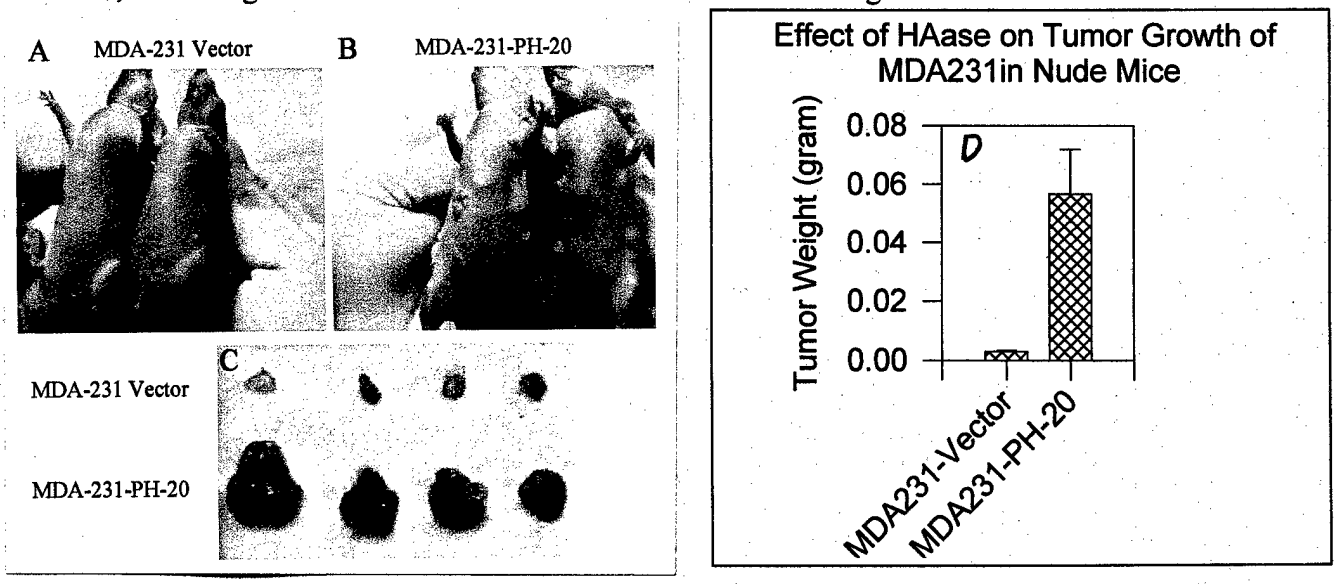

Fig 15. Effect of PH-20 on tumor growth in nude mice. Two millions of MDA 231 cells transfected with either vector alone or PH-20 were subcutaneously injected into 5 weeks-old nude mice (5 /group). Four weeks after inoculation, the mice were photographed (**A** and **B**), and the tumors were harvested (**C**) and weighted (**D**). The PH-20 cells formed bigger tumors than the vector alone control.

However, when the mice lung were carefully examined, we did not find that there was an increased metastases. This may due to the "wrong seeds" or "wrong soil". The tumor metastasis is a complex process, which requires not only the enzymes to digest the ECM and basement membrane of vessels, but also the adhesion molecules to settle down. HAase alone is not enough for induction of metastasis in the cells that lack of other necessary molecules.

III. Effect of over-expressing PH-20 on endothelial cells and tumor angiogenesis.

It has been known that FGF-2 is a mitogen for both tumor cells and endothelial cells. We speculate that the HAase released FGF-2 may also act on endothelial cells. To test this, the conditioned media (CM) from transfectants was added to media of endothelial cells, and the cell number was counted on day 4 with Coulter counter. The result (**Fig 13**) showed that the growth of endothelial cells was greatly stimulated by CM of PH-20 transfectants in a dose-dependent manner as compared to the control transfectants. This dual effect of HAase enhances its promoting role in tumor progression via stimulation of both tumor cells and endothelial cells.

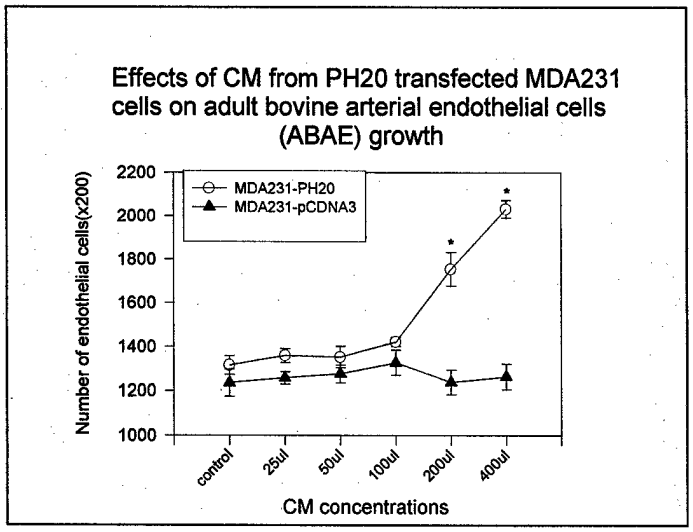

Fig 13. Effect of CM on growth of endothelial cells. The different amount of conditioned media harvested from similar density of cells was added to adult bovine aortic endothelial (ABAE) cells. The cells were harvested on day 4 and counted. The CM from PH-20 transfectants stimulated the growth of endothelium compared to the controls ($P<0.01$).

To see if the *in vitro* stimulation of growth of endothelial cells by PH-20 transfectants was translated as in vivo enhancement of tumor angiogenesis, the vessels in the tumors were examined by immunohistochemic staining with antibody against factor VIII that was expressed on endothelial cells. The results (**Fig 16**) showed that the vessels in the tumors formed by PH-20 transfectants were more than that in the control tumors, indicating the angiogenesis is enhanced by high expression of HAase. The underlying mechanisms may be: 1) the release of FGF-2 was increased due to HAase digestion; and 2) the small molecule weight HA digested by HAase may also contribute to this increased angiogenesis (26). Whether there are other angiogenic molecules involved needs to be investigated.

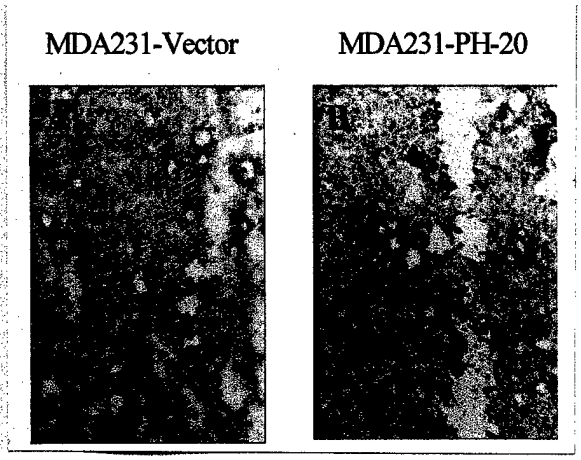

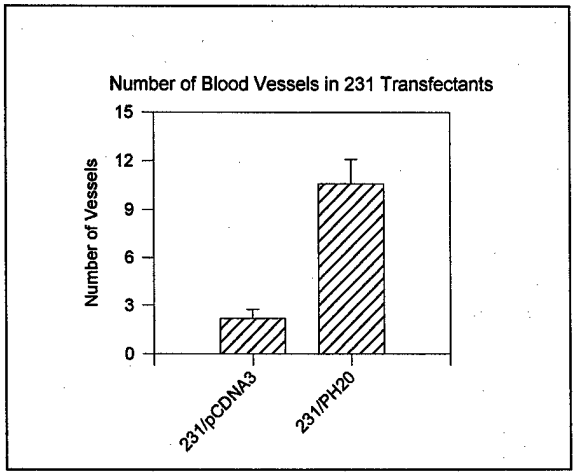

Fig 16. Effect of PH-20 on tumor angiogenesis. The frozen sections of tumors formed by vector or PH-20 transfectants were stained for vessels with anti-endothelial antibody followed by AEC substrate (in red, **A** and **B**). The numbers of vessels stained were counted from 10 random fields and the PH-20 group had more vessels than the vector group (**C**).

Aim 2. To study the expression of membrane-bound HAase in human breast cancer tissues.

In this project, one of the major tasks is to study the expression pattern of membrane-bound HAase in human breast cancer tissues. It has been demonstrated that membrane-bound HAase is expressed in some types of tumor (17), however the expression pattern of this enzyme in breast cancer has not been explored. We have applied two methods to study this both in mRNA level and protein level.

I. **Expression of <u>mRNA</u> of membrane-bound HAase in human breast cancer tissues.**

First, we want to see the expression level of mRNA of membrane-bound HAase in human breast cancer tissues with in situ hybridization method.

Two oligonuecleotide probes were designed according to the cDNA sequence of PH20:

5'-TATGTTGATAGACTTGGCTACTATCCTTACATAGATTCAATCACAGGAGTAACTGTG-3' (431-375)

5'-AACACTCAGCAGTCTCCTGTAGCTGCTACACTCTATGTGCGCAATCGAGTTCGGGAA- 3' (952-897).

These two cDNA probes were biotinylated at 3'-end during the synthesis.

Human breast samples (19 cases of normal breast tissues, 5 cases of tumor adjaction tissues and 28 cases of breast infiltrating duct carcinoma) in microarray sections were de-paraffined, treated with 0.1 N HCl for 20 minutes, and digested with Proteinase K(25 μg/ml) for 15 minutes at 37°C, and then post-fixed in 4% paraformaldehyde for 15 minutes. The sections were then prehybridized in mRNA in situ hybridization solution (DAKO) for 1 hour, and then hybridized with 500 ng /ml of biotin labeled oligonuecleotide probes in hybridization solution at 37°C overnight. Next day, the sections were washed in 50% formamide-2 x SSC (V/V) at 52°C for 30 minutes, followed by 2 x SSC, 1 x SSC and 0.1 x SSC. Then, the sections were blocked with 5% BSA for 1 hour and the hybridized probes were detected by incubation with phosphatase labeled streptavidin (1:1000) and followed by NBT/BCIP substrate for blue color. The sections were sealed with crystal mounter. The positive staining was visualized under microscopy and counted for positive spots (7). The positive spots in >20 % cells were counted as positive.

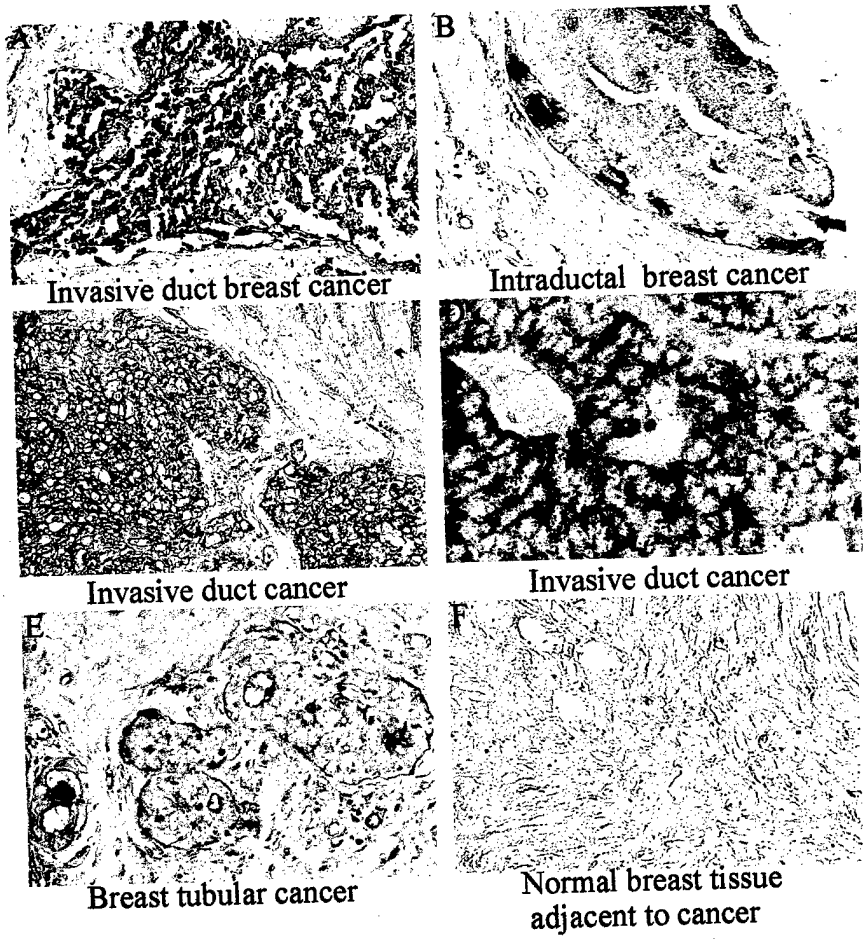

Fig. 17. In situ hybridization for the expression level of mRNA of membrane-bound HAase in human breast cancer tissues.

The results showed that in 19 cases of **normal** breast tissues, 16 cases showed **no** expression of PH20 and only 2 cases (15%) of breast lobular had a very weak signal. Similarly, only 1 out of 5 (20%) tumor margin tissue had a weak positive staining. However, 21 out of 28 **(75.0%)** breast infiltrating duct **carcinoma** were PH20 mRNA positive while there were no staining in the surrounding stromal tissues. The intensive staining of PH20 mRNA of cancer cells makes them easily to be distinguished from the normal lobular epithelial cells. The difference between the normal breast tissues and breast cancer tissues was statistically significance ($P<0.001$).

Table 1. mRNA Expression of PH20 in Breast Tissue and Cancer

Type of Histology	Case of No	positive Case	Negetive Case	Positive(%)
Breast duct Infiltrating Cancer	28	21	7	75
Breast Margin Cancer Tissue	5	1	4	20
Normal Breast Tissue	19	3	16	15.7
Total	52	25	27	

The result of in situ hybridization indicates that the mRNA of PH20 is increased in human breast cancer cells.

II. Expression of protein of membrane-bound HAase in human breast cancer tissues.

To determine if the protein of PH-20 is indeed expressed in human breast cancer tissues, we need to use immunohistochemistry staining (IHC) method. However, no anti-PH-20 antibody is commercially available. We have to generate the antibody.

As planned in the proposal, in the third year, we were concentrated on the production of high quality anti-membrane-bound HAase. We also collected human breast tissue samples, optimize the conditions for the immunohistochemic staining, stained the samples and analyzed them. The results were reported as following:

1. Preparation of antibody against human PH-20: For the determination of antigenic domain of PH-20, the GCG computer program was used to search the hydrophilic region and the surface region as well as other secondary structures of PH-20 HAase. The results (**Fig. 18**) indicated that the amino acid sequences 140 – 200 was the mostly likelihood to sever as antigenic domains.

From 140 –200 region, we picked two sequences (148-167: EEWRPTWARNWKPKDVYKNR, and 180-200: LTEATEKAKQEFEKAGKDFL, **Fig. 19**) as antigens and commercially had them synthesized. Two synthetic peptides were conjugated with KLH to make the full antigen. Two rabbits were immunized with each peptide.

In addition, the highly purified bovine sperm HAase was purchased from Sigma, which was used a native from of whole protein antigen. Six rabbits were immunized with these three antigens (two rabbits for each antigen) for three months. The serum was collected at different time points and the antibody titer was tested with ELISA. Briefly, the 96-well plate was coated with 10 μg/ml of HAase and blocked with 5% bovine albumin. The rabbit serum was serially diluted (from 1:1000 to 1:100,000) and added to the plate. After appropriate incubation and wash, the anti-rabbit secondary antibody conjugated with peroxidase was added followed by the substrate colorization. The results suggested that the titer of our anti-HAase were 1:10,000 to 1:100, 000.

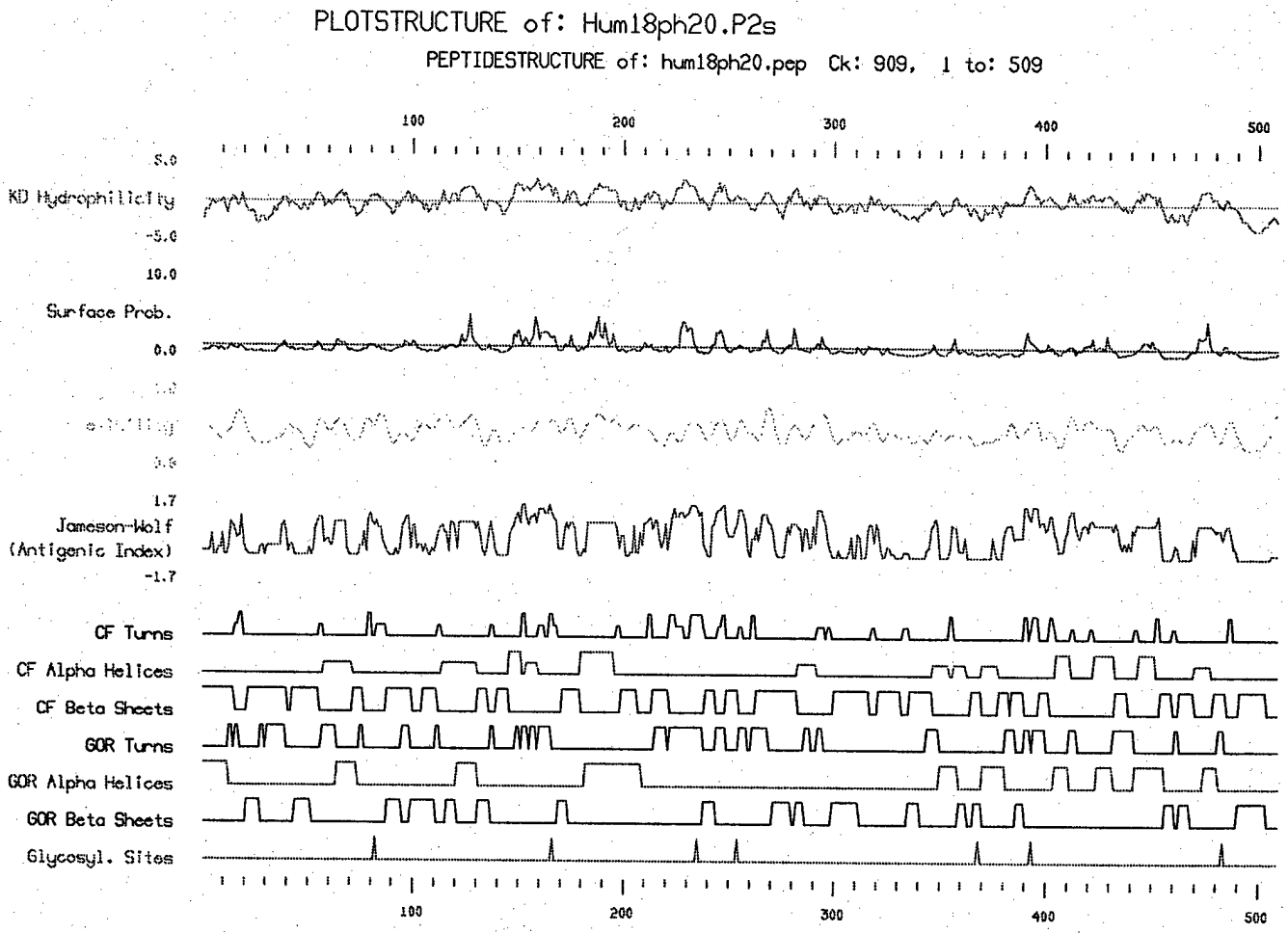

Figure 18. Determination of antigenic domains of PH-20. The profile of hydrophilic region, the surface region and other secondary structures of PH-20 were analyzed with GCG program and expressed as Plotstructure.

1 MGVLKFKHIF FRSFVKSSGV SQIVFTFLLI PCCLTLNFRA PPVIPNVPFL

51 WAWNAPSEFC LGKFDEPLDM SLFSFIGSPR INATGQGVTI FYVDRLGYYP

101 YIDSITGVTV NGGIPQKISL QDHLDKAKKD ITFYMPVDNL GMAVIDWEEW

151 RPTWARNWKP KDVYKNRSIE LVQQQNVQLS LTEATEKAKQ EFEKAGKDFL

201 VETIKLGKLL RPNHLWGYYL FPDCYNHHYK KPGYNGSCFN VEIKRNDDLS

251 WLWNESTALY PSIYLNTQQS PVAATLYVRN RVREAIRVSK IPDAKSPLPV

301 FAYTRIVFTD QVLKFLSQDE LVYTFGETVA LGASGIVIWG TLSIMRSMKS

351 CLLLDNYMET ILNPYIINVT LAAKMCSQVL CQEQGVCIRK NWNSSDYLHL

401 NPDNFAIQLE KGGKFTVRGK PTLEDLEQFS EKFYCSCYST LSCKEKADVK

451 DTDAVDVCIA DGVCIDAFLK PPMETEEPQI FYNASPSTLS ATMFIVSILF

501 LIISSVASL*

Figure 19. The position and amino acid sequence of antigenic domains of PH-20. The amino acids (148 to 167 and 180 to 200) were chosen to synthesize as antigen according to the antigenicity analysis of GCG program.

When we directly used the antibody serum to stain the paraffin section, we found that the background of immunohistochemic staining was relatively high. To reduce the background, the antibody IgG portion from the rabbit serum was purified with protein G column. In addition, we also optimized the stain condition with the following approaches: **1)** reiterative antigen of samples with microwave; **2)** reduce the antibody concentration from 1:250 to 1: 1,000; and 3) intensively wash between each step. With these cares, the background staining was greatly reduced. While the tumor cells were strongly stained, the stromal was negative.

When the normal rabbit serum (prior to immunization) was used as first antibody instead of anti-PH 20 serum, there was no staining (**Fig 20** top panel) in a paired primary cancer (left) and lymph node metastases (right) collected from same patient, however, there was a strong staining with anti-PH 20 (Fig 20 bottom panel). These data indicated that the antibody was specific.

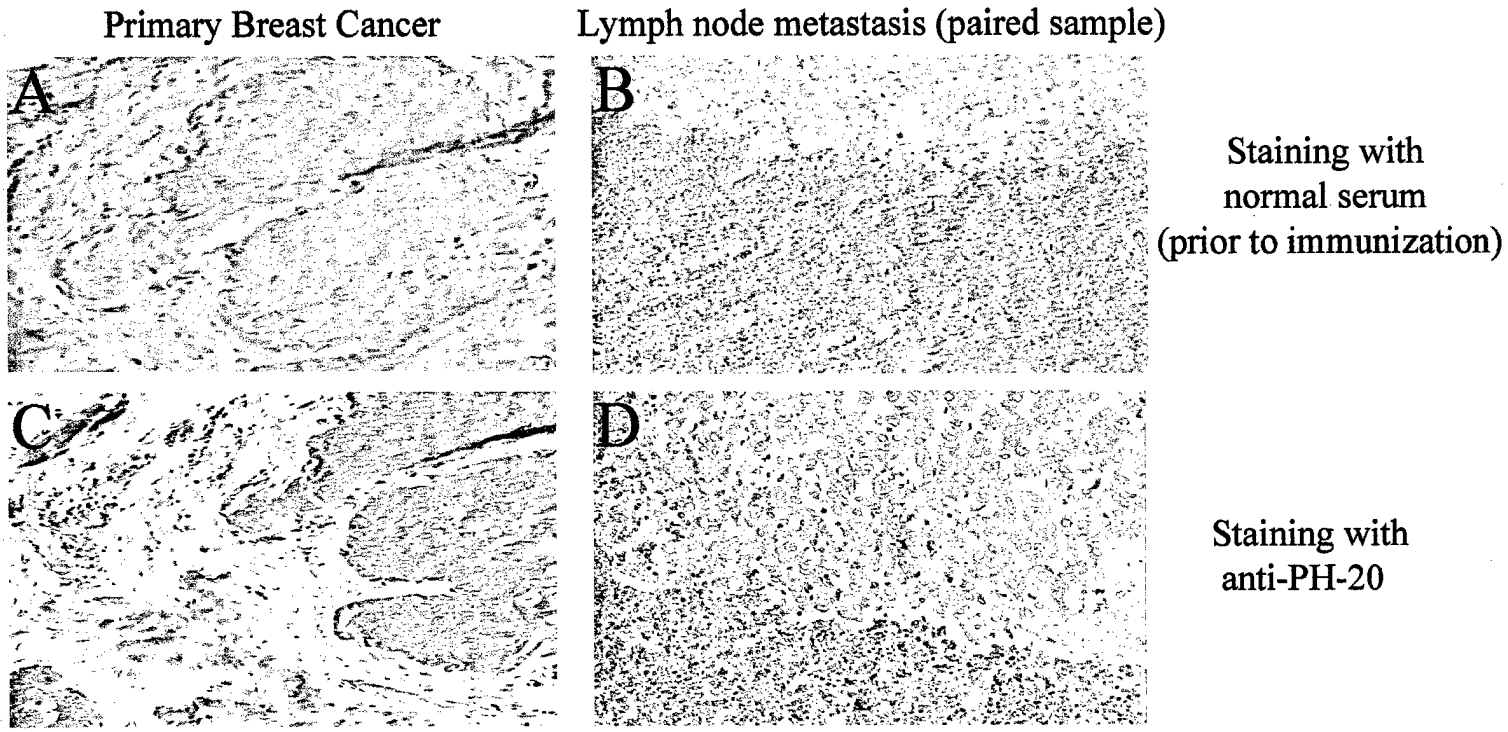

Figure 20. Determination of specificity of anti-PH-20 antibody. The serum collected from the rabbit prior to its immunization with HAase antigen or after immunization was used as primary reagent to stain a paired breast cancer sample. **Top panel**: staining with normal serum; **Bottom panel**: staining with anti- HAase; **Left side**: Primary cancer; **Right side**: Metastatic cancer in lymph node. There was no staining with normal serum (top panel), while a strong staining with anti-PH 20 was observed (bottom panel), indicating that the antibody was specific.

Then, the collected paraffin samples of human breast cancer were organized as groups: **1)** normal breast tissues; **2)** primary breast cancer **without** metastasis; **3)** primary breast cancer **with** metastasis; **4)** lymph node **metastatic** breast cancer. The group 3 and 4 were **paired samples** from the same patient, which was very valuable for the determination of the significance of sperm-type membrane-bound hyaluronidase in breast cancer progression.

First, the samples of breast cancer without metastasis were stained. While the background in stroma was relatively low, the cancer cells stained strongly with anti-HAase, indicating that breast cancer cells did express the PH-20 HAase as compared to normal breast tissue (**Fig. 21**). In Fig. 21 A and D, the red positive staining was obviously **surrounding** the cancer cells, suggesting that it was the **membrane-bound form**. In 29 cases

stained, there were 14 cases positive and 15 cases negative. The PH-20 positive rate in breast cancer without metastasis was 48.2%.

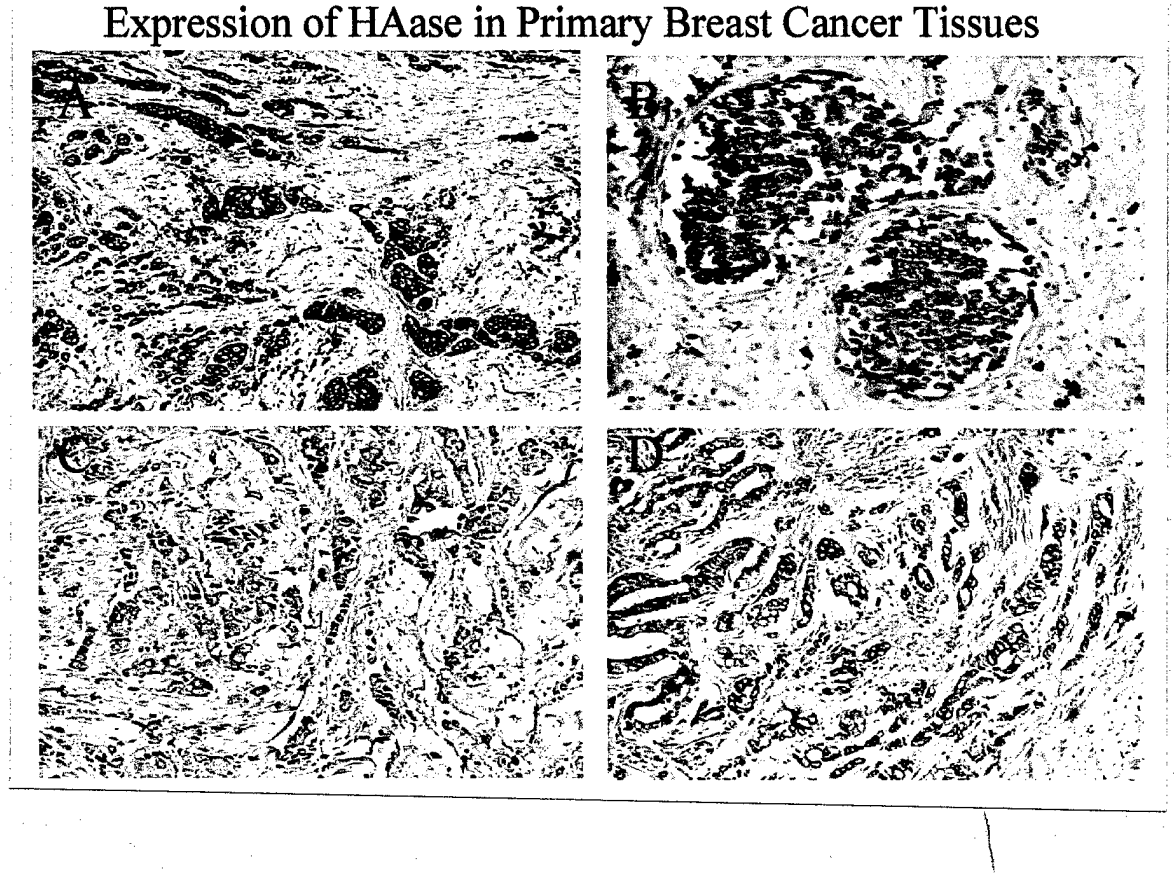

Figure 21. Expression of HAase in human primary breast cancer tissues. The five μm thick de-paraffin sections were stained with 1:500 diluted rabbit anti-PH-20 at 4°C overnight and then followed with ABC secondary staining kit (purchased from Bio-Media Inc. CA) and clorized with AEC in red. The cancer cells stained strongly with anti-PH-20 while little staining in surrounding stromal. A and D showed a membrane-bound staining.

Secondly, the samples of metastatic breast cancer in lymph node were stained. The staining was also very intensive (**Fig 22**). In 24 cases, there were 20 cases stained positive and 4 cases negative. The positive rate was 83.3%, which is much higher compared to the breast cancer without metastasis (83.3% v.s. 48.2%). This suggests that the cancer cells expressing PH-20 are preferentially to have the ability to metastasize to distant sites, settle-down and grow into new tumors. The clear membrane staining pattern was also observed (**Fig 22 D and E**). Again, this further confirmed the cellular location of this enzyme.

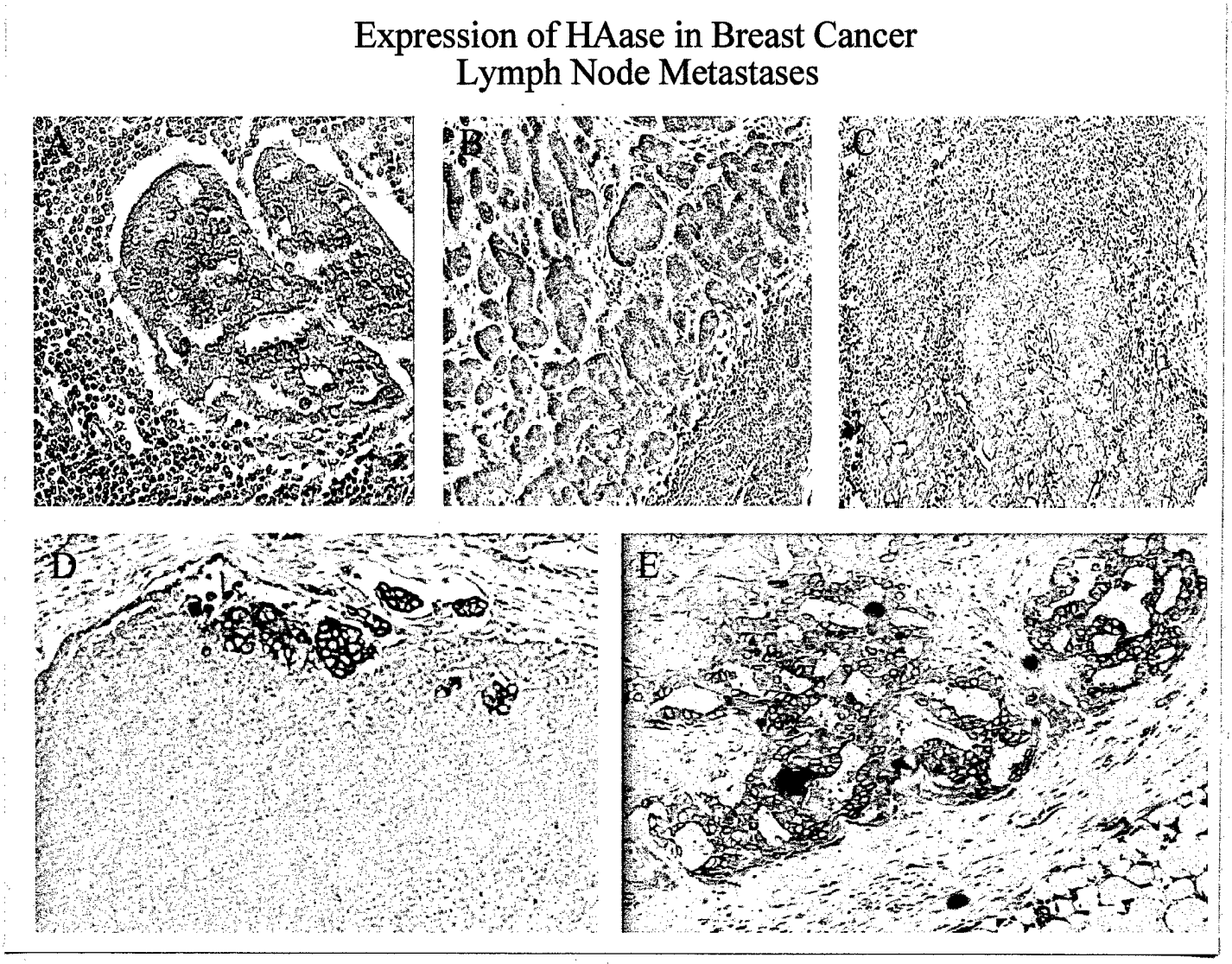

Figure 22. Expression of HAase in human metastatic breast cancer in lymph node. The five μm thick de-paraffin sections were stained with 1:500 diluted rabbit anti-PH-20 at 4°C overnight and then followed with ABC secondary staining kit (purchased from Bio-Media Inc. CA) and clorized with AEC in red. While the staining of surrounding lymph tissue was negative, the metastatic cancer cells stained strongly with anti-PH-20. D and E indicated that the staining was surrounding the membrane. The positive rate was 83.3%, much higher than that in primary cancer without metastasis (48.2%).

It seems that metastatic cancer express PH-20 HAase in a much higher rate than those primary cancers without metastasis. To see if there is any difference in the expression level of PH-20 HAase between the primary tumors **with** and **without** metastasis, the primary breast cancer samples with diagnosis in lymph node status were examined. The results (**Fig 23** and **Table 2**) indicated that the HAase expression rate of breast cancer patients **with** metastasis was 70.8%, which was higher than that of patients **without** metastasis (**70.8% v.s. 48.2%**). This suggests that the cells expressing PH-20 HAase may have stronger ability to make their way to distant site via utilizing this matrix enzyme to destroy the integrity of surrounding tissue and vessels and to gain more support from the released growth factors.

When we compared the HAase expression rate among 24 paired samples (primary and metastatic samples from the same patient), it was found that the expression rate in the metastatic samples was higher than

that in their counterparts (83.3% v.s. 70.8%). This suggests that the metastasis process may preferentially select the cells that express high level of PH-20 HAase, which would favor them to invade and colonize.

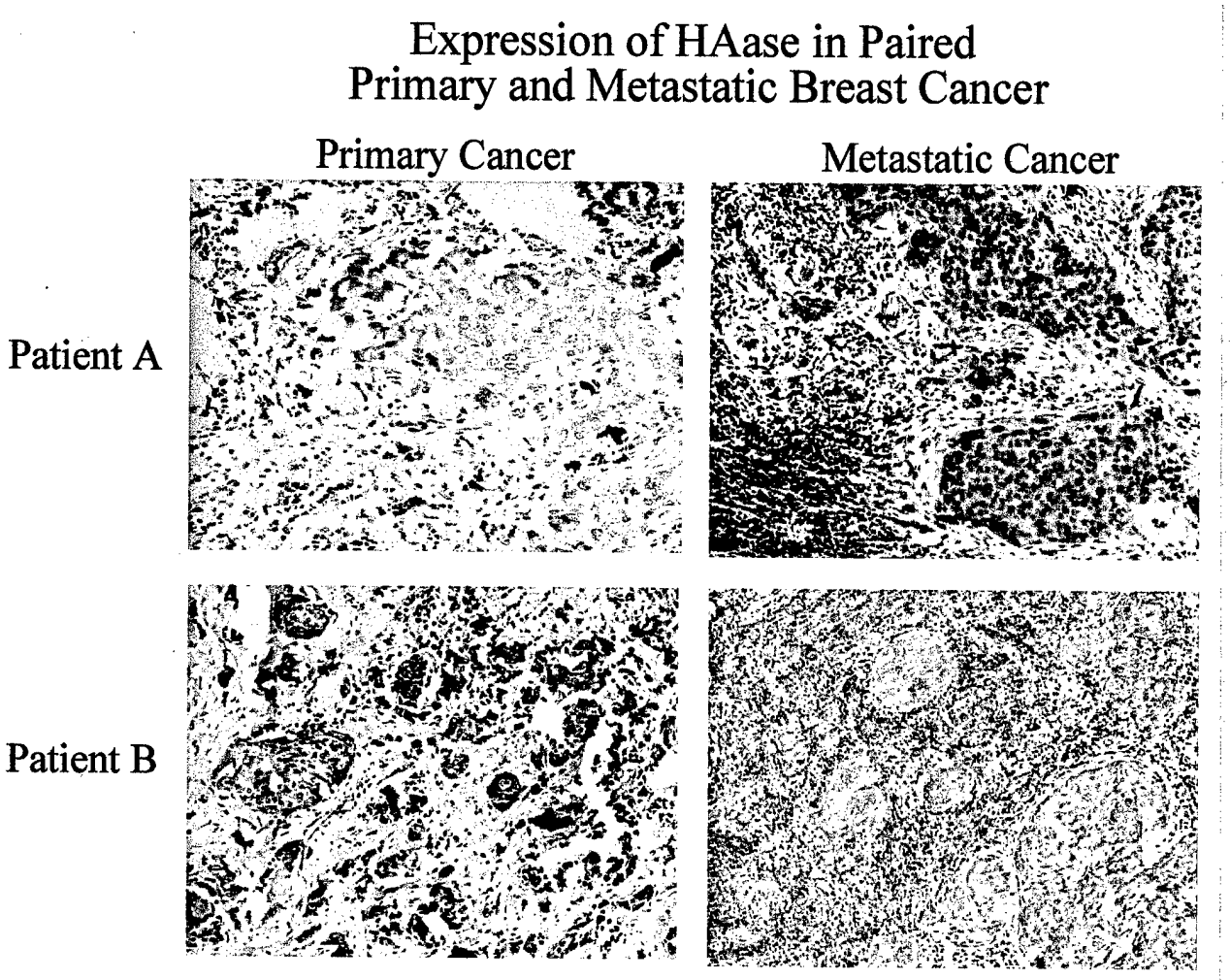

Figure 23. Expression of HAase in primary and metastatic breast cancer. The paired samples of the primary and metastatic breast cancer were stained positively with anti-PH20. However, the positive staining rate in metastatic tumors was 83.3%, higher than that (70.8%) in primary tumors.

Table 2. Expression of PH20 in Breast cancer

Histopathology Type	Total # Cases	Positive cases	Negetive Cases	Positive (%)
Normal breast tissue	3	0	3	0
BreastCancer without Lymph node metastasis	29	14	15	48.2
Breast Cancer with Lymph node metastasis	24	17	7	70.8
Lymph node metastases	24	20	4	83.3
Total	80	51	29	63.7

In summary, our results in this set of study show that: **1)** PH-20 HAase in paraffin sections of human breast cancer could be stained with antibody generated with two peptides of PH-20 and bovine testes HAase from rabbit; **2)** the staining was in a peri-cellular pattern, indicating PH-20 HAase indeed is a membrane-bound enzyme; **3)** while there was little staining in normal breast cancer tissues, the positive staining rate in primary breast cancer without metastasis is 48.2%; in breast cancer with metastasis 70.8%; and in lymph node metastatic breast cancer 83.3%. These results suggest that PH-20 HAase is likely to play a role in breast cancer progression.

Key Research Accomplishments

1. Our data demonstrated at first time that PH-20 HAase serves as a switch for release of the immobilized, inactive form of FGF2 to an active, free form. This, in turn, stimulates the growth of tumor cells both anchorage-dependent and –independent conditions via paracrine effect.

2. It is first time to transfect cDNA of PH-20 HAase into human breast cancer cells and demonstrate that the over-expression of PH-20 HAase can release PH-20 HAase, enhance tyrosine phosphorylation and activation of MAPK, enhance colony formation *in vitro* and promote tumor growth *in vivo*.

3. The over-expression of PH-20 HAase stimulates the growth of endothelial cells *in vitro* and tumor angiogenesis *in vivo*.

4. The results of in situ hybridization and immunohistochemistry staining indicate that both mRNA and protein of PH-20 HAase are expressed in breast cancer cells. While there is little staining in normal breast tissues, there is a strong staining in breast cancer cells. The expressing rate increases from primary breast tumors without metastasis (48.2%) to those with metastasis (70.8%) to those lymph node metastasis (83.3%), strongly suggesting that the PH-20 HAase is utilized by malignant breast cancer cells to promote their progression.

Materials and methods generated in this project

Materials

- Mammalian expression vector for membrane-bound PH-20 HAase;
- MDA231 breast cancer cells over-expressing of PH-20 HAase;
- cDNA probes for in situ hybridization for mRNA level of PH-20 HAase;
- Antibodies against membrane-bound PH-20 HAase for detection of its protein level in paraffin sections;
- A collection of valuable paired samples of human primary breast cancer and their lymph node metastases.

Methods

- ELISA-like method for detection of activity of membrane-bound PH-20 HAase;
- In situ hybridization for mRNA level of PH-20 HAase;
- Immunohistochemistry staining for the protein level of PH-20 HAase in paraffin sections;

CONCLUSION

Using highly purified sperm hyaluronidase and PH-20 cDNA transfection approaches, we have demonstrated that: PH-20 HAase can release FGF2, stimulates the growth of both tumor cells in both anchorage -dependent and independent conditions. It can also stimulate the proliferation of endothelial cells and enhance the tumor angiogenesis. As the result of the dual effect, PH-20 HAase promotes the tumor growth *in vivo*.

The results of in situ hybridization and immunohistochemistry staining indicate that both mRNA and protein of PH-20 HAase are expressed in breast cancer cells. While there is little staining in normal breast tissues, there is a strong staining in breast cancer cells. The expressing rate increases from primary breast tumors without metastasis (48.2%) to those with metastasis (70.8%) to those lymph node metastasis (83.3%), strongly suggesting that the PH-20 HAase is utilized by malignant breast cancer cells to promote their progression.

The detection of the level of PH-20 HAase may serve as a poor prognosis index for human breast cancer.

The reduction of the expression or the function of PH-20 HAase by genetic modification (anti-sense, ribozymes or siRNA) or small molecules may be an novel approach in anti-breast cancer.

References

1. Stetler-Stevenson WG.: The role of matrix metalloproteinases in tumor invasion, metastasis, and angiogenesis.Surg Oncol Clin N Am 2001 Apr;10(2):383-92
2. Rabbani SA, Xing RH.: Role of urokinase (uPA) and its receptor (uPAR) in invasion and metastasis of hormone-dependent malignancies.Int J Oncol 1998 Apr;12(4):911-20
3. Schmitt M, Harbeck N, Thomssen C, Wilhelm O, Magdolen V, Reuning U, Ulm K, Hofler H, Janicke F, Graeff H.: Clinical impact of the plasminogen activation system in tumor invasion and metastasis: prognostic relevance and target for therapy. Thromb Haemost 1997 Jul;78(1):285-96
4. Friesel RE, Maciag T. Molecular mechanisms of angiogenesis: fibroblast growth factor signal transduction. FASEB J, 9(10): 919-25, 1995
5. Bikfalvi A, Klein S, Pintucci G, Rifkin DB. Biological roles of fibroblast growth factor-2. Endocr Rev, 18(1): 26-45, 1997
6. Bikfalvi A. Significance of angiogenesis in tumour progression and metastasis. Eur J Cancer, 31A(7-8): 1101-4, 1995
7. Fidler IJ, Kumar R, Bielenberg DR, Ellis LM. Molecular determinants of angiogenesis in cancer metastasis. Cancer J Sci Am, 4 Suppl 1:S58-66 1998
8. Zetter BR. Angiogenesis and tumor metastasis. Annu Rev Med, 49:407-24. 1998
9. Engelberg, H.: Action of heparin that may affect the malignant process. Cancer 85 (2): 257-272; 1999
10. Rak, J and Kerbel, R. S.: b-FGF and tumor angiogenesis—Back in the limelight. Nat. Med. 3 (10): 1083-1084; 1997
11. Czubayko, F., Smith, R.V., Chung, H. C., and Wellstein, A. Tumor growth and angiogenesis induced by a secreted binding protein for fibroblast growth factors. J. Biol. Chem. 269: 28243-28248, 1994
12. Czubayko F, Liaudet-Coopman ED, Aigner A, Tuveson AT, Berchem GJ, Wellstein A: A secreted FGF-binding protein can serve as the angiogenic switch in human cancer. Nat. Med. 3(10):1137-40; 1997
13. Gmachl, M., Sagan, S.. Ketter, S and Kreil, G.: The human sperm protein PH-20 has hyaluronidase activity. FEBS 1993; 336 (3): 545-548.
14. Lin, Y., Kimmel,L. H., Myles, D. G., and Primakoff, P.: Molecular cloning of the human and monkey sperm surface protein PH-20. Proc. Natl. Acad. Sci. USA 1993; 90: 10071-10075.
15. Primakoff, P., Hyatt, H. and Myles, D. G. J. Cell Biol. 1985; 101: 2239-2244.
16. Madan AK, Yu K, Dhurandhar N, Cullinane C, Pang Y, Beech DJ: Association of hyaluronidase and breast adenocarcinoma invasiveness. Oncol Rep 6(3):607-9; 1999
17. Liu D, Pearlman E, Diaconu E, Guo K, Mori H, Haqqi T, Markowitz S, Willson J, Sy MS: Expression of hyaluronidase by tumor cells induces angiogenesis in vivo. Proc Natl Acad Sci U S A. 93(15):7832-7; 1996
18. Pham, H. T., Block, N. L., Lokeshwar, V. B.: Tumor-derived hyaluronidase: A diagnostic urine marker for high-grade bladder cancer. Cancer Res. 1997; 57: 778-783
19. Lokeshwar VB, Lokeshwar BL, Pham HT, Block NL: Association of elevated levels of hyaluronidase, a matrix-degrading enzyme, with prostate cancer progression. Cancer Res 1996; 56(3):651-7
20. Cameron, E.: Hyaluronidase and Cancer. Pergamon Press 1966
21. Lin, R.Y., Argenta, P. A., Sullivan, K. M. Stern, R., and Adzick, N. S.: Urinary hyaluronic acid is a Wilms' tumor marker. J. Pedistr. Surg. 1995; 30: 304-308
22. Bok SW : Hyaluronidase, from wound healing to cancer (II). Med Hypotheses 1982; 8(5):455-9
23. Stern, M., Longaker, M. T., Adzick, N. S., Harrison, M. R., and stern, R.: Hyaluronidase levels in urine from Wilms' tumor patients J. Natl. Cancer. Inst. 1991; 83: 1569-1574
24. Lin, R.Y., Argenta, P. A., Sullivan, K. M. Stern, R., and Adzick, N. S.: Urinary hyaluronic acid is a Wilms' tumor marker. J. Pedistr. Surg. 1995; 30: 304-308
25. Pham, H. T., Block, N. L., Lokeshwar, V. B.: Tumor-derived hyaluronidase: A diagnostic urine marker for high-grade bladder cancer. Cancer Res. 1997; 57: 778-783
26. West, D.C., Hampson, I. N., Arnold, F. and Kumar, S.: Angiogenesis induced by degradation products of hyaluronic acid. Science 1985; 228: 1324-1326.

Reportable outcomes

Publications

- Feng Gao, Zeqiu Han, Ivan Ding, Ningfei Liu, Weiming Liu, Jianzhong Xie, Charles B. Underhill and Lurong Zhang,: Hyaluronidase acts as a switch for fobroblast growth factor. (International J. Cancer cells, in press)
- Gao F, Zhang L, Underhill CB.: Promotion of growth of human breast cancer cells MDA231 by human sperm membrane-bound hyaluronidase: an experimental study. Zhonghua Yi Xue Za Zhi. 2002; 82(3):207-10

Manuscripts in preparation:

- Feng Gao, Ningfei Liu, Zeqiu Han, Charles B. Underhill, Lurong Zhang: Over-expression of human membrane-bound hyaluronidase enhance the tumorigenicity.

- Luping Wang, Feng Gao, Xue-Ming Xu, Shanmin Yang, Jinguo Chen, Charles B. Underhill and Lurong Zhang: Expression of PH-20 in human breast cancer.

Meeting abstracts

1. Lurong Zhang, Zeqiu Han and Charles B. Underhill: Hyaluronidase serves as a switch for basic fibroblast growth factor. Proc. Annu. Meet. Am. Assoc. Cancer Res 1999; 40: 460:3041

2. Ningfei Liu, Feng Gao, Zeqiu Han, Charles B. Underhill and Lurong Zhang Overexpression of human hyaluronan synthase 3 promotes tumor growth. Proc. Annu. Meet. Am. Assoc. Cancer Res 2000; 41: 799: 5077

3. Zeqiu Han, Jian Ni, Patrick Smits, Charles B. Underhill, Bin Xie, Ningfei Liu, Przemko Tylzanowski, David Parmelee, Ping Feng, Ivan Ding, Feng Gao, Reiner Gentz, Danny Huylebroeck, Jozef Merregaert and Lurong Zhang. Extracellular matrix protein 1 (ECM1) is a novel angiogenic factor expressed by breast cancer tumor cells. Proc. Annu. Meet. Am. Assoc. Cancer Res 2000; 41: 795; 5055

4. Feng Gao, Ningfei Liu, Zeqiu Han, Charles B. Underhill and Lurong Zhang Over-expression of human membrane-bound hyaluronidase (PH-20) promotes tumor growth. Proc. Annu. Meet. Am. Assoc. Cancer Res 2000; 41: 133: 847

5. Xue-Ming Xu, Yixin Chen[1], Ningfei Liu, Jinguo Chen, Feng Gao, Zequi Han, Charles B. Underhill and Lurong Zhang. Targeted peptide of human brain hyaluronan binding protein inhibits tumor growth. Proc. Annu. Meet. Am. Assoc. Cancer Res 2001; 42: 71:383

6. Feng Gao, Xue-Ming Xu, Charles B. Underhill, Shimin Zhang, Ningfei Liu, Zeqiu Han, Jiaying Zhang and Lurong Zhang. Human brain hyaluronan binding protein inhibits tumor growth via induction of apoptosis. Proc. Annu. Meet. Am. Assoc. Cancer Res 2001; 42: 815:4375

7. Ningfei Liu, Xue-Ming Xu, Charles B. Underhill, Susette Mueller, Karen Creswell, Yixin Chen, Jinguo Chen and Lurong Zhang. Inhibition of tumor growth by hyaluronan binding motifs (P4) is mediated by apoptosis pathway related with lysosome and mitochondria. Proc. Annu. Meet. Am. Assoc. Cancer Res 2001; 42: 644: 3465

8. Ningfei Liu, Xue-Ming Xu, Charles B. Underhill, Yixin Chen, Jinguo Chen, Feng Gao, Zeqiu Han and Lurong Zhang. Hyaluronan binding motifs inhibit tumor growth. Proc. Annu. Meet. Am. Assoc. Cancer Res 2001; 42: 71:382

9. Yixin Chen, Xue-Ming Xu, Jinguo Chen, Ningfei Liu, Charles B. Underhill, Karen Creswell, and Lurong Zhang. Anti-tumor effect of RGD-tachyplesin. Proc. Annu. Meet. Am. Assoc. Cancer Res 2001; 42: 69: 369

10. Jinguo Chen, Yixin Chen, Shuigen Hong, Fabio Leonessa, Robert Clake, Xue-Ming Xu, Ningfei Liu, Charles B. Underhill, Karen Creswell and Lurong Zhang. Effect of tachyplesin on MDR overexpressing tumor cells. Proc. Annu. Meet. Am. Assoc. Cancer Res 2001; 42: 812:4358

11. Xue-Ming Xu, Jinguo Chen, Luping Wang, Xu-Fang Pei, Shanmin Yang, Charles B. Underhill and Lurong Zhang: Peptides derived endostatin and angiostatin inhibits tumor growth. Proc. Annu. Meet. Am. Assoc. Cancer Res 2002; 43:1084:5364

12. Luping Wang, Jianjin Wang, Jiyao Yu, Haoyong Ning, Xu-Fang Pei, Jinguo Chen, Xue-Ming Xu, Shanmin Yang, Charles B. Underhill, Lei Liu and Lurong Zhang: Expression pattern of ECM1 in human tumors. Proc. Annu. Meet. Am. Assoc. Cancer Res 2002; 43: 729: 3618

13. Luping Wang, Xu-Fang Pei, Jinguo Chen, Xue-Ming Xu, Shanmin Yang, Ningfei Liu, Charles B. Underhill and Lurong Zhang: A peptide derived from hemopexin-like domain of MMP9 exerts anti-tumor effect. Proc. Annu. Meet. Am. Assoc. Cancer Res 2002; 43: 159:794

14. Shanmin Yang, Jinguo Chen, Xue-Ming Xu, Luping Wang, Shimin Zhang, Xu-Fang Pei, Jing Yang, Charles B. Underhill and Lurong Zhang: Triptolide, a potent anti-tumor/metastasis agent. Proc. Annu. Meet. Am. Assoc. Cancer Res 2002; 43: 854: 4233

15. Yixin Chen, Shuigen Hong, Ningfei Liu, Xu-Fang Pei, Luping Wang, Shanmin Yang[1], Xue-Ming Xu, Jinguo Chen, Charles B. Underhill and Lurong Zhang: Targeted hyaluronan binding peptide inhibits the growth of ST88-14 Schwann cells. Proc. Annu. Meet. Am. Assoc. Cancer Res 2002; 43: 888:4404

16. Ku-chuan Hsiao, Shanmin Yang, Jinguo Chen, Xue-Ming Xu, Luping Wang, Jing Yang, Charles B. Underhill and Lurong Zhang. A peptide antagonist of Fas acts as strong stimulus for cell proliferation. Proc. Annu. Meet. Am. Assoc. Cancer Res 2002; 43: 706:3502

17. Jinguo Chen, Xueming Xu, Shanmin Yang, Luping Wang, Charles B. Underhill, Lurong Zhang: Over-expression of tumor necrosis factor-stimulated gene-6 protein (TSG-6) suppresses tumor growth *in vivo.* Proc. Annu. Meet. Am. Assoc. Cancer Res 2002; 43: 799:3962

Personel receivint pay from this award

Lurong Zhang, M.D., Ph.D.
Feng Gao, M.D., Ph.D.
Luping Wang, M.D.,
Charles B. Underhill, Ph.D.
Xueming Xu, M.D., Ph.D.
Shanmin Yang, M.D.
Ningfei Liu, M.D., Ph.D.
Yixin Chen, Ph.D.

Appendices

Publications supported in part by this award:

1. Ningfei Liu, Charles B. Underhill, Randall Lapevich, Zeqiu Han, Feng Gao, Lurong Zhang and Shawn Green: Metastatin: A hyaluronan binding complex from cartilage inhibits tumor growth. Cancer Res. 2001; 61:1022-1028

2. Zeqiu Han, Jian Ni, Patrick Smits, Charles B. Underhill, Bin Xie, Ningfei Liu, Przemko Tylzanowski, David Parmelee, Ping Feng, Ivan Ding, Feng Gao, Reiner Gentz, Danny Huylebroeck, Jozef Merregaert and Lurong Zhang : Extracellular matrix protein 1(ECM1): a novel angiogenic factor expressed in breast cancer cells. FASEB J: 2001; 988-994

3. Yixin Chen, XueMing Xu, Shuigen Hong, Jinguo Chen, Ningfei Liu, Charles B. Underhill, Karen Creswell and Lurong Zhang: RGD-Tachyplesin inhibits tumor growth. Cancer Res. 2001; 61: 2434-2438

4. Ningfei Liu, Feng Gao, Zeqiu Han, Charles B. Underhill and Lurong Zhang: Over-expression of Human Hyaluronan Synthase 3 in TSU Prostate Cancer Cells Promotes Tumor Growth. Cancer Res. 2001; 61: 5207-5214

5. Liu N, Shao L, Xu X, Chen J, Song H, He Q, Lin Z, Zhang L, Underhill CB.: Hyaluronan metabolism in rat tail skin following blockage of the lymphatic circulation. Lymphology 2002; 35 (1):15-22

Appendices

Proceedings of the American Association for Cancer Research • Volume 40 • March 1999

#3041 Hyaluronidase acts as a switch for immobilized FGF2. Lurong Zhang, Zequi Han, Ivan Ding*, Jianzhong Xie*, Ningfei Liu and Charles B. Underhill. *Dept. of Cell Biology, Georgetown Univ. Med. Center, 3900 Reservoir Road, NW, Washington DC 20007; *Dept of Radiation Oncology, Univ. of Rochester School of Med and Dent., Rochester, NY.*

When many types of growth factors (GFs) are released by cancer cells, they are initially immobilized by the extracellular matrix (ECM) and can be active only after release. These GFs may be associated with the negatively-charged glycosaminoglycans, hyaluronan and chondroitin sulfate. Previous studies have shown that some types of malignant tumors express hyaluronidase (HAase), the enzyme that breaks down hyaluronan and chondroitin sulfate. Based on these observations, we hypothesized that HAase may induce the release of GFs associated with glycosaminoglycans and thereby stimulate tumor growth and angiogenesis. To test this possibility, we treated two human tumor cell lines, SW 13 and MDA 435, with testicular HAase, and found that in both cases, their ability to form colonies (>60 μm) in soft agar was increased by 4–5 fold compared to the control groups. The treatment with HAase also promoted the release of fibroblast growth factor 2 (FGF2) from the cell layer into the culture media, as detected by an ELISA. However, VEGF was not released by the treatment with HAase. These results suggest that the HAase-induced stimulation of tumor colony formation may be due to the release of FGF2 from the ECM. Interestingly, however, HAase did not stimulate the growth of these cells when they were directly attached to plastic substratum. This suggests that the effects of HAase are masked by the anchorage culture conditions through some unknown mechanism.

Proceedings of the American Association for Cancer Research • Volume 41 • March 2000

#847 OVER-EXPRESSION OF HUMAN MEMBRANE-BOUND HYALURONIDASE (PH-20) PROMOTES TUMOR GROWTH. Feng Goa, Ningfei Lui, Zeqiu Han, Charles B Underhill, and Lurong Zhang, *Changzheng Hosp, Shanghai, P.R. China, and Lombardi Cancer Ctr, Georgetown Univ, Washington, DC*

Membrane-bound hyaluronidase (PH-20), that is normally only present on sperm, is expressed by some tumor cells, and by metastatic cells in particular. In previous studies, we have found that the addition of testicular hyaluronidase to cultured cells can release immobilized FGF2 and activate its biological activity. To further examine the function of PH-20 in tumor progression, we transfected the cDNA for PH-20 into MDA231, a human breast cancer cell line. The cells expressing PH-20 were confirmed by Western blotting and by an ELISA using hyaluronar (HA) as substrate. The PH-20 transfected cells were then characterized and found to have the following properties: 1) the colony formation ability was greatly enhanced; 2) medium conditioned by these cells stimulated the growth of cultured endothelial cells, perhaps as a result of the activation of FGF2 or by the angiogenic properties of the fragments of HA; 3) when placed on the chorioallantoic membrane of chicken embryos or injected into nude mice, the resulting xenografts were larger than those formed by control cells (mock transfectants); and 4) immunohistochemical staining revealed increased levels of angiogenesis in the xenografts. The results of this study suggest that membrane-bound hyaluronidase can play an important role in the progression of malignant tumor cells.

#382 Hyaluronan Binding Motifs Inhibit Tumor Growth. Ningfei Liu, Xue-Ming Xu, Charles B. Underhill, Yixin Chen, Jinguo Chen Chen, Feng Gao, Zeqiu Han, and Lurong Zhang. *Lombardi Cancer Center, Washington, DC.*

Cartilage, enriched with hyaluronan (HA) binding proteins, has been proved to have anti-tumor effect in some clinical trails. To explore if HA binding motif is responsible for anti-tumor effect, a 39 peptide (called P4) containing three HA binding motifs was linked with NGR homing motif on its N-terminal and tested for anti-tumor function. The synthetic P4 could bind to 3H-HA with high capacity. When TSU prostate cancer cells, MDA-435 breast cancer cells and/or endothelial cells were treated with 50-100 ug/ml of P4, their growth was strongly inhibited in either anchorage-dependent or anchorage-independent conditions. This inhibitory effect was abolished by pre-incubation of P4 with HA, indicating the activated HA binding sites are crucial for the effect. In addition, when 100 ug of P4 was i.v. injected into CAM of chicken embryo bearing with tumors formed by B16 melanoma or MDA-435 cells, the tumor sizes were greatly reduced compared to the control. To see the potential of P4 for gene therapy, the amino acid sequence of P4 was back-translated into nucleotide sequence. The cDNA coding for P4 was inserted into the pSecTag2 vector with a signal peptide and transfected into TSU and MDA-435 cells. The growth of tumors formed by cells expressing P4 was inhibited compared to the control cells in both CAM and nude mice models. The angiogenesis in P4 tumors was reduced as determined by endothelial cells staining. Furthermore, the apoptotic indexes (Annexin−π staining and nuclear fragmentation) were increased in both tumor cells and endothelial cells upon the treatment of P4, indicating that the inducing of apoptosis is one of action mechanisms by which P4 exerts anti-tumor effect. The involvement of lysosome and mitochondria in the P4 induced cell death has been investigated.

#383 Targeted Peptide of Human Brain Hyaluronan Binding Protein Inhibits Tumor Growth. Xueming Xu, Yixin Chen, Ningfei Liu, Jinguo Chen, Feng Gao, Zeqiu Han, Charles B. Underhill, and Lurong Zhang. *Dept. of Biology, Xiamen University, Xiamen, China, and Lombardi Cancer Ctr., Washington, DC.*

In previous studies, we have found that human brain hyaluronan binding protein (b-HABP) inhibits tumor growth. To explore the functional domain of this anti-tumor protein, 33 amino acids containing three hyaluronan binding motifs from N-terminal of b-HABP were linked with NGR homing motif to better target tumor cells. The synthetic peptide exerted an inhibitory effect on the proliferation of both TSU prostate cancer cells and HUVEC endothelial cells at a dose of 100 ug/ml. It also inhibited the colony formation of TSU and MDA-435 cells. When the targeted b-HABP peptide was tropically administrated to TSU and MD-A435 cells on top of the chorioallantoic membranes (CAM) of 10 days chicken embryos, the tumor growth was greatly inhibited. In addition, when 100 ug of b-HABP peptide was i.v. injected once into CAM bearing with established B16 melanomas, the growth of tumor xenografts was greatly inhibited. Then, the peptide sequence was back-translated into nucleotide sequence. The cDNA coding for the peptide was obtained using overlap-PCR and inserted into the pSecTag2 vector with a signal peptide for the secretion. The pSecTag2 vector alone (as control) or pSecTag2-peptide vectors (as tests) were transfected into MDA-435 cells. The in vivo results indicated that cells expressing targeted b-HABP peptide formed smaller tumors as compared to vector alone in both the CAM and nude mice model systems. Additional studies indicated that the targeted b-HABP peptide could damage the both the plasma membrane and mitochondrial membrane that triggered the apoptosis cascade.

#369 Anti-Tumor Effect of RGD-Tachyplesin. Yixin Chen, Xue-Ming Xu, Jinguo Chen, Ningfei Liu, Charles B. Underhill, Karen Creswell, Shuigen Hong, and Lurong Zhang. *Dept.of Biology, Xiamen University, Xiamen, China, and Lombardi Cancer Center, Washington, DC.*

Tachyplesin, an anti-microbial peptide present in leukocytes of horseshoe crab (Tachypleus tridentatus), was conjugated to the integrin homing domain RGD and tested for anti-tumor activity. Initial experiments indicated that RGD-tachyplesin could inhibit the proliferation of both cultured tumor and endothelial cells and could block the colony formation of TSU prostate cancer cells. The RGD-tachyplesin appeared to compromise the integrity of the plasma membrane as well as those associated with the mitochondria and nuclei, as evidenced by the changes in the staining with the fluorescent probes JC-1, annexin V, dextran-FITC and YO-PRO-1. In addition, Western blotting showed that the Fas ligand, FADD, Caspase 7, Caspase 6 and activated subunits of Caspase 8 (18 kDa) and Caspase 3 (20 kDa) were up-regulated following treatment with RGD-tachyplesin, suggesting that it induces apoptosis through elements of the Fas dependent pathway. And finally, in vivo studies indicated that the RGD-tachyplesin could inhibit the growth of tumor cells on the chorioallantoic membranes of chicken embryos and in syngenic mice. The results of this study suggests that the RGD-tachyplesin can inhibit tumor growth by impairing the function of vital membranes and by inducing apoptosis in both tumor cells and endothelial cells.

#4375 Human Brain Hyaluronan Binding Protein Inhibits Tumor Growth VIA Induction of Apoptosis. Feng Gao, Xue-Ming Xu, Charles B. Underhill, Shimin Zhang, Ningfei Liu, Zeqiu Han, Jiaying Zhang, and Lurong Zhang. *Lombardi Cancer Ctr., Washington, DC.*

Naturally existing anti-tumor substance are less toxic and implicated a promising feature in cancer therapy. In this study, a new protein, termed human brain hyaluronan (HA) binding protein (b-HABP) was found to have an anti-tumor effect. The cDNA coding for N-terminal of human b-HABP was cloned and found to consist of 1,548 bp coding for 516 amino acids with signal peptide. When malignant MDA-435 breast cancer cells were transfected with b-HABP-pcDNA3, their ability to grow in anchorage-dependent conditions and to form colonies was greatly reduced compared to the mock transfectants. In addition, the conditioned media from b-HABP-pcDNA3 transfectants inhibited the growth of endothelial cells. Furthermore, studies revealed that the FasL, Caspase 3, p53, p27 were induced while bcl2 and cyclin E were reduced in b-HABP-pcDNA3 transfectants. Finally, the growth of tumors formed by b-HABP-pcDNA3 transfectants was greatly inhibited compared to the mock transfectants in CAM system and in nude mice model. This study suggests that HABP may represent a new category of naturally existing anti-tumor substance via induction of apoptosis.

#3465 Inhibition of Tumor Growth by Hyaluronan Binding Motifs (P4) is Mediated by Apoptosis Pathway Related with Lysosome and Mitochondria. Ningfei Liu, Xue-Ming Xu, Charles Underhill, Susette Mueller, Karen Creswell, Yixin Chen, Jinguo Chen, and Lurong Zhang. *Lombardi Cancer Ctr., Washington, DC.*

We have demonstrated that the tumor growth can be greatly suppressed by hyaluronan binding motifs (P4) either exogenous administration of synthetic P4 peptide or endogenous expressing of P4. To explore the underlying mechanism for the anti-tumor effect, FITC-P4 was used for its intracellular tracing and the alterations in apoptotic molecules were studied. The results of confocal microscopy indicated that the P4 bound to cell surface, which could be partially blocked by anti-CD44, heparin and chondroitin sulfate, indicating that the binding may indirectly mediated by CD44 and interaction anionic substances on the membrane. Following the binding on cell surface, the FITC-P4 was up-taken by lysosomes and partially entered mitochondria, as evidenced by co-localization staining. At the molecular level, Fas ligand, FADD, caspase 8 (activated 18 kDa subunit) and caspase 3 were up-regulated upon the treatment of P4 in both MDA-435 tumor cells and ABAE endothelial cells, indicating that the apoptosis is triggered by P4. As a result, other vital membranes were greatly damaged as demonstrated by 1) positive Annexin V staining, an increased inflow of FITC-Dextran (MW 40,000) and exflow of LDH for the damage of plasma membrane; 2) an increased inflow of YO-Pro-1 for the damage of nuclear membrane; and 3) the shifted JC-1 staining for the depolarization of mitochondrial potential. Furthermore, the P4-induced cell death could be partially reversed by inhibitors (NH4Cl) specific for lysosomal functions and inhibitor (Z-VAD-FMK) for caspases, suggesting that the pro-apoptotic molecules associated with lysosome and mitochondria might be released by P4 and then activate the caspases in cytoplasm.

#4358 Effect of Tachyplesin on MDR Overexpressing Tumor Cells. Jinguo Chen, Yixin Chen, Shuigen Hong, Fabio Leonessa, Robert Clarke, Xue-Ming Xu, Ningfei Liu, Charles B. Underhill, Karen Creswell, and Lurong Zhang. *Lombardi Cancer Center, Georgetown University, Washington, DC, and The Key Lab of China Education Ministry on Cell Biology and Tumor Engineering, Xiamen University, Xiamen, China.*

Tachyplesin is an anti-microbial peptide, consisting of 17 amino acids with a molecular weight of 2,269 Dalton and pI of 9.93. It has two disulfide linkages, which exposes all six positively charged basic amino acids on its surface. This cationic peptide can interact with anionic phospholipids present in the prokaryotic cytoplasmic membrane and eukaryotic mitochondrial membrane. We have found that tachyplesin could inhibit the growth of tumor cells. To see the effect of tachyplesin on the tumor cells that are resistant to first line chemotherapeutic drugs, we used a pair of breast cancer cell lines, LCC6-MDR (a MDA435 cells transduced with MDR1-retroviral vector) and LCC6-vector as control. Due to the over-expression of MDR1, LCC6-MDR cells resisted to Taxol with an EC50 of 1000 nM, while LCC6-vector had an EC50 of 10 nM. However, when treated with tachyplesin, both cell lines showed a similar sensitivity (EC50 of 40 nM) in response to the inhibitory effect of tachyplesin. The confocal analysis indicated that the FITC- tachyplesin bound to cell surface, entered the cells and localized in mitochondria. The flow cytometer analysis indicated that the mitochondria potential was depolarized and that both plasma membrane and nuclei membrane were damaged, as evidenced by staining with JC-1, FITC-Dextran and YO-Pro-1. This study suggests that the cationic peptide, such as tachyplesin, may be a promising alternative agent to treat the chemotherapy resistant tumor cells.

#4404 Targeted hyaluronan binding peptide inhibits the growth of ST88-14 Schwann cells. Yixin Chen, Shuigen Hong, Xiaolin Chen, Shanmin Yang, Ningfei Liu, Xu-Fang Pei, Luping Wang, Xue-Ming Xu, Jinguo Chen, Charles B. Underhill, and Lurong Zhang. *The Cell and Tumor Key Lab of China Education Ministry at Xiamen University, Xiamen, China, and Georgetown University Medical Center, Washington, DC.*

We have reported that the hyaluronan (HA) binding proteins/peptides possess anti-tumor effect, in part, due to the induction of apoptosis and p53. The loss of neurofibromin, a tumor suppressor corded by NF1 (Neurofibromatosis Type 1) gene, results in the accumulation of hyperactive Ras-GTP due to a reduced conversion of active Ras-GTP to inactive Ras-GDP, which turns on uncontrolled mitogenic signals in the nucleus. Therefore, neurofibromatosis can be regarded as a disease resulting from the disruption of the balance between cell proliferation and apoptosis. To determine if the abnormality of neurofibromatosis can be interrupted by HA binding peptide, a naturally existing HA binding peptide, tachyplesin with RGD domain (for a better targeting) and its scramble peptide were synthesized. When ST88-14 Schwann cells were treated with this targeted peptide for 24 hours, the cells underwent apoptosis and began to die. The 3H-TdR incorporation rate of targeted HA binding peptide treated cells was greatly reduced compared to that of the control peptide treated cells. This inhibitory effect was in a dose-dependent manner. Similarly, the ability to form colony in soft agar was also remarkably reduced. Western blot analysis showed that the cell cycle key molecules, such as cyclin B1 and cdc2, were reduced. In addition, the targeted HA binding peptide could reduce the phosphorylation of mitogen-activated protein kinase. The data suggest that the targeted HA binding peptide could inhibit the growth of ST88-14 Schwann cells via suppression of some key molecules in cell proliferation process.

#5364 Peptides derived endostatin and angiostatin inhibits tumor growth. Xueming Xu, Jinguo Chen, Luping Wang, Xue-Fang Pei, Shanmin Yang, Charles B. Underhill, and Lurong Zhang. *Georgetown University, Washington, DC.*

Endostatin and angiostatin are well-known anti-tumor/angiogenesis agents. We have found that there are several hyaluronan (HA) binding motifs existing in these two proteins. In previous studies, we have found that HA binding proteins / peptides inhibited the growth of tumor cells. In this study, two peptides with HA binding motifs derived from endostatin and angiostatin were tested to confirm that the HA binding motifs are the critical effector in the bioactivity of their parental molecules. Two peptides that containing 2-3 HA binding motifs and NGR homing domain or the control scramble peptide were chemically synthesized. When the peptides were added to endothelial cells (HUVEC and ABAE) or tumor cells (TSU prostate or MDA435 breast cancer), they inhibited the cell growth in a dose-dependent manner. When 100 μg of peptides was tropically administrated to TSU tumors grown on chorioallantoic membrane of chicken embryo, the sizes of tumors in the peptide-treated groups were smaller than the control, while the development of chick embryos were not affected. The results of Western blot and flow cytometry analysis indicated that the peptides could trigger the depolarization of mitochondrial, induce the expression of p16 and p21 and increase the cleaved caspase 8. It seems that the HA binding motifs in endostatin and angiostatin are the key factor for the anti-tumor/angiogenesis effects of their parental proteins.

#4404 Targeted hyaluronan binding peptide inhibits the growth of ST88-14 Schwann cells. Yixin Chen, Shuigen Hong, Xiaolin Chen, Shanmin Yang, Ningfei Liu, Xu-Fang Pei, Luping Wang, Xue-Ming Xu, Jinguo Chen, Charles B. Underhill, and Lurong Zhang. *The Cell and Tumor Key Lab of China Education Ministry at Xiamen University, Xiamen, China, and Georgetown University Medical Center, Washington, DC.*

We have reported that the hyaluronan (HA) binding proteins/peptides possess anti-tumor effect, in part, due to the induction of apoptosis and p53. The loss of neurofibromin, a tumor suppressor corded by NF1 (Neurofibromatosis Type 1) gene, results in the accumulation of hyperactive Ras-GTP due to a reduced conversion of active Ras-GTP to inactive Ras-GDP, which turns on uncontrolled mitogenic signals in the nucleus. Therefore, neurofibromatosis can be regarded as a disease resulting from the disruption of the balance between cell proliferation and apoptosis. To determine if the abnormality of neurofibromatosis can be interrupted by HA binding peptide, a naturally existing HA binding peptide, tachyplesin with RGD domain (for a better targeting) and its scramble peptide were synthesized. When ST88-14 Schwann cells were treated with this targeted peptide for 24 hours, the cells underwent apoptosis and began to die. The 3H-TdR incorporation rate of targeted HA binding peptide treated cells was greatly reduced compared to that of the control peptide treated cells. This inhibitory effect was in a dose-dependent manner. Similarly, the ability to form colony in soft agar was also remarkably reduced. Western blot analysis showed that the cell cycle key molecules, such as cyclin B1 and cdc2, were reduced. In addition, the targeted HA binding peptide could reduce the phosphorylation of mitogen-activated protein kinase. The data suggest that the targeted HA binding peptide could inhibit the growth of ST88-14 Schwann cells via suppression of some key molecules in cell proliferation process.

Proceedings of the American Association for Cancer Research • Volume 43 • March 2002

#5364 Peptides derived endostatin and angiostatin inhibits tumor growth. Xueming Xu, Jinguo Chen, Luping Wang, Xue-Fang Pei, Shanmin Yang, Charles B. Underhill, and Lurong Zhang. *Georgetown University, Washington, DC.*

Endostatin and angiostatin are well-known anti-tumor/angiogenesis agents. We have found that there are several hyaluronan (HA) binding motifs existing in these two proteins. In previous studies, we have found that HA binding proteins / peptides inhibited the growth of tumor cells. In this study, two peptides with HA binding motifs derived from endostatin and angiostatin were tested to confirm that the HA binding motifs are the critical effector in the bioactivity of their parental molecules. Two peptides that containing 2-3 HA binding motifs and NGR homing domain or the control scramble peptide were chemically synthesized. When the peptides were added to endothelial cells (HUVEC and ABAE) or tumor cells (TSU prostate or MDA435 breast cancer), they inhibited the cell growth in a dose-dependent manner. When 100 μg of peptides was tropically administrated to TSU tumors grown on chorioallantoic membrane of chicken embryo, the sizes of tumors in the peptide-treated groups were smaller than the control, while the development of chick embryos were not affected. The results of Western blot and flow cytometry analysis indicated that the peptides could trigger the depolarization of mitochondrial, induce the expression of p16 and p21 and increase the cleaved caspase 8. It seems that the HA binding motifs in endostatin and angiostatin are the key factor for the anti-tumor/angiogenesis effects of their parental proteins.

#4233 Triptolide, a potent antitumor agent. Shanmin Yang, Jinguo Chen, Xue-Ming Xu, Luping Wang, Shimin Zhang, Xu-Fang Pei, Jing Yang, Charles B. Underhill, and Lurong Zhang. *the Cell and Tumor Key Lab of China Education Ministry at Xiamen University, Xiamen, China, Georgetown University Medical Center, Washington, DC, and PowerTech Inc., Bethesda, MD.*

Triptolide (TPL) is a compound (MW 360) purified from the herb Tripterygium wilfordii Hook F that has been used in China as a natural medicine for hundreds of years. In China, clinical trials have indicated that TPL could achieve complete or partial remission in patients with leukemia. In the present study, we examined the effects of TPL on cell lines derived from human cancers of the breast, prostate, stomach and liver. In addition, mouse B16 melanoma cells were used as an experimental model of metastasis. In the case of cultured tumor cells, TPL at 4 ng/ml inhibited cell growth to a similar extent as taxol at 100 ng/ml both under anchorage-dependent and -independent conditions. When mice with tumor xenografts formed by several different cell lines were injected i.v. with TPL at a dose of 0.25 mg/kg/ twice a week, the sizes of the tumor xenografts were reduced to 10-50% of the controls. This was comparable or superior to that achieved with the commonly used chemotherapeutic drugs adrimycin, cisplatin and mitomycin. Importantly, TPL could inhibit both spontaneous and experimental metastasis. Additional studies revealed that treatment of tumor cells with 10 ng/ml of TPL for 24 hours resulted in decreased levels of c-myc, cyclin A/cdk2 and cyclin B/cdc2 while increasing the level of cleaved PARP, an indicator of apoptosis. Furthermore, TPL also decreased the telomerase activity as measured by both the TRAP assay and PicoGreen staining. These results strongly suggest that TPL can potentially be developed as a new anti-tumor/metastasis agent.

Proceedings of the American Association for Cancer Research • Volume 43 • March 2002

#3962 Overexpression of tumor necrosis factor-stimulated gene-6 protein (TSG-6) suppresses tumor growth *in vivo*. Jinguo Chen, Xue-Ming Xu, Shanmin Yang, Luping Wang, Charles B. Underhill, and Lurong Zhang. *Georgetown University Medical Center, Washington, DC, The Cell and Tumor Key Lab of China Education Ministry at Xiamen University; Xiamen, China, and Beijing General Hospital, Beijing, China.*

Tumor necrosis factor-stimulated gene-6 protein (TSG-6) is an anti-inflammatory factor that is produced in response to TNF and contains a link module that allows it to bind hyaluronan. In this study, we examined the effects of overexpression of TSG-6 on tumor progression. The cDNA coding for human TSG-6 gene (782bp) was cloned, inserted into an expression vector (pSecTag2/Hygro B) and transfected into TSU human prostate cancer cells. The positive clones were identified by RT-PCR and the biological activity of the TSG-6 protein was confirmed by its ability to bind hyaluronan. The TSG-6 positive clones were then pooled and compared with control cells (transfected with vector) with regard to cell behaviors. In culture, the TSG-6 transfected TSU cells grew at the same rate as control cells as measured by cell number and by incorporation of radioactive thymidine. However, when the cells were inoculated on the chorioallantoic membrane of chicken embryos, the TSG-6 transfected TSU cells grew at a slower rate than the control cells (mean xenograft weight in TSG-6 16.3 mg vs. control 39.6 mg). Similarly, when cells were injected s.c. into nude mice, the xenografts formed by the TSG-6-transfected cells were smaller than that of the control cells (mean xenograft weight 0.72 g vs. 2.16 g). Western Blot analysis of lysates from these xenografts indicated that the TSG-6 transfected cells had increased levels of Fas, cleaved caspase 8 and cleaved PARP, but no change in the levels of cyclin D1, B1, Rb, ERK. These preliminary results suggest that TSG-6 could function as a tumor suppressor *in vivo*, in part, through the induction of apoptosis.

[CANCER RESEARCH 61, 5207–5214, July 1, 2001]

Hyaluronan Synthase 3 Overexpression Promotes the Growth of TSU Prostate Cancer Cells[1]

Ningfei Liu, Feng Gao, Zeqiu Han, Xueming Xu, Charles B. Underhill, and Lurong Zhang[2]

Department of Oncology, Lombardi Cancer Center, Georgetown University Medical School, Washington DC 20007

ABSTRACT

Hyaluronan synthase 3 (HAS3) is responsible for the production of both secreted and cell-associated forms of hyaluronan and is the most active of the three isoforms of this enzyme in adults. In this study, the cDNA for human HAS3 was cloned and characterized. The open reading frame consisted of 1659 bp coding for 553 amino acids with a deduced molecular weight of about 63,000 and isoelectric pH of 8.70. The sequence of human HAS3 displayed a 53% identity to HAS1 and a 67% identity to HAS2. It also contained a signal peptide and six potential transmembrane domains, suggesting that it was associated with the plasma membrane. To evaluate the physiological role of human HAS3, expression vectors for this protein were transfected into TSU cells (a prostate cancer cell line), and the phenotypic changes in these cells were examined. The enhanced expression of hyaluronan in the transfected cells was demonstrated by dot blot analysis and ELISA. These cells were found to differ from their vector-transfected counterparts with respect to the following: (*a*) they grew at a faster rate in high (but not low) density cultures; (*b*) conditioned media from these cells stimulated the proliferation and migration of endothelial cells; (*c*) when placed on the chorioallantoic membrane of chicken embryos, these cells formed large, dispersed xenografts, whereas the control transfectants formed compact masses; and (*d*) when injected s.c. into nude mice, the xenografts formed by HAS3 transfectants were bigger than those formed by control transfectants. Histological examination of these xenografts revealed the presence of extracellular hyaluronan that could act as conduits for the diffusion of nutrients. In addition, they had a greater number of blood vessels. However, the HAS3-transfected TSU cells did not display increased metastatic properties as judged by their ability to form lung masses after i.v. injection. These results suggested that the HAS3-induced overexpression of hyaluronan enhanced tumor cell growth, extracellular matrix deposition, and angiogenesis but was not sufficient to induce metastatic behavior in TSU cells.

INTRODUCTION

A number of studies have suggested that the production of hyaluronan is associated with the metastatic behavior of tumor cells (1–11); *e.g.*, Toole *et al.* (1) have shown that invasive tumors formed by V2 carcinoma cells in rabbits have higher concentrations of hyaluronan than noninvasive tumors formed by these same cells in nude mice. Similarly, Kimata *et al.* (2) found that a strain of mouse mammary carcinoma cells with a high metastatic potential produced significantly greater amounts of hyaluronan than a similar strain with a low metastatic potential. In a previous study (3), we found that the amount of hyaluronan on the surfaces of mouse B16 melanoma cells was directly correlated with their ability to form lung metastases. Finally, increased levels of hyaluronan production have been correlated with a variety of metastatic tumors, including carcinomas of the breast, lung, liver, pancreas, and kidney (Wilms' tumor) (4–9). Indeed, in the case of Wilms' tumor (10) and mesotheliomas (11), the increased levels of hyaluronan in the serum of these patients has been regarded as a diagnostic marker for the clinical course of these conditions. Thus, there appears to be a correlation between hyaluronan production and metastatic behavior.

At present, three closely related isoforms for HAS[3] have been described, termed HAS1, 2, and 3, each of which appears to be associated with the plasma membrane (12–19). They have a predicted molecular mass of approximately 63 kDa, and transfection of cells with expression vectors for each of these isoforms can induce the synthesis of hyaluronan and the formation of a pericellular coat. However, the three isoforms are distinguished from each other with respect to: (*a*) their expression pattern during embryonic development and distribution in adult tissues; (*b*) the phenotype of knockout mutants in mice in which loss of HAS2 resulted in an embryonic lethality, whereas ones deficient in HAS1 and HAS3 were viable and had no obvious phenotype; (*c*) the rate at which they carry out hyaluronan synthesis, with HAS3 being more active than either HAS1 and HAS2; and (*d*) the size of the hyaluronan produced by the different isoforms with HAS3 giving rise to a somewhat smaller product than either HAS1 or 2 (17, 18).

Several recent studies have shown that transfection of tumor cells with expression vectors for hyaluronan synthase alters their behavior; *e.g.*, Kosaki *et al.* (20) reported that the transfection of human fibrosarcoma cells with HAS2 enhanced both anchorage-independent growth and tumorigenicity. In addition, Itano *et al.* (21) have found that clones of mouse mammary cancer cells that had low levels of hyaluronan synthesis demonstrated decreased metastatic properties, which could be restored if the cells were transfected with an expression vector for HAS1.

In this study, we have cloned and characterized the full-length cDNA for human HAS3 and examined its potential role in tumor progression. An expression vector carrying HAS3 was transfected into TSU prostate cancer cells, and alterations in the phenotype of the resulting cells were examined. We found that the HAS3-induced overexpression of hyaluronan enhanced the rate of tumor cell growth both *in vitro* and *in vivo*. Xenografts of the HAS3-transfected cells grew faster and larger, demonstrated a hyaluronan-rich stroma and increased vascularization. However, transfection with HAS3 did not shift the TSU cells to a more metastatic phenotype, suggesting that hyaluronan alone is not sufficient for metastasis in the case of TSU cells.

MATERIALS AND METHODS

Cell Lines. The TSU human prostate cancer cell line was obtained from the Tumor Cell Line Bank of the Lombardi Cancer Center (Georgetown University, Washington DC) and maintained in 10% calf serum, 90% DMEM. ABAE cells were kindly provided by Dr. Luyuan Li (Lombardi Cancer Center, Washington DC) and were cultured in 10% fetal bovine serum, 90% DMEM containing 2 ng/ml basic fibroblast growth factor.

Received 12/18/00; accepted 4/25/01.

The costs of publication of this article were defrayed in part by the payment of page charges. This article must therefore be hereby marked *advertisement* in accordance with 18 U.S.C. Section 1734 solely to indicate this fact.

[1] Supported in part by National Cancer Institute/NIH (R29 CA71545), United States Army Medical Research and Materiel Command (DAMD 17-99-1-9031; DAMD 17-98-1-8099; PC970502) and Susan G. Komen Breast Cancer Foundation (to L. Z. and C. B. U.). The animal protocols used in this study were approved by the Georgetown University Animal Care and Use Committee.

[2] To whom requests for reprints should be addressed, at Department of Oncology, Lombardi Cancer Center, Georgetown University Medical School, 3970 Reservoir Road, NW, Washington DC 20007. Phone: (202) 687-6397; Fax: (202) 687-7505; E-mail: Zhangl@gusun.georgetown.edu.

[3] The abbreviations used are: HAS, hyaluronan synthase; ABAE, adult bovine aorta endothelial cells; b-HABP, biotinylated hyaluronan-binding protein from cartilage; RT-PCR, reverse transcription-polymerase chain reaction.

Cloning and Characterization of cDNA for Human HAS3. Oligonucleotide primers for PCR of a partial sequence of cDNA for human HAS3 were designed according to the published sequence of Spicer and McDonald (Ref. 17; GenBank accession no. U86409) and consisted of the following: 5′-TCCTACTTTGGCTGTGTGCAG and 3′-AGATTTGTTGATGGTAGCA-AT. A human brain cDNA library (Clontech, Palo Alto, CA) was used as a template, and PCR was performed to generate a 570-bp fragment of human HAS3 cDNA. This fragment was then used to probe the human brain cDNA library. Positive clones were isolated, amplified, and sequenced. The MacVector program was used to carry out homologue analysis of the cloned human HAS3 with other human and mouse HASs.

Construction and Transfection of Human HAS3 Expression Vector. The cDNA for HAS3 was subcloned into the pcDNA3 mammalian expression vector (Invitrogen, Carlsbad, CA), and correct clones were identified by restriction endonuclease map analysis. The HAS3-pcDNA3 or pcDNA3 (control vector) were transfected into TSU cells using the calcium precipitation method (22). The clones that survived in 1 mg/ml of Geneticin (G418) (>100 individual clones in each case) were pooled and expanded for further characterization.

Characterization of Transfected Cells. The presence of HAS3 message was determined by RT-PCR using the GeneAmp RNA PCR kit (Perkin-Elmer, Branchburg, NJ). The primers consisted of the following: 5′-TCATGGTGGT-GGATGGCAACCGC and 3′-CTAAGCCACCTGATGTACGTCCA, which gave rise to a 283-bp reaction product with HAS3 and a 324-bp product with HAS1. The amplified sequences were analyzed by agarose gel electrophoresis followed by staining with ethidium bromide.

Two methods were used to determine hyaluronan production by the transfected cells. The first consisted of dot blot analysis of secreted hyaluronan, in which conditioned media from vector-TSU and HAS3-TSU cells that had been cultured at similar densities for 3 days were applied to nitrocellulose membrane using a dot blot apparatus. After washing with PBS containing 0.1% Tween 20, the membrane was blocked with 5% nonfat milk and 1% polyvinylpyrrolidone in PBS for 30 min. The hyaluronan was detected by sequential incubations in 1 μg/ml of b-HABP (23) for 1 h, 0.25 μg/ml of peroxidase-labeled streptavidin for 1 h, and finally a chemiluminescent substrate for peroxidase.

The second method for quantitation of hyaluronan consisted of a modified enzyme-linked assay (23). For this assay, a high-bound ELISA plate (Falcon, Lincoln Park, NJ) was coated with 100 μg/ml of crude human umbilical cord hyaluronan (Sigma Chemical Co., St. Louis, MO) in PBS at room temperature overnight and blocked with 10% calf serum, 90% PBS. The samples of conditioned media and cell lysates were adjusted to equal protein concentrations, and 25-μl samples were mixed with 100 μl of 50 μg/ml of b-HABP at 37°C for 1 h and then transferred to the hyaluronan-coated ELISA plate. The unbound b-HABP remaining in the sample mixture could then bind to the hyaluronan-coated plate and was detected by incubation with 0.5 μg/ml of peroxidase-labeled streptavidin followed by a peroxidase substrate consisting of H_2O_2 and azinobis (3-ethyl-benzthiazoline sulfonic acid) in 0.1 M Na citrate (pH 5.0). The plate was read at A^{405}, and the concentration of hyaluronan in the samples was calculated from a standard curve.

The expression of CD44 by the vector-TSU and HAS3-TSU cells was examined by Western blotting. For this, both low- and high-density cultures were harvested with EDTA in PBS, and equivalent amounts of protein were dissolved in Laemmli sample buffer under nonreducing conditions and electrophoresed on a 10% SDS polyacrylamide gel. The resulting gel was electrophoretically transferred to a sheet of nitrocellulose and stained for CD44 using the BU52 monoclonal antibody (The Binding Site, Birmingham, United Kingdom) as described previously (24).

Anchorage-dependent Growth. Aliquots of medium (10% calf serum, 90% DMEM) containing 5000 transfected cells were added to 24-well dishes. At various times, the cells were harvested in 5 mM EDTA in PBS, and the cell number was determined with a Coulter counter. In some experiments, the cells were grown in the presence of 2 to 200 μg/ml of high molecular weight hyaluronan (Lifecore Biomedical, Chaska, MN) for 7 days.

Colony Formation. Vector-TSU or HAS3-TSU cells (20,000) were suspended in 1 ml of 0.36% agarose, 10% fetal bovine serum, 90% DMEM and then immediately placed on top of a layer of 0.6% solid agarose with 10% fetal bovine serum, 90% DMEM. Two weeks later, the number of colonies larger than 50 μm in diameter was quantified using an Omnicon Image Analysis system (Imaging Products International, Chantilly, VA).

Endothelial Cell Proliferation and Migration. For the proliferation assay, 2×10^3 ABAE cells were subcultured into 96-well plates and allowed to grow overnight. The next day, the media was replaced with 150 μl of 1% calf serum, 99% DMEM along with 50 μl of conditioned medium from either vector-TSU or HAS3-TSU cells. After 36 h, 0.3 μCi of [^{3}H]thymidine was added to each well, and 8 h later the cells were processed with an autoharvester. The incorporated [^{3}H]thymidine was determined with a β-counter.

For the migration assay, 25-μl aliquots of 10% FCS, 90% DMEM containing 5×10^3 ABAE cells were added to bottom wells of a 48-well Boyden chamber (Nucleopore, Pleasanton, CA) and then covered with a nucleopore membrane (5-μm pore size) coated with 0.1 mg/ml gelatin (25). The top well chamber was assembled and inverted for 2 h to allow the cells to adhere to the bottom side of membrane and then turned upright. Conditioned medium (50 μl) from either the vector-TSU or HAS3-TSU cells was added to top wells of the chamber and incubated for 2 h. The membrane was removed, the bottom side was carefully wiped to remove cells that had not migrated, and then the cells on the topside were stained with Hema 3 (Biochemical Science, Swedenboro, NJ). The membrane was placed on a slide, and the number of cells that had migrated to the topside were counted in 10 random high-powered fields.

Tumor Growth and Metastasis Assay. Two assay systems were used to determine tumor growth *in vivo*. In the first assay, 2×10^6 vector-TSU and

```
                                G TGC GTT CGC GGC TGC TTT GAC CTG GTG GGC GCC GCC TCC
GGC ACT GCA CCG AGG CGG GGC GCC AGC GCC CAG GTT GCT GGG CTG GCC TTG GCG CCC CCT
TCC CCT ACC CAG AGC GCA GGC AGG CAG GGG GGT CCC GCC GCG CCC CTT CAG CAT ATG CCG160
                                                                        M  P   2
GTG CAG CTG ACG ACA GCC CTG CGT GTG GTG GGC ACC AGC CTG TTT GCC CTG GCA GTG CTG 220
V  Q  L  T  T  A  L  R  V  V  G  T  S  L  F  A  L  A  V  L   22
GGT GGC ATC CTG GCA GCC TAT GTG ACG GGC TAC CAG TTC ATC CAC ACG GAA AAG CAC TAC 280
G  G  I  L  A  A  Y  V  T  G  Y  Q  F  I  H  T  E  K  H  Y   42
CTG TCC TTC GGC CTG TAC GGC GCC ATC CTG GGC CTG CAC CTG CTC ATT CAG AGC CTT TTT 340
L  S  F  G  L  Y  G  A  I  L  G  L  H  L  L  I  Q  S  L  F   62
GCC TTC CTG GAG CAC CGG CGC ATG CAA CGT GCC GGC CAG GCC CTG AAG CTG CCC TCC CCG 400
A  F  L  E  H  R  R  M  Q  R  A  G  Q  A  L  K  L  P  S  P   82
CGG CGG GGC TCG GTG GCA CTG TGC ATT GCC GCA TAC CAG GAG GAC CCT GAC TAC TTG CGC 460
R  R  G  S  V  A  L  C  I  A  A  Y  Q  E  D  P  D  Y  L  R  102
AAG TGC CTG CGC TCG GCC CAG CGC ATC TCC TTC CCT GAC CTC AAG GTG GTC ATG GTG GTG 520
K  C  L  R  S  A  Q  R  I  S  F  P  D  L  K  V  V  M  V  V  122
GAT GGC AAC CGC CAG GAG GAC GCC TAC ATG CTG GAC ATC TTC CAC GAG GTG CTG GGC GGC 580
D  G  N  R  Q  E  D  A  Y  M  L  D  I  F  H  E  V  L  G  G  142
ACC GAG CAG GCC GGC TTC TTT GTG TGG CGC AGC AAC TTC CAT GAG GCA GGC GAG GGT GAG 640
T  E  Q  A  G  F  F  V  W  R  S  N  F  H  E  A  G  E  G  E  162
ACG GAG GCC AGC CTG CAG GAG GGC ATG GAC CGT GTG CGG GAT GTG GTG CGG GCC AGC ACC 700
T  E  A  S  L  Q  E  G  M  D  R  V  R  D  V  V  R  A  S  T  182
TTC TCG TGC ATC ATG CAG AAG TGG GGA GGC AAG CGC GAG GTC ATG TAC ACG GCC TTC AAG 760
F  S  C  I  M  Q  K  W  G  G  K  R  E  V  M  Y  T  A  F  K  202
GCC CTC GGC GAT TCG GTG GAC TAC ATC CAG GTG TGC GAC TCT GAC ACT GTG CTG GAT CCA 820
A  L  G  D  S  V  D  Y  I  Q  V  C  D  S  D  T  V  L  D  P  222
GCC TGC ACC ATC GAG ATG CTT CGA GTC CTG GAG GAG GAT CCC CAA GTA GGG GGA GTC GGG 880
A  C  T  I  E  M  L  R  V  L  E  E  D  P  Q  V  G  G  V  G  242
GGA GAT GTC CAG ATC CTC AAC AAG TAC GAC TCA TGG ATT TCC TTC CTG AGC AGC GTG CGG 940
G  D  V  Q  I  L  N  K  Y  D  S  W  I  S  F  L  S  S  V  R  262
TAC TGG ATG GCC TTC AAC GTG GAG CGG GCC TGC CAG TCC TAC TTT GGC TGT GTG CAG TGT1000
Y  W  M  A  F  N  V  E  R  A  C  Q  S  Y  F  G  C  V  Q  C  282
ATT AGT GGG CCC TTG GGC ATG TAC CGC AAC AGC CTC CTC CAG CAG TTC CTG GAG GAC TGG1060
I  S  G  P  L  G  M  Y  R  N  S  L  L  Q  Q  F  L  E  D  W  302
TAC CAT CAG AAG TTC CTA GGC AGC AAG TGC AGC TTC GGG GAT GAC CGG CAC CTC ACC AAC1120
Y  H  Q  K  F  L  G  S  K  C  S  F  G  D  D  R  H  L  T  N  322
CGA GTC CTG AGC CTT GGC TAC CGA ACT AAG TAT ACC GCG CGC TCC AAG TGC CTC ACA GAG1180
R  V  L  S  L  G  Y  R  T  K  Y  T  A  R  S  K  C  L  T  E  342
ACC CCC ACT AAG TAC CTC CGG TGG CTC AAC CAG CAA ACC CGC TGG AGC AAG TCT TAC TTC1240
T  P  T  K  Y  L  R  W  L  N  Q  Q  T  R  W  S  K  S  Y  F  362
CGG GAG TGG CTC TAC AAC TCT CTG TGG TTC CAT AAG CAC CAC CTC TGG ATG ACC TAC GAG1300
R  E  W  L  Y  N  S  L  W  F  H  K  H  H  L  W  M  T  Y  E  382
TCA GTG GTC ACG GGT TTC TTC CCC TTC TTC CTC ATT GCC ACG GTT ATA CAG CTT TTC TAC1360
S  V  V  T  G  F  F  P  F  F  L  I  A  T  V  I  Q  L  F  Y  402
CGG GGC CGC ATC TGG AAC ATT CTC CTC TTC CTG CTG ACG GTG CAG CTG GTG GGC ATT ATC1420
R  G  R  I  W  N  I  L  L  F  L  L  T  V  Q  L  V  G  I  I  422
AAG GCC ACC TAC GCC TGC TTC CTT CGG GGC AAT GCA GAG ATG ATC TTC ATG TCC CTC TAC1480
K  A  T  Y  A  C  F  L  R  G  N  A  E  M  I  F  M  S  L  Y  442
TCC GTC CTC TAT ATG TCC AGC CTT CTG CCG GCC AAG ATC TTT GCC ATT GCT ACC ATC AAC1540
S  L  L  Y  M  S  S  L  L  P  A  K  I  F  A  I  A  T  I  N  462
AAA TCT GGC TGG GGC ACC TCT GGC CGA AAA ACC ATT GTG GTG AAC TTC ATT GGC CTC ATT1600
K  S  G  W  G  T  S  G  R  K  T  I  V  V  N  F  I  G  L  I  482
CCT GTG TCC ATC TGG GTG GCA GTT CTC CTG GGA GGG CTG GCC TAC ACA GCT TAT TGC CAG1660
P  V  S  I  W  V  A  V  L  L  G  G  L  A  Y  T  A  Y  C  Q  502
GAC CTG TTC AGT GAG ACA GAG CTA GCC TTC CTT GTC TCT GGG GCT ATA CTG TAT GGC TGC1720
D  L  F  S  E  T  E  L  A  F  L  V  S  G  A  I  L  Y  G  C  522
TAC TGG GTG GCC CTC CTC ATG CTA TAT CTG GCC ATC ATC GCC CGG CGA TGT GGG AAG AAG1780
Y  W  V  A  L  L  M  L  Y  L  A  I  I  A  R  R  C  G  K  K  542
CCG GAG CAG TCA AGC TTG GCT TTT GCT GAG GTG TGA CAT GGC CCC CAA GCA GAG CGG GTA1840
                                                                        553
P  E  Q  S  S  L  A  F  A  E  V  *
AAG TGC AAT GGG TAA GGG AGG GAA GGG GAA TGG AAG AGA AAA GAC AGG GTG GGA GGG AGG1900
AGG GAG TGC TGT GTT TTA GTC TCT TAA TGG TCC AAA GGA CAA ATC TAA AAT GCA AAG AAC1960
GGT GAT GTA GTA TGG CCT GAC AGC TCT GTT TA                                1992
```

Fig. 1. Nucleotide sequence and derived amino acid sequence of human HAS3. The open reading frame of human HAS3 consists of 1659 bp coding for 553 amino acids. The signal peptide (first 27 amino acids) and the six transmembrane domains are *underlined*. Between the first transmembrane domain (amino acids 43 to 65) and the second transmembrane domain (amino acids 384 to 402) there is a stretch of 319 amino acids located outside of the plasma membrane, which is probably the major functional region for the synthase activity. The remaining 170 amino acids in the COOH terminus (amino acids 384 to 553) contain five transmembrane domains that can form loops that span the plasma membrane. The GenBank accession no. is AF234839.

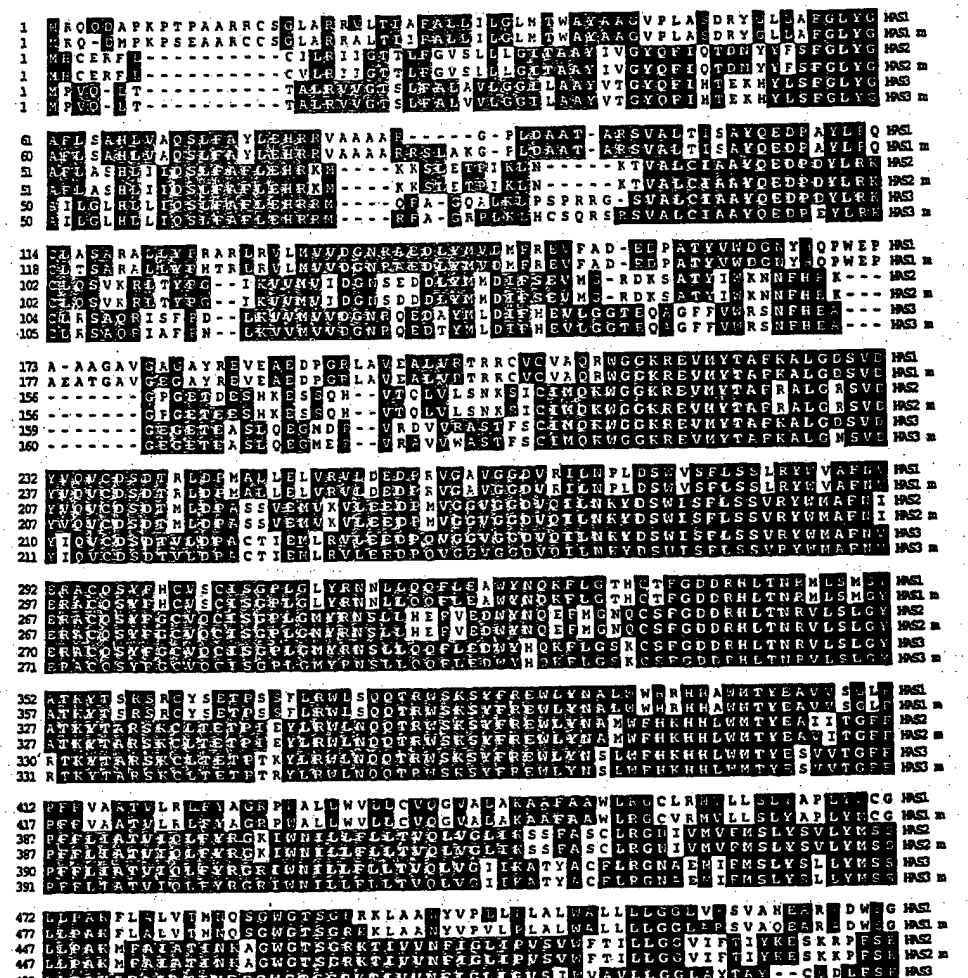

Fig. 2. Comparison of the human HAS3 with other members of the HAS family. Human HAS3 is about 53% identical to HAS1, 67% identical to HAS2 of both human and mouse (*m*), and 96% identical to mouse HAS3.

HAS3-TSU cells were placed on the chorioallantoic membranes of 10-day-old chicken embryos (15 eggs/group) and incubated at 37°C for 5 days. The tumor masses that grew on the chorioallantoic membranes were removed, photographed, and weighed. In the second assay system, the transfected cells were injected s.c. into 5-week-old male nude mice (2×10^6 cells/site; five mice/group), and the size of the xenografts was measured twice a week. At the end of 3 weeks, the mice were sacrificed, and the xenografts were photographed, weighted, and then fixed with 3.7% formaldehyde or frozen in liquid nitrogen for immunohistochemical staining.

To examine experimental metastasis, 5×10^5 vector-TSU and HAS3-TSU cells were injected into the tail veins of 5-week-old nude mice (five mice/group). Three weeks later, the mice were sacrificed, and the lungs were examined under a dissecting microscope for metastases.

Histological Staining. To stain cultured cells for hyaluronan, the transfected cells were seeded into an 8-well chamber slide (Nunc, Naperville, IL) and allowed to grow to confluence. After fixation in 3.7% formaldehyde for 5 min, the cells were washed and stained with 10 μg/ml b-HABP in 10% calf serum, 90% PBS, followed by 4 μg/ml of peroxidase-conjugated streptavidin and finally a substrate consisting of 3-amino-9-ethyl-carbazole and H_2O_2 that gives a dark red reaction product (23).

To stain xenografts for hyaluronan, the tissue was fixed with formaldehyde, embedded in paraffin, and cut into 5-μm thick sections. After the removal of the paraffin, the sections were processed as described above. After the immunoperoxidase reaction step, the sections were counter-stained with Mayer's hematoxylin and then preserved with Crystal/Mount (Biomeda, Foster City, CA).

To stain for endothelial cells, samples of the xenografts were rapidly frozen, cut into 10-μm thick sections, fixed in acetone, and air-dried. The sections were incubated sequentially with: (*a*) a 1:30 dilution of rat antimouse CD31 (PharMigen, San Diego, CA) in 10% calf serum, 90% PBS for 1 h; (*b*) avidin-biotin complex method reagents for rat IgG (ABC kits; Biomeda); (*c*) a peroxidase substrate consisting of H_2O_2 and 3-amino-9-ethyl-carbazole; and (*d*) counter-stained with Mayer's hematoxylin. The numbers of immunopositive spots corresponding to small blood vessels were counted in 10 random fields of three samples from each group.

Statistical Analysis. The mean and SE were calculated from the raw data and then subjected to Student's *t* test. The $P < 0.05$ was regarded as statistically significant.

RESULTS

Cloning and Characterization of Human HAS3. The full-length cDNA for HAS3 was cloned from a cDNA library of human brain using a probe consisting of a known partial sequence of the gene. The open reading frame contained 1659 bp coding for 553 amino acids and is shown in Fig. 1. The HAS3 protein had a deduced molecular weight of about 63,000 and a pI of 8.70. The first 27 amino acids represented

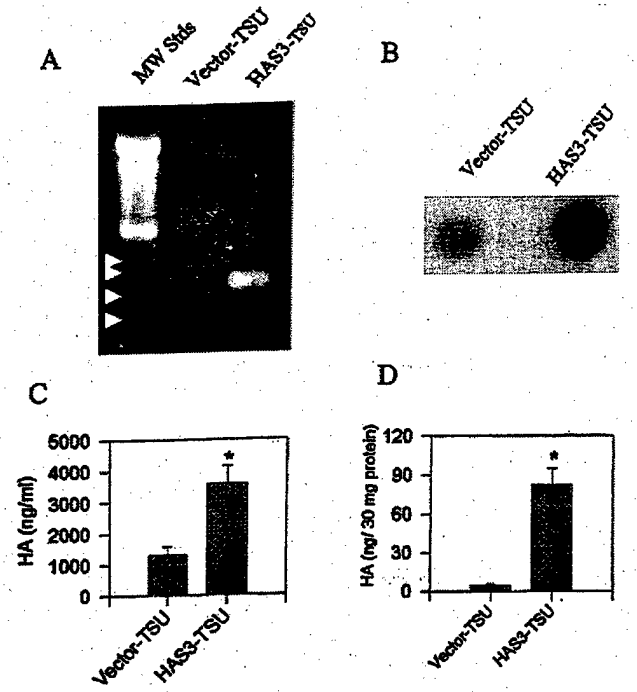

Fig. 3. Analysis of vector-TSU and HAS3-TSU cells for HAS3 mRNA and hyaluronan production. *A*, for the analysis of HAS3 message, RNA was extracted from the cultured cells and subjected to RT-PCR as described in "Materials and Methods." Agarose gel electrophoresis of the reaction products showed that the HAS3-TSU cells contained a prominent band of approximately 280 bp that was absent from the vector-TSU cells. The positions of markers for 100 through 400 bp are indicated by the *arrowheads* in the first *lane*. *B*, for the analysis of hyaluronan production, conditioned media from the transfected cells was applied to nitrocellulose using a dot blot apparatus and stained for hyaluronan using b-HABP, followed by peroxidase-labeled streptavidin and a chemiluminescence reagent. The dots represent the hyaluronan in conditioned media of vector-TSU cells (*left*) and HAS3-TSU cells (*right*). *C* and *D*, the amount of hyaluronan in conditioned media and cell lysates as determined by an ELISA are shown respectively. The increase of hyaluronan in conditioned media and lysates from HAS3-TSU cells as compared with the vector-TSU cells was statistically significant ($P < 0.05$).

the signal peptide (the cleavage site is between ILA and AY). There were six transmembrane sequences, one in the NH_2 terminus and five in the COOH terminus. Between the first transmembrane sequence (from amino acid 43 to 65) and second transmembrane sequence (from amino acid 384 to 402), there was a stretch of 319 amino acids located outside of plasma membrane, which appeared to be the major functional region for polysaccharide synthesis. The 170 amino acids in the COOH terminus (from amino acid 384 to 553) contained five transmembrane domains that can form loops spanning in and out of the plasma membrane. A potential *N*-glycosylation site was present at amino acid position 462, a glycosaminoglycan attachment site at position 464, and several phosphorylation sites for tyrosine kinase, casein kinase, protein kinase C, and cyclic AMP- and cyclic GMP-dependent protein kinases. HAS3 also contained seven hyaluronan-binding motifs of $B(X_7)B$ in which B is either R or K, and X_7 contains no acidic residues and at least one basic amino acid (26). Similar domains are present in other hyaluronan-binding proteins such as RHAMM, CD44, hyaluronidase, link protein, aggrecan, human GHAP, and TSG-6. Fig. 2 shows that compared with related enzymes, human HAS3 was about 53% identical to HAS1 (both human and mouse forms), 67% identical to HAS2, and 96% identical to mouse HAS3. These results are consistent with earlier studies of this and related genes (13–19).

Overexpression of Hyaluronan in TSU Cells Transfected with HAS3. To examine the role of HAS3 in tumor progression, the cloned cDNA was inserted into a mammalian expression vector (pcDNA3) under the control of a cytomegalovirus promoter and then transfected into TSU cells (human prostate cancer). To avoid complications associated with clonal variations, all of the clones (>100) that survived in 1 mg/ml of Geneticin (G418) were pooled and expanded for experimental analysis throughout this study. The presence of HAS3 message in the transfected cells was examined by RT-PCR as described in "Materials and Methods." When analyzed by agarose gel electrophoresis (Fig. 3*A*), the HAS3-TSU cells gave rise to a PCR product of approximately 280 bp corresponding to HAS3, whereas no such band was detected in the vector-TSU cells. In addition, no reaction product of 314 bp was apparent, indicating that the message for HAS1 was absent from these cells.

The production of hyaluronan by the transfected cells was initially examined by dot blot analysis. As showed in Fig. 3*B*, conditioned medium from HAS3-TSU cells contained a significantly greater amount of hyaluronan than that from vector-TSU cells. To quantitatively measure the hyaluronan, a competitive enzyme-linked assay was performed. Fig. 3, *C* and *D* show that both conditioned medium and lysates of HAS3-TSU cells contained greater amounts of hyaluronan as compared with those of the control vector-TSU cells. However, there was no obvious difference in the level of CD44, a cell surface receptor for hyaluronan, on the two cell types at either low or high density as determined by Western blotting (data not shown). Taken together, these results indicate that the transfection of TSU cells with cDNA for HAS3 stimulated their production of hyaluronan.

HAS3 Promotes Cell Growth at High Densities. We then compared the growth rates of the vector-TSU and HAS3-TSU cells. For this, the transfected cells were subcultured at similar starting densities, and at various times thereafter the cells were harvested and enumerated with a Coulter counter. Fig. 4*A* shows that during the first 4 days, there was no obvious difference in the proliferation rates of the vector-TSU and HAS3-TSU cells. However, after day 5, the HAS3-TSU cells began to proliferate at a faster rate than the vector-TSU cells. Thus, at high densities, the HAS3-transfected cells grew at a faster rate. This conclusion was also suggested by our recent finding that transfection of MDA-231 human breast cancer cells with antisense to HAS3 results in decreased expression of hyaluronan and inhibition of their growth at high densities.[4] Together, these results indicate that HAS3 plays a role in cell proliferation at high densities.

Cultures of the vector-TSU and HAS3-TSU cells were then compared with respect to their patterns of growth and hyaluronan staining. As shown in Fig. 4*B* (*top*), the vector-TSU cells displayed a cobblestone appearance indicative of contact inhibition of growth with relatively little staining of pericellular hyaluronan. In contrast, the HAS3-TSU cells (Fig. 4*B*, *bottom*) appeared to have lost contact-inhibition of growth, forming numerous multilayered clusters of cells, which were associated with most of the hyaluronan staining. In addition, the HAS3-TSU cells displayed an enhanced ability to form colonies in soft agar as compared with the vector-TSU cells (Fig. 4*C*). Thus, at high densities, the HAS3-transfected cells grew at a faster rate, presumably because they had partially lost contact inhibition of growth.

Conditioned Medium from HAS3-TSU Stimulated the Proliferation and Migration of Endothelial Cells. Because several studies (27–29) reported that hyaluronan can modulate angiogenesis, we examined the effects of conditioned medium from HAS3-TSU cells on the behavior of cultured endothelial cells. When conditioned medium from HAS3-TSU cells was added to the medium of ABAE cells, it stimulated their proliferation by 66% as compared with that from vector-TSU cells (Fig. 5*A*). Furthermore, conditioned medium from the HAS3-TSU also stimulated the migration of ABAE cells through

[4] Unpublished data.

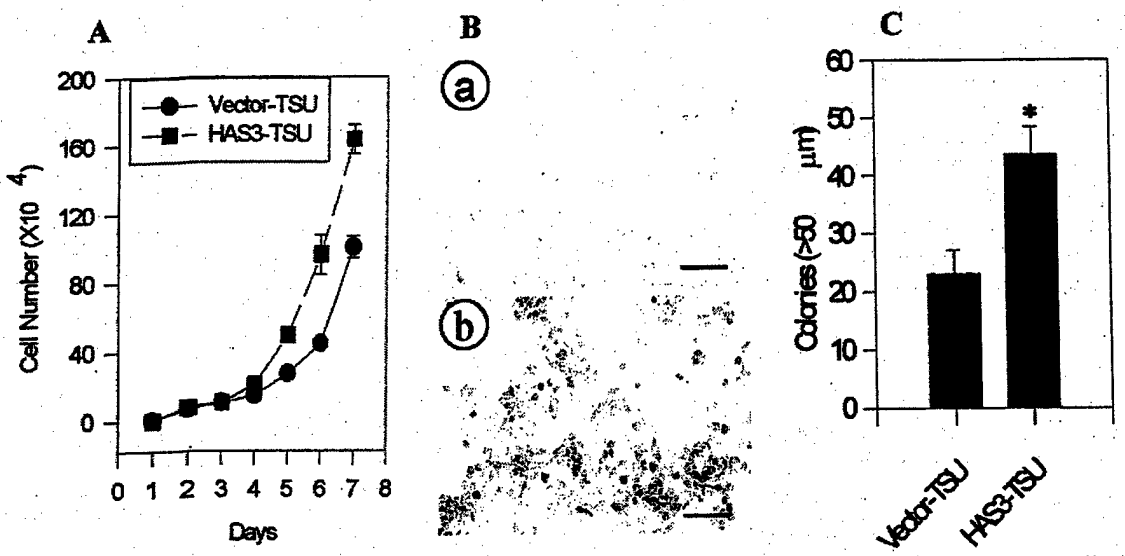

Fig. 4. *In vitro* growth pattern of vector-TSU and HAS3-TSU cells. *A*, cell growth curves for the transfected TSU cells are shown. The cells were plated in 24-well dishes, and the cell number was determined at the indicated times. Although the rate of cell growth was the same at low densities, at higher densities, the HAS3-TSU cells grew faster than the vector-TSU cells. Three independent experiments yielded similar results. *B*, transfected cells at high density were stained for hyaluronan. The transfected cells were grown to confluence, briefly fixed in formaldehyde, and stained for hyaluronan with b-HABP, followed by peroxidase-labeled streptavidin and finally a substrate for peroxidase that gives a red color. The vector-TSU cells (*part a*) formed a confluent monolayer with little hyaluronan staining, whereas the HAS3-TSU cells (*part b*) formed numerous multilayered clusters that stain for hyaluronan (*bar*, 100 μm). *C*, anchorage-independent growth of the transfected cells is shown. Equal numbers of vector-TSU and HAS3-TSU cells were cultured in soft agar for 2 weeks, and the number of colonies were counted with Omnicon Image Analysis system. The HAS3-TSU cells formed a greater number of colonies larger than 50 μm than did the vector-TSU cells (*, $P < 0.05$). This experiment was performed in triplicate.

nucleopore filters by more than 300% as compared with conditioned medium from control cells (Fig. 5*B*). These results further suggest that the hyaluronan produced by HAS3-TSU cells could exert a stimulatory effect on endothelial cells.

The Growth of Transfected Cells on the Chicken Chorioallantoic Membrane. To determine whether the increased growth rate of HAS3-TSU cells *in vitro* also occurred *in vivo*, we examined their growth on the chorioallantoic membranes of chicken eggs. In this experiment, equal numbers of vector-TSU and HAS3-TSU cells were placed on the chorioallantoic membranes of 10-day-old chicken embryos and allowed to grow for 5 days. The xenografts showed a striking divergence in morphology. The vector-TSU cells formed rounded, nodular xenografts that grew out of the membrane surface, with necrotic tissue in the center, whereas the HAS3-TSU cells gave rise to xenografts with a dispersed morphology within the membrane and without any obvious signs of necrosis. As shown in Fig. 6, *A* and *B*, the HAS3-TSU xenografts were significantly larger than those of the vector-TSU cells. Histological examination of the xenografts revealed that, whereas the vector-TSU cells were compact, the HAS3-TSU cells were more dispersed with increased intercellular spaces (data not shown). These results suggested that overexpression of hyaluronan enhanced the tumor growth on the chorioallantoic membrane system.

HAS3 Promotes the Primary Growth of TSU Cells but Not Metastasis in Nude Mice. The *in vivo* growth characteristics of these cells were further examined by injecting them s.c. into nude mice. After 2 weeks, the xenografts formed by HAS3-TSU cells grew at a faster rate and appeared to be more vascularized than the control cells. After 3 weeks of growth, the HAS-3 xenografts were three times larger than those formed by the vector-TSU cells (Fig. 7, *A* and *B*), suggesting that HAS3 promotes the growth of TSU tumor cells in mice. These results are consistent with those obtained from the chicken chorioallantoic membrane system.

However, when transfected cells were injected into the tail veins of nude mice (five mice/group), no lung metastases were detected with either cell type. Thus, the overexpression of hyaluronan by itself is not sufficient to induce metastatic behavior in TSU cells.

Increased Extracellular Hyaluronan and Angiogenesis in HAS3-TSU Xenografts. The xenografts from nude mice were processed for histology, and the resulting sections were stained for hyaluronan (Fig. 8*A*). Although the xenografts varied from region to region, in general, the cells in the vector-TSU xenografts were relatively homogeneous and compact, and most of the hyaluronan appeared to be present in the cytoplasm of the cells (Fig. 8*A*). In contrast, the HAS3-TSU cells formed small clusters or nests of cells that were

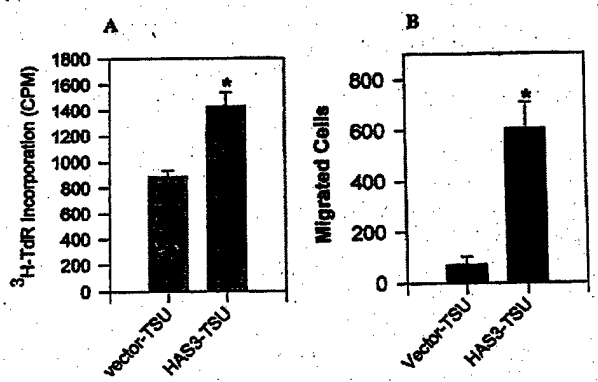

Fig. 5. Effect of conditioned media from vector-TSU and HAS3-TSU cells on endothelial cells. *A*, effects of conditioned media on the proliferation of endothelial cell are demonstrated. ABAE cells were cultured for 36 h in the presence of conditioned media from either vector-TSU or HAS3-TSU cells, pulsed with [^{3}H]thymidine for 8 h, harvested, and processed for incorporated radioactivity. The conditioned media from HAS3-TSU cells stimulated the ABAE cells to a greater extent than that from vector-TSU cells. *B*, effects of conditioned medium on the migration of endothelial cells is shown. Aliquots containing 5×10^3 ABAE cells were added to bottom wells of a 48-well Boyden chamber, covered with a nucleopore membrane, and then treated with 50 μl of conditioned medium for 2 h. The membrane was stained with Hema 3 and placed on a slide, and the migrated cells were counted in 10 random fields. Conditioned medium from HAS3-TSU cells significantly increased the migration of the endothelial cells as compared with that from the vector-TSU cells ($P < 0.05$).

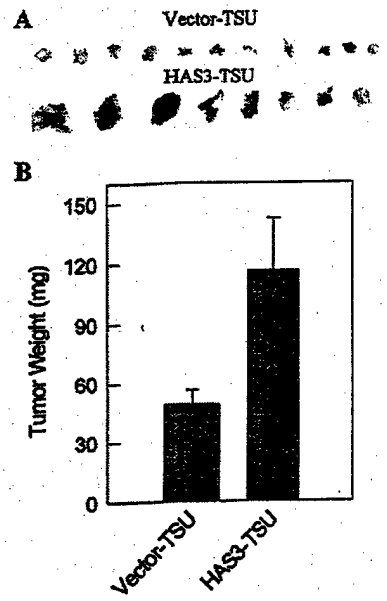

Fig. 6. Growth of transfected TSU cells on the chicken chorioallantoic membrane. Samples of vector-TSU and HAS3-TSU cells (2×10^6 cells) were placed on the chorioallantoic membranes of 10-day-old chicken embryos (15 eggs/group), incubated at 37°C for 5 days, and then photographed. *A*, the xenografts of vector-TSU cells (*top row*) and HAS3-TSU cells (*bottom row*) from the chorioallantoic membrane are shown. The vector-TSU xenografts formed compact nodules, whereas the HAS3-TSU xenografts were more spread out and larger. *B*, the weights of the HAS3-TSU xenografts were significantly greater than that of the vector-TSU cells ($P < 0.05$).

surrounded by a matrix rich in hyaluronan (Fig. 8*A*). Such structures were not observed in the control-TSU xenografts.

The extent of angiogenesis in these xenografts was examined by staining for mouse endothelial cells using antibodies to CD31. Fig. 8*B* shows that there was strong positive staining in HAS3-TSU xenografts as compared with the control vector-TSU xenografts. The number of vessels in 10–15 random fields was significantly higher in the HAS3-TSU xenografts than in the control xenografts (Fig. 8*C*). This suggests that increased levels of hyaluronan can stimulate angiogenesis in mice, and this may, in part, account for the faster growth rate of tumors formed by HAS3-TSU cells.

DISCUSSION

In this study, we have characterized human HAS3 with regard to both its structure and its function in tumor progression. On the basis of its deduced amino acid sequence, HAS3 shares significant homology with HAS1 and HAS2, containing a signal peptide as well as six transmembrane regions strongly suggesting that it is associated with the plasma membrane. Its enzymatic activity was demonstrated by the fact that TSU cells transfected with expression vectors for HAS3 produced larger amounts of hyaluronan as determined by histochemical staining, dot blot analysis, and quantitative ELISA. These findings are consistent with earlier studies of HAS proteins (12–19).

This study also suggested that stimulation of hyaluronan synthesis in TSU cells by transfecting them with HAS3 expression vectors enhanced their growth both in chicken embryos and in nude mice. This enhanced tumor growth appeared to be attributable to two distinct mechanisms. The first involved a direct effect on the tumor cells themselves, as indicated by the fact that in tissue culture, HAS3-transfected cells grew at a faster rate at high density. The second mechanism promoting tumor growth rate resulted from an increase in vascularization, as reflected by the greater density of blood vessels in xenografts from nude mice. Together, these two factors contribute to the increased tumor growth rate.

At present, we believe that the effects of HAS3 transfection on TSU cell phenotype are a direct consequence of increased hyaluronan synthesis. Along these lines, it is important to note that HAS3 overexpression increases the production of both secreted and cell-associated hyaluronan. These two pools of hyaluronan may have different effects on cell behavior. This was suggested by preliminary experiments in which we found that the addition of high molecular weight hyaluronan to cultures of vector-TSU or HAS3-TSU cells had no obvious effect on their growth rates (data not shown). We believe that under these specific conditions, free hyaluronan of high molecular weight did not affect the behavior of these cells. Rather, we believe that it was the cell-associated fraction of hyaluronan induced by HAS3 that played a more important role in stimulating cell growth. However, we cannot eliminate the possibility that hyaluronan of the appropriate size and concentration may indeed influence the behavior of TSU cells, similar to the effects that it has on endothelial cells (27, 28). It is also possible that HAS3 may have effects on the TSU cells independent of its function to promote hyaluronan synthesis; *e.g.*, HAS3 could influence the interaction of the plasma membrane with elements of the cytoskeleton and thereby alter cell behavior.

The hyaluronan on the surface of cultured cells can form a pericellular coat that can be directly visualized by its ability to exclude small particles such as erythrocytes (30). In the case of rat fibrosarcoma cells, this coat is composed of small, microvilli-like projections that extend out from the surface of the cells to which the hyaluronan is attached (31). This pericellular coat could stimulate the growth of cells by several different mechanisms. One possible mechanism is that it disrupts intercellular junctions and thereby allows the cells to detach from the substrate so that they can divide and occupy new space (32–34). This would allow cells to overcome contact inhibition of growth that is characteristic of TSU cells and allow them to from multilayers at high-density cultures as we have observed. Another possibility is that the hyaluronan interacts with receptors on the surfaces of cells such as CD44 or RHAMM to influence their migratory and proliferative behavior (35, 36).

Extracellular hyaluronan can also stimulate cell proliferation by

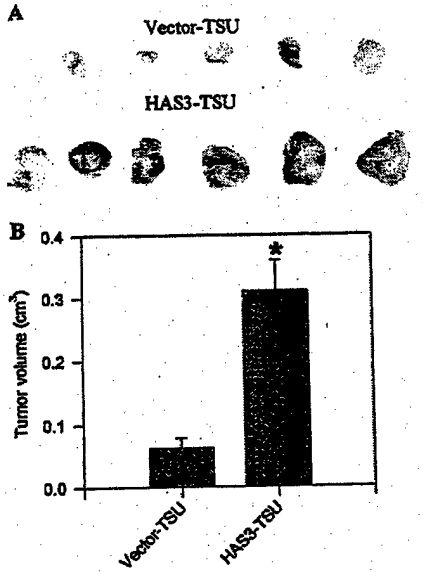

Fig. 7. Xenografts formed by transfected TSU cells in nude mice. *A*, the appearance of xenografts formed in nude mice is shown. Mice received injections of 2×10^6 vector-TSU cells (*top*) or HAS3-TSU cells (*bottom*), and the xenografts were harvested 21 days later. The HAS3-TSU xenografts were larger than those of the vector-TSU cells. *B*, the weights of the HAS3-TSU xenografts were significantly greater than that of the vector-TSU ($P < 0.05$).

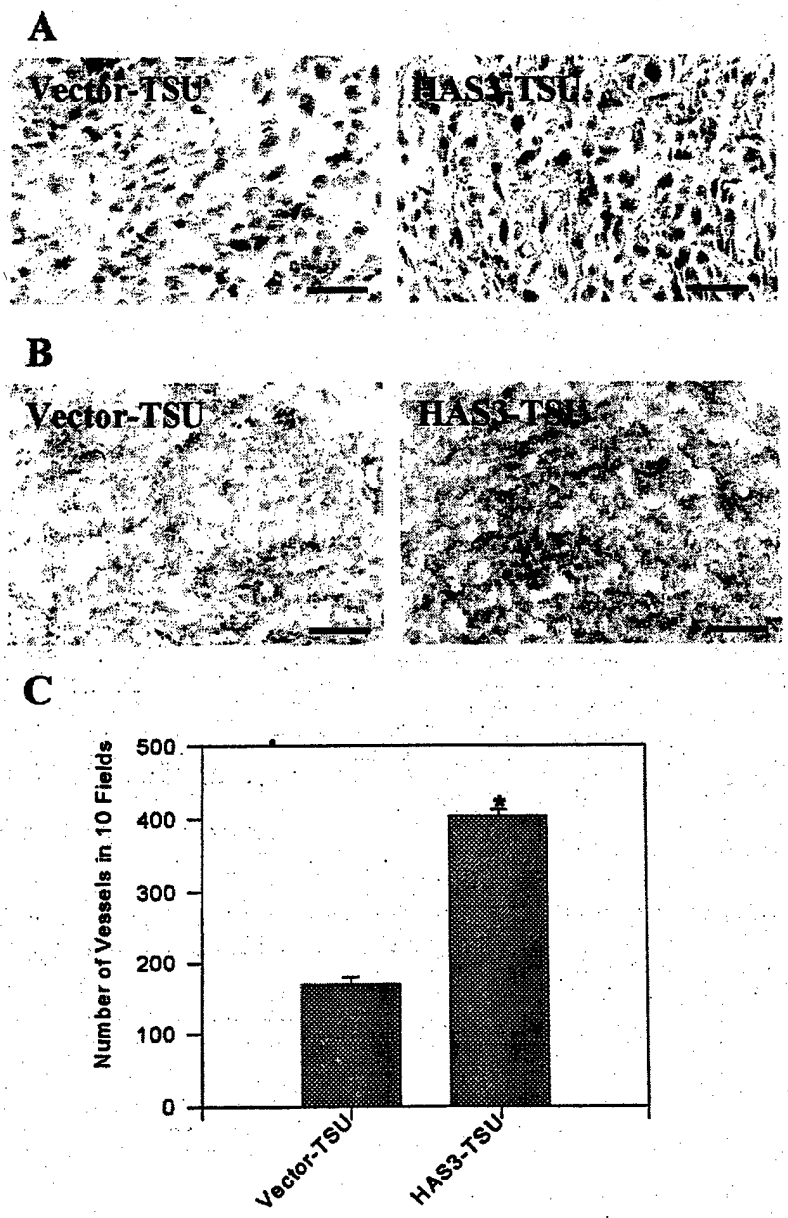

Fig. 8. Staining of xenografts for hyaluronan and endothelial cells. *A*, paraffin sections of vector-TSU and HAS3-TSU xenografts from nude mice were stained for hyaluronan (*red*) and counter-stained with hematoxylin (*blue*). A representative section of a vector-TSU xenograft shows that most of the hyaluronan staining was associated with the cytoplasm of the cells, whereas in a similar section from a HAS3-TSU xenograft, the cells were present in small clusters, surrounded by a stroma rich in hyaluronan. Although the microscopic morphology of the xenografts varied from region to region, the hyaluronan-rich stroma was prevalent in the HAS3-TSU xenografts and absent from the vector-TSU xenografts. *Bar*, 50 μm. *B*, cryostat sections of the xenografts were stained for endothelial cells using an antibody against mouse CD31. Representative fields show that xenografts formed from HAS3-TSU cells have a higher concentration of endothelial cells than those from vector-TSU cells. *Bar*, 100 μm. *C*, the number of blood vessels in 10 random fields from three samples of each group are shown. The HAS3-TSU xenografts had a significantly higher concentration of blood vessels than that of the vector-TSU cells ($P < 0.05$).

increasing the flow of nutrients. Indeed, the extracellular hyaluronan apparent in xenografts of HAS3-TSU cells in nude mice could serve as conduits through which nutrients diffuse to support cells located some distance from the blood supply and thus facilitate their growth. In the xenografts of vector-TSU cells that lacked these hyaluronan rich spaces, the tumor cells formed a continuous mass and were more susceptible to necrosis. Along these lines, extracellular hyaluronan is prominent in the lower regions of most, if not all, stratified epithelium, where it is believed to maintain spaces so that nutrients can diffuse to the more superficial epithelial cells (37, 38).

Hyaluronan also appeared to promote vascularization that is clearly important in regulating tumor growth (39, 40). This was indicated by our observation that xenografts of HAS3-TSU cells formed in nude mice had a greater density of blood vessels than did control xenografts. Part of this increased vascularization may be attributable to the pericellular spaces generated by the hyaluronan that provides space that facilitates the invasion of endothelial cells. In addition, the hyaluronan itself can stimulate the migration of endothelial cells. This was also indirectly suggested by experiments showing that conditioned media from the HAS3-transfected cells stimulated the growth and migration of cultured endothelial cells. This is consistent with the earlier studies of West *et al.* (27, 28) who have shown that oligosaccharide fragments of hyaluronan stimulated the formation of new blood vessels in the chorioallantoic membrane of chicken embryos.

Although the results of this study suggest that overexpression of HAS3 in TSU prostate cancer cells promotes their tumorigenicity, there are some aspects that appear to contradict the findings of other studies; *e.g.*, although we found that TSU transfectants grew faster in culture, Kosaki *et al.* (20) found no such increase in the growth of HT1080 cells transfected with HAS2 under anchorage-dependent conditions; however, these cells did form larger colonies in suspension culture. We believe that this difference may be attributable in part to the different target cells that were used in these studies. The TSU cells used as targets in this study are of epithelial origin, whereas HT1080 cells are derived from a fibrosarcoma of connective tissue cells. This could also account for the differences seen with regard to growth behavior and the production of hyaluronan in the connective tissue and their ability to stimulate angiogenesis. Alternatively, the

differences could be attributed to the characteristics of the particular HASs that were used in these studies, because they differ with respect to both their synthetic activity as well as the size of the hyaluronan that they produce (16–18).

Another apparent discrepancy was our observation that transfection of TSU cells with HAS3 did not appear to stimulate their ability to form lung metastases in nude mice. In contrast, we had reported previously (3) that the levels of hyaluronan on the surface of B16 cells were directly correlated with their metastatic behavior. Similarly, Itano *et al.* (21) found that transfection of FM3A with HAS1 enhanced their metastatic properties. Again, we believe that these divergent results were attributable to the different cell types that were used as targets for transfection. In the case of B16 and FM3A, these cell lines originally possessed the ability to undergo metastasis, and stimulation of hyaluronan synthesis in these cells enhanced this innate property. In contrast, TSU cells appeared to lack this ability (at least in nude mice), and increased hyaluronan synthesis, by itself, is not sufficient to promote metastatic properties. Clearly, the process of metastasis is a complex phenomenon involving the collaboration of many molecules. Although the production of hyaluronan is one of the factors, it is not sufficient for tumor metastasis in the case of TSU cells.

In conclusion, the results of this study indicate that HAS3 expression plays a role in tumor progression and are consistent with earlier studies demonstrating a correlation between hyaluronan levels and tumorigenicity. Furthermore, the hyaluronan may be acting through several different mechanisms, including: (*a*) a direct effect on the growth of the tumor cells themselves; (*b*) the formation of extracellular conduits through which nutrients can flow; and (*c*) the stimulation of blood vessel growth. However, these effects depend upon the particular cell type and the specific environment. Given the complexity of the effects of hyaluronan, it may be difficult to predict exactly how it will influence the behavior of tumor cells. In the case of TSU cells, hyaluronan may be more of a facilitator of tumor growth rather than an instigator of metastasis.

REFERENCES

1. Toole, B. P., Biswas, C., and Gross, J. Hyaluronate and invasiveness of the rabbit V2 carcinoma. Proc. Natl. Acad. Sci. USA, *76:* 6299–6303, 1979.
2. Kimata, K., Honma, Y., Okayama, M., Oguri, K., Hozumi, M., and Suzuki, S. Increased synthesis of hyaluronic acid by mouse mammary carcinoma cell variants with high metastatic potential. Cancer Res., *43:* 1347–1354, 1983.
3. Zhang, L., Underhill, C. B., and Chen, L. Hyaluronan on the surface of tumor cells is correlated with metastatic behavior. Cancer Res., *55:* 428–433, 1995.
4. Marotta, M., D'Armiento, F. P., Martino, G., Donato, G., Nazzaro, A., Vecchione, R., and Rosati, P. Glycosaminoglycans in human breast cancer: morphological and biochemical study. Appl. Pathol., *3:* 164–169, 1985.
5. Coppes, M. J. Serum biological markers and paraneoplastic syndromes in Wilm's tumor. Med. Pediatr. Oncol., *21:* 213–221, 1993.
6. Horai, T., Nakamura, N., Tateshi, R., and Hattori, S. Glycosaminoglycans in human lung cancer. Cancer (Phila.), *48:* 2016–2021, 1981.
7. Roboz, J., Greaves, J., Silides, D., Chahinian, A. P., and Holland, J. F. Hyaluronic acid content of effusions as a diagnostic aid for malignant mesothelioma. Cancer Res., *45:* 1850–1854, 1985.
8. Kojima, J., Nakamura, N., Kanatani, M., and Omori, K. The glycosaminoglycans in human hepatic cancer. Cancer Res., *35:* 542–547, 1975.
9. Azumi, N., Underhill, C. B., Kagan, E., and Sheibani, K. A novel biotinylated probe specific for hyaluronate: its diagnostic value in diffuse malignant mesothelioma. Am. J. Surg. Pathol., *16:* 116–121, 1992.
10. Dahl, I. M. S., and Laurent, T. C. Concentration of hyaluronan in serum of untreated cancer patients reference to patients with mesothelioma. Cancer (Phila.), *62:* 326–330, 1988.
11. Frebourg, T., Lerebours, G., Delpech, B., Benhamou, D., Bertrand, P., Maingonnat, C., Boutin, C., and Nouvet, G. Serum hyaluronate in malignant pleural mesothelioma. Cancer (Phila.), *59:* 2104–2107, 1987.
12. Shyjan, A. M., Heldin, P., Butcher, E. C., Yoshino, T., and Briskin, M. J. Functional cloning of the cDNA for a human hyaluronan synthase. J. Biol. Chem., *271:* 23395–23399, 1996.
13. Watanabe, K., and Yamaguchi, Y. Molecular identification of a putative human hyaluronan synthase. J. Biol. Chem., *271:* 22945–22948, 1996.
14. Itano, N., and Kimata, K. Molecular cloning of human hyaluronan synthase. Biochem. Biophys. Res. Commun., *222:* 816–820, 1996.
15. Itano, N., and Kimata, K. Expression cloning and molecular characterization of HAS protein, a eukaryotic hyaluronan synthase. J. Biol. Chem., *271:* 9875–9878, 1996.
16. Spicer, A. P., Olson, J. S., and McDonald, J. A. Molecular cloning and characterization of a cDNA encoding the third putative mammalian hyaluronan synthase. J. Biol. Chem., *272:* 8957–9861, 1997.
17. Spicer, A. P., and McDonald, J. A. Characterization and molecular evolution of a vertebrate hyaluronan synthase gene family. J. Biol. Chem., *273:* 1923–1932, 1998.
18. Spicer, A. P., and Nguyen, T. K. Mammalian hyaluronan synthases: investigation of functional relationships *in vivo*. Biochem. Soc. Trans., *27:* 109–115, 1999.
19. Itano, N., Sawai, T., Yoshida, M., Lenas, P., Yamada, Y., Imagawa, M., Shinomura, T., Hamaguchi, M., Yoshida, Y., Ohnuki, Y., Miyauchi, S., Spicer, A. P., McDonald, J. A., and Kimata, K. Three isoforms of mammalian hyaluronan synthases have distinct enzymatic properties. J. Biol. Chem., *274:* 25085–25092, 1999.
20. Kosaki, R., Watanabe, K., and Yamaguchi, Y. Overproduction of hyaluronan by expression of the hyaluronan synthase Has2 enhances anchorage-independent growth and tumorigenicity. Cancer Res., *59:* 1141–1145, 1999.
21. Itano, N., Sawai, T., Miyaishi, O., and Kimata, K. Relationship between hyaluronan production and metastatic potential of mouse mammary carcinoma cells. Cancer Res., *59:* 2499–2504, 1999.
22. Chen, C., and Okayama, H. High-efficiency transformation of mammalian cells by plasmid DNA. Mol. Cell. Biol., *7:* 2745–2752, 1987.
23. Underhill, C. B., and Zhang, L. Analysis of hyaluronan using biotinylated hyaluronan-binding proteins. Methods Mol. Biol., *137:* 441–447, 1999.
24. Culty, M., Shizari, M., Nguyen, H. A., Clarke, R., Thompson, E. W., and Underhill, C. B. Degradation of hyaluronan and expression of CD44 by human breast cancer cell lines correlate with their invasive potential. J. Cell. Physiol., *160:* 275–286, 1994.
25. Falk, W., Goodwin, R. H., and Leonard, E. J. A 48-well micro chemotaxis assembly for rapid and accurate measurement of leukocyte migration. J. Immunol. Methods, *33:* 239–247, 1980.
26. Yang, B., Yang, B. L., Savani, R. C., and Turley, E. A. Identification of a common hyaluronan binding motif in the hyaluronan binding proteins RHAMM, CD44 and link protein. EMBO J., *13:* 286–296, 1994.
27. West, D. C., Hampson, I. N., Arnold, F., and Kumar, S. Angiogenesis induced by degradation products of hyaluronic acid. Science (Wash. DC), *228:* 1324–1326, 1985.
28. West, D. C., and Kumar, S. The effect of hyaluronate and its oligosaccharides on endothelial cell proliferation and monolayer integrity. Exp. Cell Res., *183:* 179–196, 1989.
29. Feinberg, R. N., and D. C. Beebe. Hyaluronate in vasculogenesis. Science (Wash. DC), *220:* 1177–1179, 1983.
30. Underhill, C. B., and Toole, B. P. Transformation-dependent loss of the hyaluronate-containing coats of cultured cells. J. Cell. Physiol., *110:* 123–128, 1982.
31. Koshiishi, I., Shizari, M., and Underhill, C. B. CD44 mediates the adhesion of platelets to hyaluronan. Blood, *84:* 390–396, 1994.
32. Brecht, M., Mayer, U., Schlosser, E., and Prehm, P. Increased hyaluronate synthesis is required for fibroblast detachment and mitosis. Biochem. J., *239:* 445–450, 1986.
33. Lark, M. W., and Culp, L. A. Selective solubilization of hyaluronic acid from fibroblast substratum adhesive sites. J. Biol. Chem., *257:* 14073–14080, 1982.
34. Abatangelo, G., Cortivo, R., Martelli, M., and Vecchia, P. Cell detachment mediated by hyaluronic acid. Exp. Cell Res., *137:* 73–78, 1982.
35. Zhang, S., Chang, M. C., Zylka, D., Turley, S., Harrison, R., and Turley, E. A. The hyaluronan receptor RHAMM regulates extracellular-regulated kinase. J. Biol. Chem., *273:* 11342–11348, 1998.
36. Bourguignon, L. Y., Shu, H., Shao, L., and Chen, Y. W. CD44 interaction with Tiam1 promotes Rac1 signaling and hyaluronic acid-mediated breast tumor migration. J. Biol. Chem., *275:* 1829–1338, 2000.
37. Alho, A. M., and Underhill, C. B. The hyaluronate receptor is preferentially expressed on proliferating epithelial cells. J. Cell Biol., *108:* 1557–1565, 1989.
38. Underhill, C. B. The interaction of hyaluronate with the cell surface: the hyaluronate receptor and the core protein. Ciba Found. Symp., *143:* 87–106, 1989.
39. Folkman, J. New perspectives in clinical oncology from angiogenesis research. Eur. J. Cancer, *32:* 2534–2539, 1996.
40. Folkman, J., and D'Amore, P. A. Blood vessel formation: what is its molecular basis? Cell, *87:* 1153–1155, 1996.

[CANCER RESEARCH 61, 1022–1028, February 1, 2001]

Metastatin: A Hyaluronan-binding Complex from Cartilage That Inhibits Tumor Growth[1]

Ningfei Liu,[2] Randall K. Lapcevich,[2] Charles B. Underhill, Zeqiu Han, Feng Gao, Glenn Swartz, Stacy M. Plum, Lurong Zhang,[2] and Shawn J. Green[2, 3]

Department of Oncology, Georgetown University Medical Center, Washington, D.C. 20007 [N. L., C. B. U., Z. H., F. G., L. Z.], and EntreMed, Inc., Rockville, Maryland 20902 [R. K. L., G. S., S. M. P., S. J. G.]

ABSTRACT

In this study, a hyaluronan-binding complex, which we termed Metastatin, was isolated from bovine cartilage by affinity chromatography and found to have both antitumorigenic and antiangiogenic properties. Metastatin was able to block the formation of tumor nodules in the lungs of mice inoculated with B16BL6 melanoma or Lewis lung carcinoma cells. Single i.v. administration of Metastatin into chicken embryos inhibited the growth of both B16BL6 mouse melanoma and TSU human prostate cancer cells growing on the chorioallantoic membrane. The *in vivo* biological effect may be attributed to the antiangiogenic activity because Metastatin is able to inhibit the migration and proliferation of cultured endothelial cells as well as vascular endothelial growth factor-induced angiogenesis on the chorioallantoic membrane. In each case, the effect could be blocked by either heat denaturing the Metastatin or premixing it with hyaluronan, suggesting that its activity critically depends on its ability to bind hyaluronan on the target cells. Collectively, these results suggest that Metastatin is an effective antitumor agent that exhibits antiangiogenic activity.

INTRODUCTION

A potential therapeutic target on angiogenic endothelial cells is hyaluronan, a large negatively charged glycosaminoglycan that plays a role in the formation of new blood vessels (1). Particularly high concentrations of hyaluronan are associated with endothelial cells at the growing tips or sprouts of newly forming capillaries (2, 3). Similarly, when cultured endothelial cells are stimulated to proliferate by cytokines, their synthesis of hyaluronan is significantly increased (4). Interestingly, this stimulation is restricted to endothelial cells derived from the small blood vessels and is not seen in endothelial cells derived from larger ones (4). In the case of mature blood vessels, hyaluronan is present in perivascular regions and in the junctions between the endothelial cells (5, 6). Earlier studies have shown that exogenously applied hyaluronan has different effects on angiogenesis depending on its size, with macromolecular hyaluronan inhibiting vascularization in chicken embryos, and oligosaccharide fragments of hyaluronan stimulating vascularization in the chorioallantoic membrane (7–9). Thus, hyaluronan appears to be specifically associated with the endothelial cells of newly forming blood vessels and can influence their behavior.

In addition to hyaluronan, endothelial cells involved in neovascularization also express CD44 and other cell surface receptors for hyaluronan (10–12). In particular, endothelial cells associated with tumors express large amounts of CD44 (11). In previous studies, we have shown that CD44 allows cells to bind hyaluronan so that it can be internalized into endosomal compartments, where the hyaluronan is degraded by the action of acid hydrolases (13, 14). Thus, the expression of CD44 by endothelial cells allows them to bind and internalize hyaluronan as well as any associated proteins. The fact that both hyaluronan and CD44 are up-regulated in endothelial cells involved in neovascularization suggests that the turnover of hyaluronan by these cells is much greater than that by cells lining mature blood vessels.

The increased turnover of hyaluronan in tumor-associated endothelial cells suggested a possible mechanism to specifically target these cells. Our initial idea was to use a hyaluronan-binding complex isolated from cartilage to deliver chemotherapeutic agents specifically to these endothelial cells. Purified by affinity chromatography, this hyaluronan-binding complex consists of tryptic fragments of the link protein and aggrecan core protein (5, 15, 16). We intended to couple the hyaluronan-binding complex to a chemotherapeutic agent such as methotrexate and use this derivative to attack endothelial cells. We hoped that this derivative would bind to the hyaluronan on the endothelial cells and then be internalized into lysosomes, where the methotrexate would be released by the action of acid hydrolyses. Surprisingly, however, in the course of these experiments, we found that the hyaluronan-binding complex by itself (*i.e.*, in the absence of a chemotherapeutic agent) inhibited angiogenic activity. Functionally, we termed the hyaluronan-binding complex, which inhibits tumor growth, Metastatin.

In the present study, we demonstrate that Metastatin has a number of intriguing biological activities, including inhibition of endothelial cell proliferation and migration, inhibition of angiogenesis, and suppression of tumor cell growth in chicken embryos and pulmonary metastasis in mice. These effects are blocked by preincubating Metastatin with hyaluronan, suggesting that the activity of Metastatin depends on its ability to bind hyaluronan on the target cells.

MATERIALS AND METHODS

Preparation of Metastatin. The hyaluronan-binding complex was prepared by a modified version of the method originally described by Tengblad (15, 16). Briefly, bovine nasal cartilage (Pel-Freez, Rogers, AR) was shredded with a Sure-Form blade (Stanley), extracted overnight with 4 M guanidine-HCl and 0.5 M sodium acetate (pH 5.8), and dialyzed against distilled water to which 10× PBS was added to a final concentration of 1× PBS (pH 7.4). The protein concentration was measured, and for each 375 mg of protein, 1 mg of trypsin (type III; Sigma, St. Louis, MO) was added. After digestion for 2 h at 37°C, the reaction was terminated by the addition of 2 mg of soybean trypsin inhibitor (Sigma) for each milligram of trypsin. The digest was dialyzed against 4 M guanidine-HCl and 0.5 M acetate (pH 5.8), mixed with hyaluronan coupled to Sepharose, and then dialyzed against a 10-fold volume of distilled water. The hyaluronan-Sepharose beads were placed into a chromatography column and washed with 1.0 M NaCl, followed by a gradient of 1.0–3.0 M NaCl. Metastatin was eluted from the hyaluronan affinity column with 4 M guanidine-HCl and 0.5 M sodium acetate (pH 5.8), dialyzed against saline, and sterilized by passage through a 0.2-μm-pore filter. For SDS-PAGE analysis, the purified preparation was loaded onto a 10% BisTris nonreducing gel (Novex, Inc.) and subsequently stained with Coomassie Blue. To identify the

Received 7/12/00; accepted 11/28/00.

The costs of publication of this article were defrayed in part by the payment of page charges. This article must therefore be hereby marked *advertisement* in accordance with 18 U.S.C. Section 1734 solely to indicate this fact.

[1] Supported in part by the United States Army Medical Research and Materiel Command under DAMD1717-94-J-4284, DAMD17-98-1-8099, and DAMD17-99-1-9031. Additional support was obtained from the Susan G. Komen Foundation and NIH Grant R29CA71545.

[2] These authors contributed equally to this work.

[3] To whom requests for reprints should be addressed, at EntreMed, Inc., Medical Center Drive, Suite 200, Rockville, MD 20902. Phone: (301) 738-2494; Fax (301) 217-9594; E-mail shawng@entremed.com.

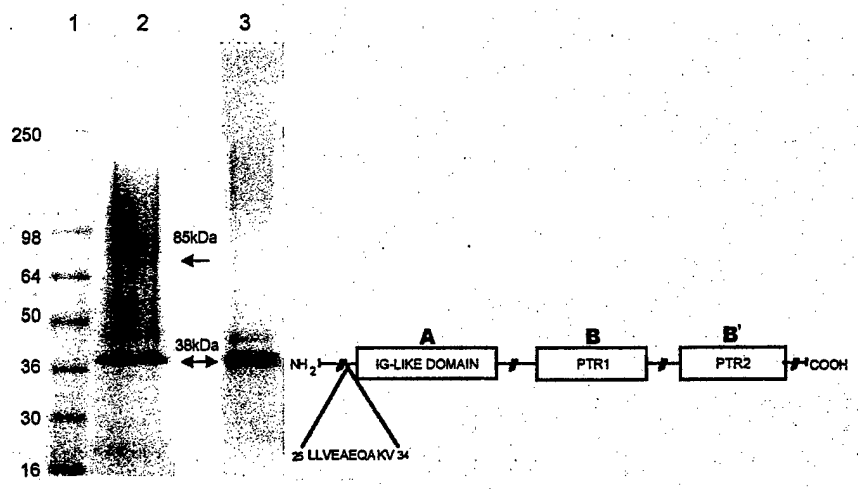

Fig. 1. SDS-PAGE and NH_2-terminal analysis of Metastatin. *Lane 1*, molecular mass markers; *Lane 2*, Metastatin stained with Coomassie blue; *Lane 3*, Western blot of Metastatin immunostained with an antibody against the link protein. The fragment of aggrecan migrated as a diffuse band at ~85 kDa, whereas the truncated link protein was at 38 kDa. NH_2-terminal sequence analysis of the 38-kDa band indicated that the first 24 amino acids of the link protein have been cleaved and is indicated on the schematic diagram.

link protein by Western blotting, the proteins on the gel were transferred to a sheet of nitrocellulose and immunostained with the 9/30/8-A-4 monoclonal antibody. (The monoclonal antibody, developed by Dr. B. Caterson, was obtained from the Developmental Studies Hybridoma Bank under the auspices of the NICHD and maintained by the University of Iowa, Department of Biological Sciences, Iowa City, IA 52242.) This identity was further confirmed by NH_2-terminal sequencing (Fig. 1). In tests of the biological activity of Metastatin, controls consisted of Metastatin mixed with an excess mass of hyaluronan (Lifecore, Chaska, MN) or a heat-inactivated preparation made by placing it in a boiling water bath for 30 min.

Endothelial and Tumor Cell Lines. HUVECs[4] were obtained from the Tumor Bank of the Lombardi Cancer Center (Georgetown University, Washington, DC). ABAEs were kindly provided by Dr. Luyuan Li (Lombardi Cancer Center), and BRECs were provided by Dr. Rosemary Higgins (Pediatrics, Georgetown University). These endothelial cells were cultured in 90% DMEM, 10% fetal bovine serum, and 10 ng/ml bFGF. The B16BL6 melanoma tumor line was obtained from the National Cancer Institute Central Repository (Frederick, MD), TSU cells were obtained from the American Type Culture Collection (Rockville, MD), and Lewis lung carcinoma cells were kindly supplied by Dr. Michael O'Reilly (Children's Hospital, Boston, MA). The tumor cells were grown in 90% DMEM, 10% fetal bovine serum, and 2 mM L-glutamine. For the mouse metastasis assays, cells were generally used between passages 6 and 18.

Mice. Specific pathogen-free, male, 6–8-week-old C57Bl/6 mice were obtained from The Jackson Laboratory (Bar Harbor, ME). Animals were cared for and treated in accordance with the procedures outlined in the Guide for the Care and Use of Laboratory Animals (NIH Publication No. 86-23). Animals were housed in a pathogen-free environment and provided with sterilized animal chow (Harlan Sprague Dawley, Indianapolis, IN) and water *ad libitum*.

Mouse Metastasis Model System. For the experimental melanoma model, mice were inoculated i.v. in the lateral tail vein with B16Bl6 cells (5×10^4 cells/animal) on day 0. Treatment was initiated on day 3 with 5 (0.2 mg/kg), 15 (0.6 mg/kg), and 49 μg (2 mg/kg) of Metastatin and continued daily until animals were sacrificed on day 14. After euthanasia, the lungs were removed, and surface metastatic lesions were enumerated under a dissecting microscope.

Mice were also inoculated with Lewis lung carcinoma cells, which aggressively form pulmonary metastases. Mice were injected i.v. in the lateral tail vein with 2.5×10^5 cells/animal (day 0), and beginning on day 3, the Metastatin was administered by daily i.p. injections of 15 (0.6 mg/kg) and 49 μg (2 mg/kg) or by three i.v. injections of 100 μg (4 mg/kg) on days 1, 3, and 5. Animals were euthanized, and their lungs were removed and weighed. To obtain the lung weight gain, the average lung weight of nontreated mice (0.2 g) was subtracted from that of the treated animals.

The number of pulmonary metastases and lung weight gains were reported as mean ± SD, and the differences were compared using Student's *t* test. The groups were considered to be different when the probability (*P*) value was <0.05.

Chicken Chorioallantoic Membrane Assays. To measure angiogenesis, a chick chorioallantoic membrane assay was performed using a modification of the methods of Brooks *et al.* (17). For this, holes were drilled in the tops of 10-day-old chicken eggs to expose the chorioallantoic membranes, and filter discs (0.5 cm in diameter) containing 20 ng of human recombinant VEGF [20 μl (1 μg/ml); Pepro, Rocky Hill, NJ] were placed on the surface of each chorioallantoic membrane (day 0). The holes were covered with parafilm, and the eggs were incubated at 37°C in a humidified atmosphere. One day later, the eggs were given injections (via a blood vessel in the chorioallantoic membrane using a 30-gauge needle) of the various substances [Metastatin (80 μg/egg) or controls consisting of PBS or heat-inactivated Metastatin]. Three days later (day 4), the chorioallantoic membranes and associated discs were cut out and immediately immersed in 3.7% formaldehyde. For computer-assisted image analysis, the discs were divided into quarters with fine wires, and the blood vessels in each quarter were digitally photographed and analyzed by an Optimas 5 program to calculate the vessel area and length normalized to the total area measured. The means and the SEs were calculated from all quadrants within each group, and the statistical significance was determined by Student's *t* test. Twelve or more eggs were used for each sample point.

For the growth of xenografts on the chorioallantoic membrane, holes were cut into the sides of 10-day-old eggs exposing the membrane (day 0), and then 1×10^6 B16BL6 or TSU cells were applied to the membranes. Two days later, the eggs were given i.v. injections of the various substances. On day 7, the tumor masses were fixed in formalin, dissected free from the normal membrane tissue, and weighed.

Cell Growth Assays. To determine the effects of Metastatin on cell growth, the cell lines were subcultured into 24-well dishes at a density of approximately 5×10^5 cells/well for the endothelial cell lines (HUVEC, ABAE, and BREC) and 5×10^4 cells/well for tumor cell lines (B16BL6, TSU, and Lewis lung carcinoma). For the dose-response experiments, the medium was changed every other day, and at the end of 6 days, the cells were released with 0.5 mM EDTA in PBS, and the cell number was determined with a Coulter counter (Hialeah, FL).

ELISA Assay for Hyaluronan. Cells were grown to confluence in 24-well dishes, and the conditioned medium was collected, incubated with a biotinylated version of the Metastatin (16), and then transferred to plates precoated with hyaluronan (umbilical cord; Sigma). The hyaluronan present in the conditioned medium interacts with the biotinylated Metastatin so that less of it will be left to bind to hyaluronan attached to the plate. At the end of the incubation, the plates were washed, and the amount of biotinylated Metastatin remaining attached was determined by incubating the plates with streptavidin coupled to peroxidase (Kirkegard & Perry, Gaithersburg, MD) followed by a soluble substrate for peroxidase. The amount of hyaluronan in the conditioned medium was calculated by comparison with a standard curve with known amounts of hyaluronan (16).

[4] The abbreviations used are: HUVEC, human umbilical vein endothelial cell; ABAE, adult bovine aorta endothelial cell; BREC, bovine retinal endothelial cell; VEGF, vascular endothelial growth factor; bFGF, basic fibroblast growth factor.

Wound Migration Assay. A suspension of HUVECs (5×10^5 cells in 5 ml of 98% M199 and 2% fetal bovine serum) was added to 60-mm tissue culture plates that had been precoated with gelatin (2 ml of 1.5% gelatin in PBS, 37°C, overnight) and allowed to grow for 3 days to confluence. An artificial "L"-shaped wound was generated in the confluent monolayer with a sterile razor blade by moving the blade down and across the plate. Plates were then washed with PBS, and 2 ml of PBS were added to each plate along with 2 ml of sample in M199 and 2% fetal bovine serum in the presence and absence of 5 ng/ml bFGF. After an overnight incubation, the plates were treated with Diff-Quik for 2 min to fix and stain the cells. The number of cells that migrated were counted under ×200 magnification using a 10-mm micrometer over a 1 cm distance along the wound edge. Ten fields for each plate were counted, and an average for the duplicate was calculated.

RESULTS

Characterization of Metastatin. Metastatin was isolated from bovine nasal cartilage by affinity chromatography on hyaluronan-Sepharose. As shown in Fig. 1, Metastatin consisted of two molecular factions as determined by SDS-PAGE, a sharp band at 38 kDa that corresponds to the link protein, and a diffuse band at approximately 85 kDa that represents a tryptic fragment of the aggrecan core protein (5, 15, 16). The diffuse nature of this latter fraction is probably due to variations in the degree of glycosylation and glycosaminoglycan content. The identity of the link protein was verified by immunoblotting with a specific monoclonal antibody against this protein (Fig. 1). In addition, NH_2-terminal sequence analysis of the 38-kDa band revealed that the purified protein was missing the first 24 amino acids. Previous studies have shown that this complex binds to hyaluronan with high affinity and specificity (5, 16). Indeed, a biotinylated version of the preparation has been widely used as a histochemical stain to localize hyaluronan in tissue sections (5, 16).

Because cartilage is known to contain various protease inhibitors, which may contribute to its antitumor properties (18), we wanted to determine whether Metastatin possessed such attributes. For this reason, we used a chromogenic assay (Diapharma Group, Inc., West Chester, OH) to assess the effect of Metastatin on the following enzymes: (*a*) trypsin; (*b*) chymotrypsin; (*c*) plasmin; and (*d*) elastase. At concentrations as high as 100 μg/ml, Metastatin did not inhibit the activity of any of the enzymes tested (data not shown).

Effect of Metastatin on Metastatic Tumors. In initial experiments, we found that Metastatin was effective at inhibiting pulmonary metastases of B16BL6 cells. When mice were given daily i.p. injections of Metastatin 3 days after tumor inoculation, lung metastases were strikingly reduced (Fig. 2*A*). Fig. 2*B* shows that the number of surface lung metastases (>0.5 mm) in the mice treated with 15 and 49 μg Metastatin/day were reduced by more than 80%. The dose-response curve shown in Fig. 2*C* was constructed from two independent experiments and shows that Metastatin decreased the number of metastatic colonies in a dose-dependent manner with an ED_{50} of approximately 10 μg (0.4 mg/kg). Significantly, when Metastatin preparations were premixed with macromolecular hyaluronan, the antimetastatic activity was blocked, and the mean number of surface pulmonary metastases was comparable to that seen in control mice (Fig. 2*B*). This suggests that the ability of Metastatin to bind hyaluronan is required for its anti-tumor activity.

Similar results were obtained with the Lewis Lung carcinoma cell line, which is a more aggressive mouse tumor model. As shown in Fig. 3. *A* and *B*, Metastatin inhibited pulmonary metastasis of Lewis lung carcinoma cells in a dose-related fashion, as reflected in the weight gain of the lungs. Furthermore, Metastatin was effective when given by two different routes, i.p. and i.v. (Fig. 3, *B* and *C*).

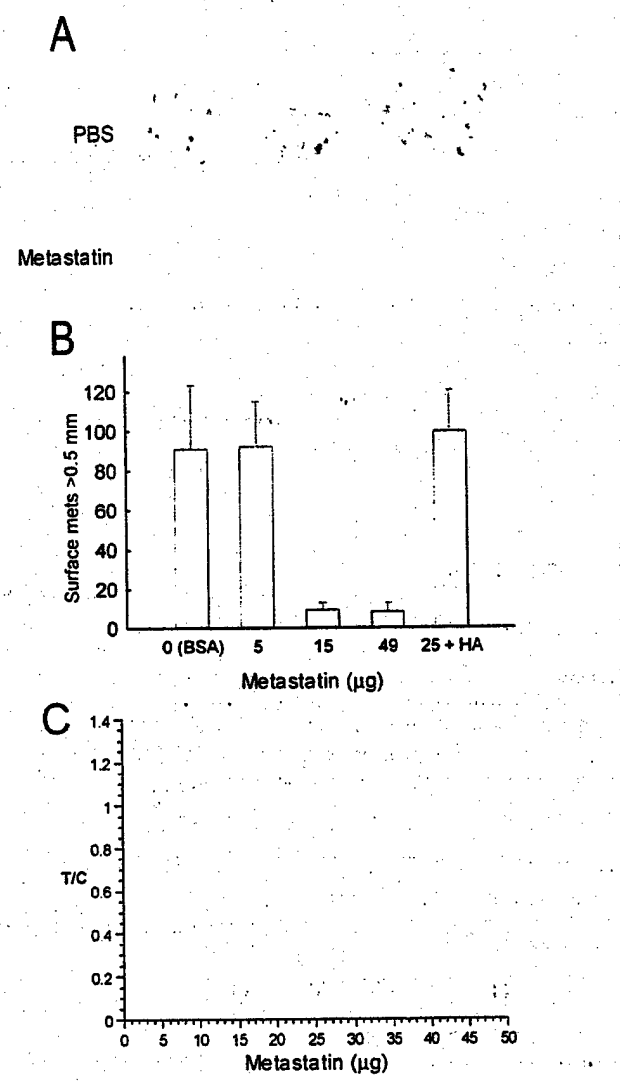

Fig. 2. Effect of Metastatin on B16BL6 melanoma metastasis. B16BL6 melanoma cells were injected into the tail veins of C57Bl/6 mice, and 3 days later, the mice were injected i.p. with increasing doses of Metastatin. After 14 days, the lungs were removed, and surface pulmonary metastases were counted. *A*, the lungs from control animals had a greater number of metastases than those from the Metastatin (49 μg)-treated animals. *B*, the number of pulmonary metastases larger than 0.5 mm is plotted against the concentration of Metastatin injected. Metastatin inhibits the number of metastases, and the addition of hyaluronan to Metastatin blocked its inhibitory activity. The values shown are the mean of at least five mice/group; *bars*, SD. *C*, this dose-response curve was derived from two independent experiments ($n = 5$ for each point) and shows the ratio of pulmonary metastasis in the test and control animals (*T/C*) as a function of the Metastatin dose.

Effect of Metastatin on *in Vitro* Cell Proliferation and Migration. In the next series of experiments, we wanted to determine whether Metastatin has any effect on the growth of either endothelial or tumor cells in tissue culture. For these experiments, the cells were grown in the presence of varying concentrations of Metastatin for 6 days, and then the final cell numbers were determined. Metastatin inhibited the proliferation of the endothelial cell lines HUVEC, ABAE, and BREC (Fig. 4*A*) and two of the tumor cell lines (B16BL6 and Lewis lung carcinoma cells) but had no effect on the TSU cells (Fig. 4*B*). Similar results were obtained when proliferation was monitored by incorporation of bromodeoxyuridine (data not shown). It is important to note that the growth inhibition of B16BL6 cells was partially blocked when the preparation of Metastatin was premixed with an excess of hyaluronan (Fig. 4*B*).

One possible explanation for the lack of TSU cell sensitivity to

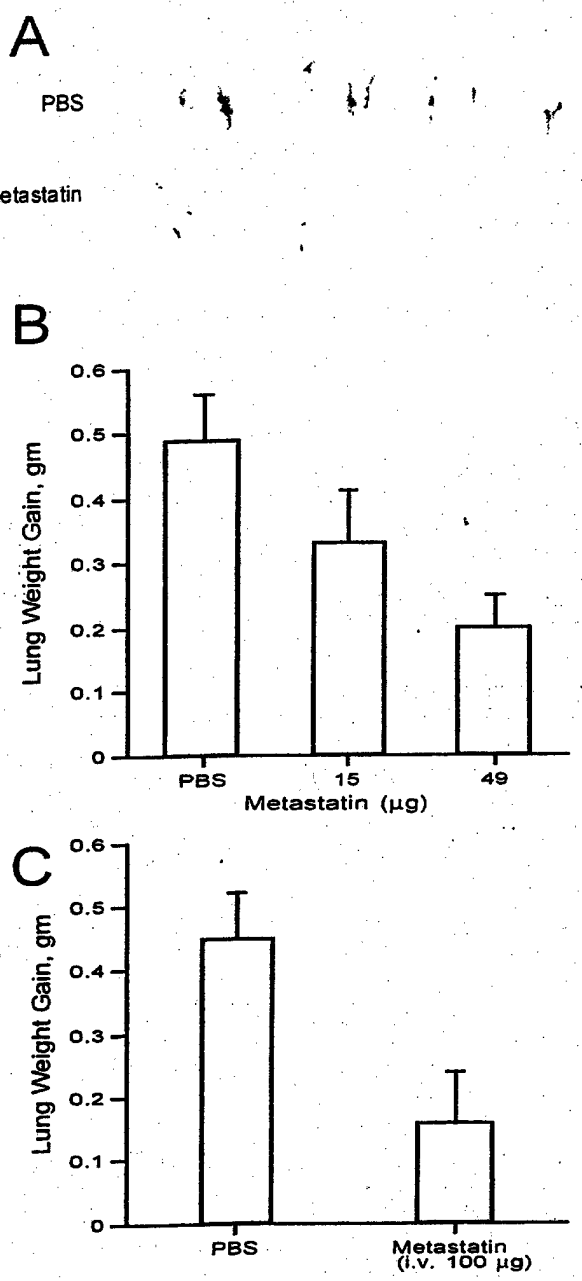

Fig. 3. Inhibition of pulmonary metastasis of Lewis lung carcinoma cells. Lewis lung carcinoma cells were injected into the tail veins of C57Bl/6 mice, and 3 days later, mice were treated with PBS or Metastatin. Once the treatment was stopped, animals were euthanized, and lungs were removed and weighed. *A*, shows representative lungs from control and treated animals and illustrates that Metastatin lowers the tumor burden. *B*, Metastatin injected i.p. daily beginning on day 4 decreased the relative lung weights in a dose-dependent fashion. *C*, the weight of the lungs in animals was also decreased when Metastatin was administered by three separate i.v. injections (100 μg/injection on days 1, 3, and 5). The values shown are the mean of at least five mice/group; *bars*, SD.

Metastatin could be the amount of hyaluronan that they secrete because it has an inhibitory effect. To test this possibility, conditioned media from confluent cultures of the different cell lines were collected and analyzed for hyaluronan by a modified ELISA. TSU cells were found to secrete significantly larger amounts of hyaluronan into the medium than the other cell lines (7 μg/ml *versus* <0.5 μg/ml, respectively). Indeed, this level of hyaluronan would be sufficient to block the effects of added Metastatin.

We also examined the effects of Metastatin on the migration of endothelial cells, another important factor in the process of angiogenesis (19). In this assay, we examined the effect of Metastatin on the migration of HUVECs using the wound migration assay. Fig. 5 shows that at a concentration of 10 μg/ml, Metastatin inhibited the migration of HUVECs by 50% as compared with controls treated with bFGF alone. Again, similar results were obtained when migration was monitored using Nucleopore filters (data not shown).

Effect of Metastatin on VEGF-induced Angiogenesis. The fact that Metastatin could inhibit both the growth and migration of endothelial cells *in vitro* suggested that it might also be able to block angiogenesis *in vivo*. To test this possibility, we examined the effect

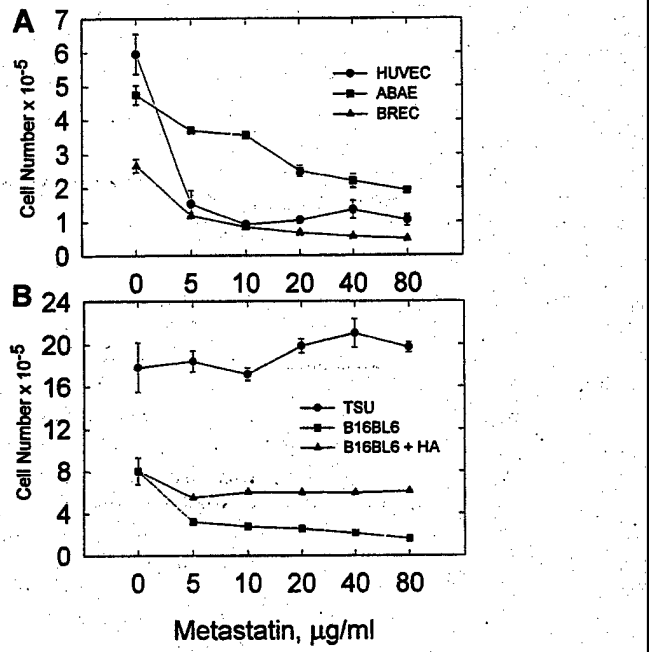

Fig. 4. The effects of varying concentrations of Metastatin on the growth of cultured cells. The cell lines were cultured in 24-well dishes in complete medium containing the indicated amounts of Metastatin, with medium changes ever other day. After 6 days, the cells were harvested with a solution of EDTA in PBS, and the cell numbers were determined with a Coulter counter. *A*, a dose-response curve is shown for the effects of Metastatin on the growth of the endothelial cell lines HUVEC, ABAE, and BREC. In each case, the growth of the cells was inhibited by Metastatin. *B*, a dose-response plot is shown for the tumor cell lines B16BL6 and TSU. Whereas Metastatin inhibited the growth of the B16BL6 cells, it had little or no effect on the TSU cells. The addition of an equal mass of hyaluronan to the Metastatin significantly reduced its effect on the proliferation of B16BL6 cells.

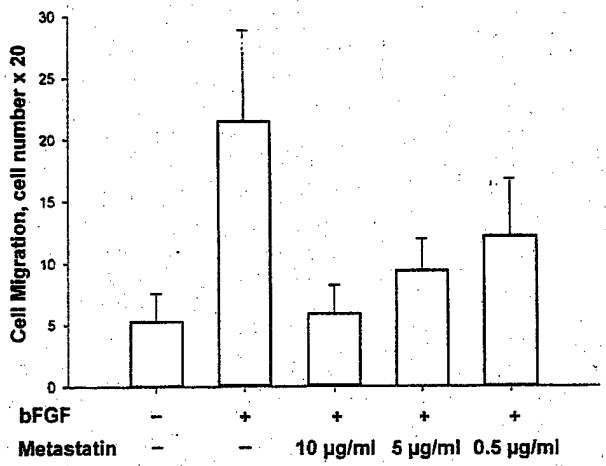

Fig. 5. Dose-dependent inhibitory effect of Metastatin on the migration of endothelial cells. HUVECs were grown to confluence on gelatin-coated culture plates, wounded with a sterile razor blade, and induced to migrate with bFGF in the presence of varying amounts of Metastatin. The number of cells that migrated were enumerated using a micrometer and microscope at ×200 magnification.

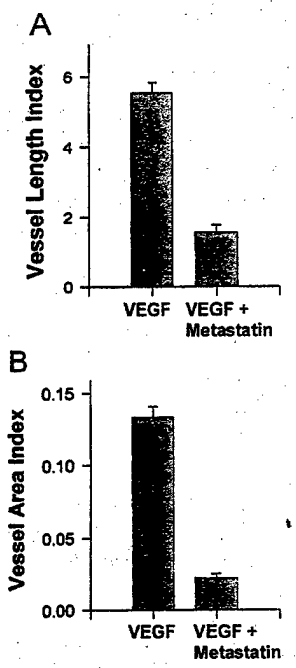

Fig. 6. Effect of Metastatin on VEGF-induced angiogenesis. The top of air sacs of 10-day-old chicken eggs were opened, exposing the chorioallantoic membranes, and filter discs containing 20 ng of VEGF were applied. The treated group was then injected i.v. with Metastatin (80 μg/egg), and the control group did not receive injections. The chorioallantoic membranes and associated discs were cut out on day 3 and analyzed by computer-assisted image analysis as described in "Materials and Methods". Metastatin had a significant inhibitory effect on both the (*A*) vessel length index and (*B*) vessel area index.

of Metastatin on angiogenesis induced in the chick chorioallantoic membrane. In this assay, filter papers containing recombinant human VEGF were placed on the chorioallantoic membrane of 10-day-old eggs, which were then given a single i.v. injection of the Metastatin or control preparations. Three days later, the extent of vascularization in the region of the filters was determined by computer-assisted image analysis. As shown in Fig. 6, treatment with Metastatin reduced both the length and area of vessels as compared with the control group, suggesting that Metastatin does indeed have the ability to block VEGF-induced angiogenesis.

Inhibition of Tumor Growth on the Chorioallantoic Membrane. To further explore the antitumor activity of Metastatin, we examined its effect on the growth of B16BL6 and TSU cells on the chicken chorioallantoic membrane. Tumor cells were applied to the chorioallantoic membranes of 10-day-old chicken embryos and allowed to grow for 1 week. Pilot experiments revealed that after inoculation with 10^6 cells, the take rate was almost 100% and resulted in xenografts with weights from 50–150 mg in 7 days. However, when the inoculated eggs were given a single i.v. injection of the Metastatin, the growth of the B16BL6 and TSU xenografts was greatly inhibited (Fig. 7). Again, this inhibitory effect was abolished if the preparation of Metastatin was heat inactivated or preincubated with its ligand, hyaluronan (Fig. 7*B*). It is important to note that Metastatin did not appear to adversely affect the development of the chicken embryos.

DISCUSSION

In this study we report that Metastatin, a cartilage-derived hyaluronan-binding complex consisting of proteolytic fragments of bovine link protein and aggrecan, is able to block the growth and metastasis of tumor cells under the following conditions: (*a*) a single i.v. injection of Metastatin into the chorioallantoic membrane of chicken embryos inhibited the growth of B16BL6 mouse melanoma cells and TSU human prostate cancer cells; (*b*) multiple i.p. injections of Metastatin prevented the experimental metastasis of B16BL6 and Lewis lung carcinoma cells to the lungs of mice; and (*c*) three i.v. injections of Metastatin were sufficient to inhibit the formation of Lewis lung carcinoma metastasis. In each case, Metastatin did not have an obvious detrimental effect on the host and was neutralized by complexing with soluble hyaluronan.

Metastatin is a member of a family of hyaluronan-binding proteins that also includes CD44, tumor necrosis factor-stimulated gene 6 (TSG-6), versican, neurocan, and brevican (20). Interestingly, Metastatin is similar to other factors that influence angiogenesis in that it is a fragment of a larger complex. For example, Angiostatin is a fragment of plasminogen, Endostatin represents a fragment of collagen XVIII, and serpin consists of a fragment of antithrombin (21–24). It is possible that the production of the peptide fragments is part of a feedback loop important in the down-regulation of angiogenesis.

In addition to Metastatin, a number of other antiangiogenic factors have been isolated from cartilage. Indeed, cartilage has been extensively studied as a source of molecules that could account for its avascular nature. Langer *et al.* (25) first reported a bovine cartilage fraction isolated by guanidine extraction and purified by trypsin affinity chromatography that inhibited tumor-induced vascular proliferation. In addition, Moses *et al.* (26) have recently isolated Troponin I from veal scapulae, which was shown to have antitumor and antiangiogenic properties. Lee and Langer (27) have described a guanidine-extracted factor from shark cartilage that inhibited angiogenesis and suppressed tumor vascularization. Similarly, Moses *et al.* (18) isolated a factor from cultures of scapular chondrocytes that inhibited angiogenesis in the chicken chorioallantoic membrane and appeared to be a protease inhibitor. However, it is likely that our preparation of Metastatin acts through a distinct mechanism because it has no detectable antiprotease activity and is inhibited by the addition of hyaluronan. It is tempting to speculate that Metastatin may contribute to the avascular nature of cartilage. Along these lines, we have previously found that hypertrophic chondrocytes produce large amounts of free hyaluronan, which may neutralize the effects of Metastatin in this region and thereby allow blood vessels to invade (28).

The results of this study suggest that Metastatin has antiangiogenic properties as demonstrated by its ability to block VEGF-induced formation of blood vessels in the chicken chorioallantoic membrane. The antiangiogenic effect of Metastatin was also consistent with our finding that it blocked both the proliferation and migration of cultured endothelial cells. Whereas Metastatin can directly attach tumor cells, we believe that most of its antitumor activity is due to its inhibition of angiogenesis because after its injection, the first cells that it would encounter are the endothelial cells, which would be exposed to the highest concentration. In addition, this antiangiogenic mechanism is suggested by the fact that Metastatin blocked the growth of TSU cells *in vivo* (*i.e.*, on the chicken chorioallantoic membrane) but had little or no effect on their proliferation *in vitro*. In this particular case, it seems likely that Metastatin was acting indirectly on the TSU tumor cells by blocking angiogenesis.

In other cases, the antitumor activity of Metastatin may be due to the combined action of direct killing of the tumor cells and the inhibition of angiogenesis. Indeed, Metastatin does appear to partially inhibit the growth of B16BL6 in tissue culture, and it could presumably have a similar effect *in vivo*. Because many blood vessels that are associated with tumors are leaky (29), Metastatin may be able to escape the circulation to interact directly with the tumor cells and block their proliferation. Along these lines, a recent study by Maniotis *et al.* (30) has indicated that some tumors have the ability to form

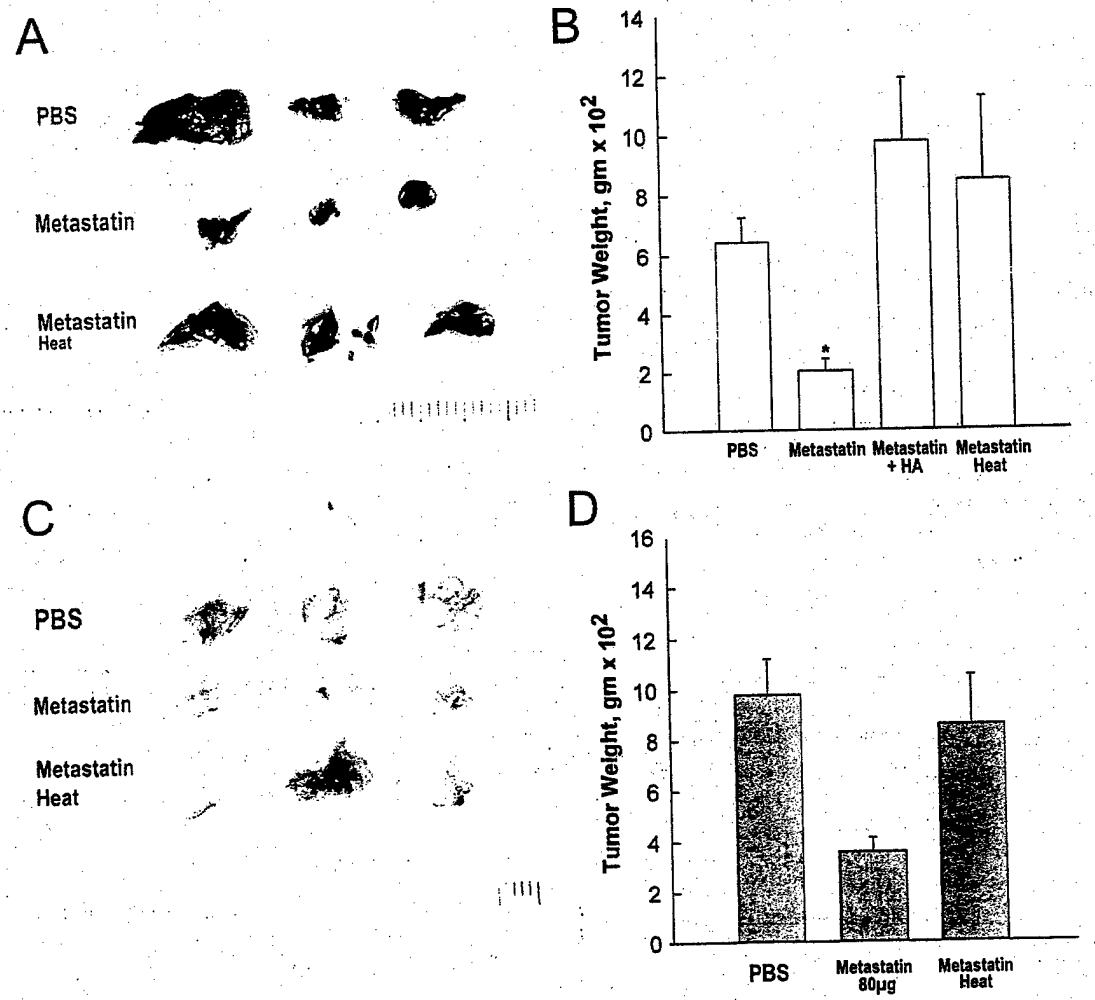

Fig. 7. Effect of Metastatin on the growth of tumor cells on the chicken chorioallantoic membrane. The top of the air sacs of 10-day-old chicken eggs were opened, exposing the chorioallantoic membrane, and pellets containing B16BL6 melanoma or TSU prostate tumor cells were placed on the membrane. On day 3, the embryos were given a single i.v. injection of PBS or Metastatin (80 µg). The tumors and associated chorioallantoic membranes were removed on day 6 and weighed. *A* and *C*, examples of the B16BL6 and TSU xenografts from eggs treated with PBS, Metastatin, or heat-denatured Metastatin. *B* and *D*, the weights of B16BL6 and TSU xenografts from eggs treated with Metastatin and control preparations are shown.

vasculature independent of endothelial cells. The tumor cells themselves appear to take on the characteristics of endothelial cells and are responsible for the formation of blood vessels. It is possible that such dual-acting tumor cells could also respond to Metastatin.

The biological effects of Metastatin appear to be closely linked to its ability to bind hyaluronan. If the preparation of Metastatin was premixed with hyaluronan, then this reversed its inhibitory effects on tumor growth *in vivo* and *in vitro* and its effects on the growth and migration of cultured endothelial cells. This indirectly suggests that Metastatin is binding to hyaluronan associated with the target cell. In the case of endothelial cells, particularly high levels of hyaluronan are localized to the tips of newly forming capillaries in the chicken chorioallantoic membrane and rabbit cornea (2, 3). A variety of other cell types show a similar relationship between proliferation and the production of hyaluronan (31–34). Whereas the hyaluronan present on proliferating tumor and endothelial cells could interact directly with Metastatin in the blood, the hyaluronan in other locations would not be exposed to high concentrations of the complex. Most normal cells would be protected by the fact that high concentrations of hyaluronan are present in connective tissues such as the dermis, lamina propria, and capsules (5, 35, 36), which would help to neutralize the Metastatin that diffused into these regions. It is important to note that under normal physiological conditions, hyaluronan in the blood is maintained at low levels by the liver and lymphatic system (37, 38). Thus, the circulating Metastatin should retain its hyaluronan binding activity.

Cell surface hyaluronan may serve as a target for other inhibitors of angiogenesis and tumor growth. For example, Endostatin, a ~20-kDa fragment of the COOH-terminal of collagen XVIII that inhibits angiogenesis (21, 22), may also be able to bind hyaluronan, as suggested by the presence of specific structural motifs (39). Secondly, a soluble, recombinant version of immunoglobulin fused with CD44 that binds to hyaluronan can inhibit the growth of human lymphoma cells that express CD44 in nude mice (40, 41). TSG-6, which is secreted by a variety of cells after stimulation with inflammatory cytokines, is able to both bind hyaluronan and block tumor cell growth (42). In each of these cases, these factors may be interacting with hyaluronan on the surfaces of target cells to exert their effects on angiogenesis and tumor growth.

In preliminary studies, we have found that Metastatin induces apoptosis in the target cells. However, at present, the mechanism by which Metastatin is able to do this is unclear. One possibility is that after Metastatin has bound to hyaluronan on the cell surface, it is taken up by the cells into lysosomes, where it is broken down into smaller fragments that enter the cytoplasm and induce apoptosis, perhaps by interacting with the mitochondrial membrane. Alternatively, Metasta-

tin could be interacting directly with the plasma membrane of the target cells, causing damage that in turn induces the apoptotic cascade. Clearly, future experiments will be directed toward elucidating the mechanism by which Metastatin induces apoptosis in the target cells.

In conclusion, we have found that Metastatin is able to block tumor growth in two model systems, and this effect depends on its ability to bind hyaluronan. Metastatin appears to target both tumor cells and endothelial cells that are involved in neovascularization. We postulate that during angiogenesis, the endothelial cells up-regulate their synthesis of hyaluronan, which then serves as a target for the injected Metastatin. Thus, Metastatin may represent a new type of antitumor agent, which targets cell surface hyaluronan.

ACKNOWLEDGMENTS

We are grateful to Dr. Theresa LaVallee and Wendy Hembrough for their assistance with the migration assay.

REFERENCES

1. Rooney, P., Kumar, S., Ponting, J., and Wang, M. The role of hyaluronan in tumor neovascularization. Int. J. Cancer, *60:* 632–636, 1995.
2. Ausprunk, D. H., Boudreau, C. L., and Nelson, D. A. Proteoglycans in the microvasculature. II. Histochemical localization in proliferating capillaries of the rabbit cornea. Am. J. Pathol., *103:* 367–375, 1981.
3. Ausprunk, D. H. Distribution of hyaluronic acid and sulfated glycosaminoglycans during blood vessel development in the chick chorioallantoic membrane. Am. J. Pathol., *177:* 313–331, 1986.
4. Mohamadzadeh, M., DeGrendele, H., Arizpe, H., Estess, P., and Siegelman, M. Proinflammatory stimuli regulate endothelial hyaluronan expression and CD44/HA-dependent primary adhesion. J. Clin. Investig., *101:* 97–108, 1998.
5. Green, S. J., Tarone, G., and Underhill, C. B. The distribution of hyaluronate and hyaluronate receptors in the adult lungs. J. Cell Sci., *89:* 145–156, 1988.
6. Eggli, P. S., and Graber, W. Association of hyaluronan with rat vascular endothelial and smooth muscle cells. J. Histochem. Cytochem., *43:* 689–697, 1995.
7. Feinberg, R. N., and Beebe, D. C. Hyaluronate in vasculogenesis. Science (Washington DC), *220:* 1177–1179, 1983.
8. West, D. C., Hampson, I. N., and Kumar, S. S. Angiogenesis induced by degradation products of hyaluronic acid. Science (Washington DC), *228:* 1324–1326, 1985.
9. Deed, R. P., Rooney, P. L., Kumar, J. D., Norton, J., Smith, A., Freemont, J., and Kumar, S. Early-response gene signaling is induced by angiogenic oligosaccharides of hyaluronan in endothelial cells. Inhibition by non-angiogenic, high-molecular-weight hyaluronan. Int. J. Cancer, *71:* 251–256, 1997.
10. Banerjee, S. D., and Toole, B. P. Hyaluronan-binding protein in endothelial cell morphogenesis. J. Cell Biol., *119:* 643–652, 1992.
11. Griffioen, A. W., Goenen, M. J. H., Damen, C. A., Hellwig, S. M. M., van Weering, D. H. J., Vooys, W., Blijham, G. H., and Groenewegen, G. CD44 is involved in tumor angiogenesis; an activation antigen on human endothelial cells. Blood, *90:* 1150–1159, 1997.
12. Banerji, S., Ni, J. Wang, S-X., Clasper, S., Su, J., Tammi, R., Jones, M., and Jackson, D. G. LYVE-1, a new homologue of the CD44 glycoprotein, is a lymph-specific receptor for hyaluronan. J. Cell Biol., *144:* 789–801, 1999.
13. Culty, M., Nguyen, H. A., and Underhill, C. B. The hyaluronan receptor (CD44) participates in the uptake and degradation of hyaluronan. J. Cell Biol., *116:* 1055–1062, 1992.
14. Culty, M., Shizari, M., Thompson, E. W., and Underhill, C. B. Binding and degradation of hyaluronan by human breast cancer cell lines expressing different forms of CD44: correlation with invasive potential. J. Cell. Physiol., *160:* 275–286, 1994.
15. Tengblad, A. Affinity chromatography on immobilized hyaluronate and its applications to the isolation of hyaluronate binding proteins from cartilage. Biochim. Biophys. Acta., *578:* 281–289, 1979.
16. Underhill, C. B., and Zhang, L. Analysis of hyaluronan using biotinylated hyaluronan-binding proteins. Methods Mol. Biol., *137:* 441–447, 1999.
17. Brooks, P. C., Silletti, S., von Schalscha, T. L., Friedlander, M., and Cheresh, D. A. Disruption of angiogenesis by PEX, a noncatalytic metalloproteinase fragment with integrin binding activity. Cell, *92:* 391–400, 1998.
18. Moses, M. A., Sudhalter, J., and Langer, R. Isolation and characterization of an inhibitor of neovascularization from scapular chondrocytes. J. Cell Biol., *119:* 473–482, 1992.
19. Ausprunk, D. H., and Folkman, J. Migration and proliferation of endothelial cells in preformed and newly formed blood vessels during tumor angiogenesis. Microvasc. Res., *14:* 53–65, 1977.
20. Neame, P. J., and Barry, F. P. The link protein. Experientia (Basel), *49:* 393–402, 1993.
21. Folkman, J., and Shing, Y. Angiogenesis. J. Biol. Chem., *267:* 10931–10934, 1992.
22. O'Reilly, M. S., Boehm, T., Shing, Y., Fukai, N., Vasios, G., Lane, W. S., Flynn, E., Birkhead, J. R., Olsen, B. R., and Folkman, J. Endostatin. An endogenous inhibitor of angiogenesis and tumor growth. Cell, *88:* 277–285, 1997.
23. O'Reilly, M. S., Holmgren, L., Shing, Y., Chen, C., Rosenthal, R. A., Moses, M., Lane, W. S., Cao, Y., Sage, E. H., and Folkman, J. Angiostatin. A novel angiogenesis inhibitor that mediates the suppression of metastases by a Lewis lung carcinoma. Cell, *79:* 315–328, 1994.
24. O'Reilly, M. S., Pirie-Sheperd, S., Lane, W. S., and Folkman, J. Antiangiogenic activity of the cleaved conformation of the serpin antithrombin. Science (Washington DC), *285:* 1926–1928, 1999.
25. Langer, R., Brem, H., Falterman, K., Klein, M., and Folkman, J. Isolations of a cartilage factor that inhibits tumor neovascularization. Science (Washington DC), *193:* 70–72, 1976.
26. Moses, M. A., Wiederschain, D., Wu, I., Fernandez, C. A., Ghazizadeh, V., Lane, W. S., Flynn, E., Sytkowski, A., Tao, T., and Langer, R. Troponin I is present in human cartilage and inhibits angiogenesis. Proc. Natl. Acad. Sci. USA, *96:* 2645–2650, 1999.
27. Lee, A., and Langer, R. L. Shark cartilage contains inhibitors of tumor angiogenesis. Science (Washington DC), *221:* 1185–1187, 1983.
28. Pavasant, P., Shizari, M., and Underhill, C. B. Distribution of hyaluronan in the epiphysial growth plate: Turnover by CD44 expressing osteoprogenitor cells. J. Cell Sci., *107:* 2669–2677, 1994.
29. Dvorak, H. F., Nagy, J. A., Dvorak, J. T., and Dvorak, A. M. Identification and characterization of the blood vessels of solid tumors that are leaky to circulating macromolecules. Am. J. Pathol., *133:* 95–109, 1988.
30. Maniotis, A. J., Folberg, R., Hess, A., Seftor, E. A., Gardner, L. M. G., Pe'er, J., Trent, J. M., Meltzer, P. S., and Hendirx, M. J. Vascular channel formation by human melanoma cells *in vivo* and *in vitro*: vasculogenic mimicry. Am. J. Pathol., *155:* 739–752, 1999.
31. Main, N. Analysis of cell-growth-phase-related variation in hyaluronate synthase activity of isolated plasma-membrane fractions of cultured human skin fibroblasts. Biochem. J., *237:* 333–342, 1986.
32. Tomida, M., Koyama, H., and Ono, T. Induction of hyaluronic acid synthetase activity in rat fibroblasts by medium change of confluent cultures. J. Cell. Physiol., *86:* 121–130, 1975.
33. Hronowski, L., and Anastassiades, T. P. The effect of cell density on net rates of glycosaminoglycan synthesis and secretion by cultured rat fibroblasts. J. Biol. Chem., *255:* 10091–10099, 1980.
34. Matuoka, K., Namba, M., and Mitsui, Y. Hyaluronate synthetase inhibition by normal and transformed human fibroblasts during growth reduction. J. Cell Biol., *104:* 1105–1115, 1987.
35. Alho, A. M., and Underhill, C. B. The hyaluronate receptor is preferentially expressed on proliferating epithelial cells. J. Cell Biol., *108:* 1557–1565, 1989.
36. Underhill, C. B. The interaction of hyaluronate with the cell surface: the hyaluronate receptor and the core protein. CIBA Found. Symp., *143:* 87–106, 1989.
37. Fraser, J. R. E., Appelgren, L. E., and Laurent, T. C. Tissue uptake of circulating hyaluronic acid. Cell Tissue Res., *233:* 285–293, 1983.
38. Laurent, T. C., and Fraser, J. R. E. The properties and turnover of hyaluronan. Laurent, removal of HA from the blood. CIBA Found. Symp., *124:* 9–29, 1986.
39. Hobenester, E., Sasaki, T., Olsen, B. R., and Timpl, R. Crystal structure of the angiogenesis inhibitor endostatin at 1.5 A resolution. EMBO J., *17:* 1656–1664, 1998.
40. Sy, M-S., Guo, Y. J., and Stamenkovic, I. Inhibition of tumor growth *in vivo* with a soluble CD44-immunoglobulin fusion protein. J. Exp. Med., *176:* 623–627, 1992.
41. Yu, Q., Toole, B. P., and Stamenkov, I. Induction of apoptosis of metastatic mammary carcinoma cells *in vivo* by disruption of tumor cell surface CD44 function. J. Exp. Med., *186:* 1985–1996, 1997.
42. Wisniewski, H. G., Hua, J-C., Poppers, D. M., Naime, D., Vilcek, J., and Cronstein, B. N. TSG-6, a glycoprotein associated with arthritis, and its ligand hyaluronan exert opposite effects in a murine model of inflammation. J. Immunol., *156:* 1609–1615, 1996.

[CANCER RESEARCH 61, 2434–2438, March 15, 2001]

Advances in Brief

RGD-Tachyplesin Inhibits Tumor Growth[1]

Yixin Chen, Xueming Xu, Shuigen Hong, Jinguo Chen, Ningfei Liu, Charles B. Underhill, Karen Creswell, and Lurong Zhang[2]

Department of Oncology, Lombardi Cancer Center, Georgetown University Medical School, Washington, D.C. 20007 [X-M. X., J. C., N. F., C. B. U., K. C., L. Z.], and The Key Laboratory of China Education Ministry on Cell Biology and Tumor Cell Engineering, Xiamen University, Fujian 361005, People's Republic of China [Y. C., S. H.]

Abstract

Tachyplesin is an antimicrobial peptide present in leukocytes of the horseshoe crab (*Tachypleus tridentatus*). In this study, a synthetic tachyplesin conjugated to the integrin homing domain RGD was tested for antitumor activity. The *in vitro* results showed that RGD-tachyplesin inhibited the proliferation of both cultured tumor and endothelial cells and reduced the colony formation of TSU prostate cancer cells. Staining with fluorescent probes of FITC-annexin V, JC-1, YO-PRO-1, and FITC-dextran indicated that RGD-tachyplesin could induce apoptosis in both tumor and endothelial cells. Western blotting showed that treatment of cells with RGD-tachyplesin could activate caspase 9, caspase 8, and caspase 3 and increase the expression of the Fas ligand, Fas-associated death domain, caspase 7, and caspase 6, suggesting that apoptotic molecules related to both mitochondrial and Fas-dependent pathways are involved in the induction of apoptosis. The *in vivo* studies indicated that the RGD-tachyplesin could inhibit the growth of tumors on the chorioallantoic membranes of chicken embryos and in syngenic mice.

Introduction

Tachyplesin, a peptide from hemocytes of the horseshoe crab (*Tachypleus tridentatus*), can rapidly inhibit the growth of both Gram-negative and -positive bacteria at extremely low concentrations (1, 2). Tachyplesin has a unique structure, consisting of 17 amino acids (KWCFRVCYRGICYRRCR) with a molecular weight of 2,269 and a pI of 9.93. In addition, it contains two disulfide linkages, which causes all six of the basic amino acids (R, arginine; K, lysine) to be exposed on its surface (3). The cationic nature of tachyplesin allows it to interact with anionic phospholipids present in the bacterial membrane and thereby disrupt membrane function (4, 5).

The structural nature of tachyplesin suggested that it might also possess antitumor properties. Tachyplesin can interact with the neutral lipids in the plasma membrane of eukaryotic cells (4, 5). More importantly, because it can interact with the membranes of prokaryotic cells, it is likely that tachyplesin can also interact with the mitochondrial membrane of eukaryotic cells. Indeed, these membranes are structurally similar because mitochondria are widely believed to have evolved from prokaryotic cells that have established a symbiotic relationship with the primitive eukaryotic cell (6). Recent studies have indicated that mitochondria play a critical role in regulating apoptosis in eukaryotic cells (7). The disruption of mitochondrial function results in the release of proteins that normally are sequestered by this organelle. The release of factors, such as cytochrome *c* and Samc, can activate caspases that, in turn, trigger the apoptotic cascade (8, 9). Along these lines, Ellerby *et al.* (10) have found that a cationic antimicrobial peptide (KLAKLAKKLAKLAK) conjugated with a CNGRC homing domain exhibits antitumor activity through its ability to target mitochondria and trigger apoptosis. Because the proapoptotic peptide and tachyplesin belong to the same category of cationic antimicrobial peptide, it seems possible that tachyplesin could have similar antitumor activity.

To explore this possibility, we have examined a chemically synthesized preparation of tachyplesin that was linked to a RGD sequence, which corresponds to a homing domain that allows it to bind to integrins on both tumor and endothelial cells and thereby facilitates internalization of the peptide (11, 12). We found that this synthetic RGD-tachyplesin could inhibit the proliferation of TSU prostate cancer cells and B16 melanoma cells as well as endothelial cells in a dose-dependent manner *in vitro* and reduce tumor growth *in vivo*.

Materials and Methods

Synthesis of RGD-Tachyplesin. Two peptides were chemically synthesized. The test peptide was RGD-tachyplesin (CRGDCGGKWCFRVCYRGICYRRCR), and the control peptide was a scrambled sequence with a similar molecular weight and pI. To impede enzymatic degradation, the NH_2-terminal of the peptide was acetylated, and the COOH-terminal was amidated. Before use, the peptides were dissolved in dimethylformamide and 1% acetate acid, diluted with saline to a concentration of 1 mg/ml, and sterilized by boiling for 15 min in a water bath.

Cell Lines. The TSU human prostate cancer cells, B16 melanoma, Cos-7, and NIH-3T3 were maintained in 10% calf serum and 90% DMEM. The human umbilical vein endothelial cells and ABAE[3] cells were cultured in 20% fetal bovine serum and 80% DMEM containing 10 ng/ml fibroblast growth factor 2 and vascular endothelial growth factor, respectively.

Cell Proliferation Assay. Aliquots of complete medium containing 5000 cells were distributed into a 96-well tissue culture plate. The next day, the media were replaced with 160 μl of fresh media and 40 μl of a solution containing different concentrations of the peptides. One day later, 30 μl of 0.3 μCi of [^{3}H]thymidine in serum-free media were added to each well, and after 8 h, the cells were harvested, and the amount of incorporated [^{3}H]thymidine was determined with a beta counter.

Colony Formation Assay. TSU cells (2×10^4) were suspended in 1 ml of 0.36% agarose in 90% DMEM and 10% calf serum containing 100 μg/ml control peptide or RGD-tachyplesin and then immediately placed on the top of a layer of 0.6% solid agarose in 10% calf serum and 90% DMEM in 6-well plates. Two weeks later, the number of colonies larger than 60 μm in diameter was determined using an Omnicon Image Analysis system (Imaging Products International Inc., Chantilly, VA).

Analysis of Tachyplesin-damaged Cells by Flow Cytometry. Cultures of TSU cells at 80% confluence were treated overnight with 50 μg/ml control peptide or RGD-tachyplesin. The next day, the cells were harvested with 5 mM EDTA in PBS, washed, resuspended in 10% calf serum and 90% DMEM, and then stained with the fluorescent dyes annexin V and propidium iodide, JC-1,

Received 11/22/00; accepted 1/30/01.

The costs of publication of this article were defrayed in part by the payment of page charges. This article must therefore be hereby marked *advertisement* in accordance with 18 U.S.C. Section 1734 solely to indicate this fact.

[1] Supported in part by National Cancer Institute/NIH Grant R29 CA71545; United States Army Medical Research and Materiel Command Grants DAMD17-99-1-9031, DAMD17-98-1-8099, DAMD17-00-1-0081, and PC970502; and Susan G. Komen Breast Cancer Foundation (C. B. U. and L. Z.). Y. C. was a recipient of China Scholarship Council, and L. Z. was a recipient of funding from the visiting scholar foundation for key laboratory at Xiamen University, China.

[2] To whom requests for reprints should be addressed, at Department of Oncology, Lombardi Cancer Center Georgetown University Medical School, 3970 Reservoir Road, NW, Washington, D.C. 20007. Phone: (202) 687-6397; Fax: (202) 687-7505; E-mail: Zhangl@georgetown.edu.

[3] The abbreviations used are: ABAE, adult bovine aorta endothelial; FADD, Fas-associated death domain; CAM, chorioallantoic membrane.

YO-PRO-1, and FITC-dextran, according to manufacturer's instructions (Molecular Probes, Eugene, OR).

Western Blotting. Cultures of TSU and ABAE cells at approximately 80% confluence were treated overnight with 100 μg/ml peptides and then harvested with 1 ml of lysis buffer (1% Triton X-100, 0.5% sodium deoxycholate, 0.5 μg/ml leupetin, 1 mM EDTA, 1 μg/ml pepstatin, and 0.2 mM phenylmethylsulfonyl fluoride). The protein concentration was determined by the BCA method (Pierce, Rockford IL), and 20 μg of protein lysate were loaded onto 4–12% BT NuPAGE gel (Invitrogen, Carlsbad CA), electrophoresed, and transferred to a nitrocellulose membrane. The loading and transfer of equal amounts of protein were confirmed by staining with Ponceau S solution (Sigma, St. Louis, MO). The membranes were blocked with 5% nonfat milk and 1% polyvinylpyrrolidone in PBS for 30 min and then incubated for 1 h with 1 μg/ml antibodies to Fas ligand, FADD, caspase 9, caspase 8, caspase 3, caspase 7, and caspase 6 (Oncogene, Boston, MA). After washing, the membrane was incubated for 1 h with 0.2 μg/ml of peroxidase-labeled antirabbit IgG followed by a chemiluminescent substrate for peroxidase and exposed to enhanced chemiluminescence Hyperfilm MP (Amersham, Piscataway, NJ).

Effect of RGD-Tachyplesin on TSU Tumor Growth on the Chicken CAM. TSU cells (2×10^6) were mixed with equal amounts of control peptide or RGD-tachyplesin (100 μg in 200 μl of saline) and immediately placed on top of the CAMs of 10-day-old chicken embryos (15 eggs/group) and incubated at 37.8°C. Every other day thereafter, 200 μl of PBS containing 100 μg of the peptides were added tropically to the xenografts on the CAMs. Five days later, the xenografts were dissected from the membrane, photographed, and weighed.

Effect of RGD-Tachyplesin on B16 Tumor Growth in Mice. B16 melanoma cells were injected s.c. into the flank of 5-week-old male C57BL/6 mice (5×10^5 cells/site; 5 mice/group) and allowed to establish themselves for 2 days. Every other day thereafter, 250 μg of the control peptide or RGD-tachyplesin was injected i.p. into the mice. At the end of 2 weeks, the mice were sacrificed, and the tumor xenografts were removed, photographed, and weighed.

Statistical Analysis. The mean and SE were calculated from the raw data and then subjected to Student's t test. $P < 0.05$ was regarded as statistical significance.

Results

RGD-Tachyplesin Inhibits the Growth of Tumor and Endothelial Cells *in Vitro*. Because both tumor and endothelial cells play an important role in determining tumor progression, we initially examined the effects of RGD-tachyplesin on the proliferation of both of these cells *in vitro*. As shown in Fig. 1*A*, RGD-tachyplesin inhibited the growth of the cultured cells in a dose-dependent manner, with an EC_{50} of about 75 μg/ml for TSU tumor cells and 35 μg/ml for the endothelial cells. In contrast, the scrambled peptide had no obvious effect on the proliferation of the cells at 100 μg/ml. This effect was also reflected in the morphology of the cells. After exposure to 50 μg/ml RGD-tachyplesin for 12 h, a significant fraction of treated cells had become rounded and detached, whereas few cells did so after treatment with the control peptide (data not shown).

To determine whether nontumorigenic cells were also affected by RGD-tachyplesin, the immortalized cell lines, Cos-7 and NIH-3T3, were tested in the [^{3}H]thymidine incorporation assay. As shown in Fig. 1*B*, when treated with 50 μg/ml RGD-tachyplesin, the extent of inhibition of Cos-7 or NIH-3T3 (0–20%) was less than that of tumor or proliferating endothelial cells (40–75%), indicating that nontumorigenic cells are less sensitive to RGD-tachyplesin.

Next, we examined the effects of the peptides on the growth of TSU cells in soft agar. The ability of cells to grow under such anchorage-independent conditions is one of the characteristic phenotypes of aggressive tumor cells. As shown in Fig. 1*C*, RGD-tachyplesin inhibited the ability of TSU cells to form colonies as compared to the groups of control peptide and vehicle alone.

Treatment with RGD-Tachyplesin Alters Membrane Function. We then examined the mechanism by which RGD-tachyplesin inhibited the proliferation of the tumor and endothelial cells. One possibility was that RGD-tachyplesin damages cell membranes, and this damage, in turn, induces apoptosis.

To examine the extent of apoptosis, TSU cells that had been treated for 1 day with the test or control peptides were stained with FITC-annexin and propidium iodide. FITC-annexin V binds to phosphatidylserine, which is exposed on the outer leaflet of the plasma membrane of cells in the initial stages of apoptosis, whereas propidium iodide preferentially stains the nucleus of dead cells, but not living cells. Fig. 2*A* shows that treatment with RGD-tachyplesin induced apoptosis (annexin V positive, propidium iodide negative) in a greater number of cells than did treatment with the vehicle or control peptide.

This induction of apoptosis could have been due to the disruption of mitochondrial function. To examine this, we used JC-1 staining, which measures the membrane potential of mitochondria. As shown in Fig. 2, *B* and *C*, treatment with RGD-tachyplesin caused a shift in the fluorescence profile from one that was highly red (Fig. 2*B*) to one that was less red and more green (Fig. 2*C*). This indicated that the membrane potential of mitochondria was changed by treatment with RGD-tachyplesin.

We also examined the integrity of the plasma membrane and nuclear membrane after treatment with the scrambled peptide and RGD-tachyplesin using two different fluorescent markers. YO-PRO-1 dye can only stain the nuclei of cells with damaged plasma and nuclear membranes. Fig. 2*D* shows that treatment with RGD-tachyplesin allowed the YO-PRO-1 dye to pass into the nuclei, causing an increase in the fluorescence intensity. Similar results were obtained when the cells were stained with FITC-dextran, which is not taken up by viable, healthy cells but can pass through the damaged plasma membrane of unhealthy cells. Fig. 2*E* shows that cells treated with RGD-tachyplesin took up a greater amount of FITC-dextran (M_r 40,000) than did those treated with the control peptide. These results indicated that the majority of RGD-tachyplesin-treated cells allowed these big molecules to pass their damaged membranes.

The above-mentioned experiments were also carried out with ABAE cells, and similar results were obtained (data not shown). Presumably, RGD-tachyplesin induces apoptosis in both TSU and ABAE cells by damaging their membranes.

RGD-Tachyplesin Triggers Apoptotic Pathways. Apoptosis can be induced by two mechanisms: (*a*) the mitochondrial pathway; and (*b*) the death receptor pathway (13). To identify the nature of the apoptotic pathway triggered by RGD-tachyplesin, both TSU and ABAE cells were treated overnight with RGD-tachyplesin and control peptide and then analyzed by Western blotting for the alterations of molecules involved in the mitochondrial and Fas-dependent pathways. Fig. 3 shows that treatment of both TSU tumor cells and ABAE cells with RGD-tachyplesin caused the cleavage of M_r 46,000 caspase 9 into subunits of M_r 35,000 and M_r 10,000, indicating activation of the mitochondrial-related, Fas-independent pathway. In addition, RGD-tachyplesin treatment could up-regulate the expression of upstream molecules in the Fas-dependent pathway, including Fas ligand (M_r 43,000), FADD (M_r 28,000), and activate subunits of caspase 8 (M_r 18,000). Furthermore, the downstream effectors, such as caspase 3 subunits (M_r 20,000), caspase 6 (M_r 40,000), and caspase 7 (M_r 34,000), were also up-regulated by RGD-tachyplesin. These results suggest that RGD-tachyplesin induces apoptosis through both the mitochondrial-related, Fas-independent pathway and the Fas-dependent pathway. However, because there is cross-talk between these two pathways (13), we do not have enough evidence to determine which one is the initiator.

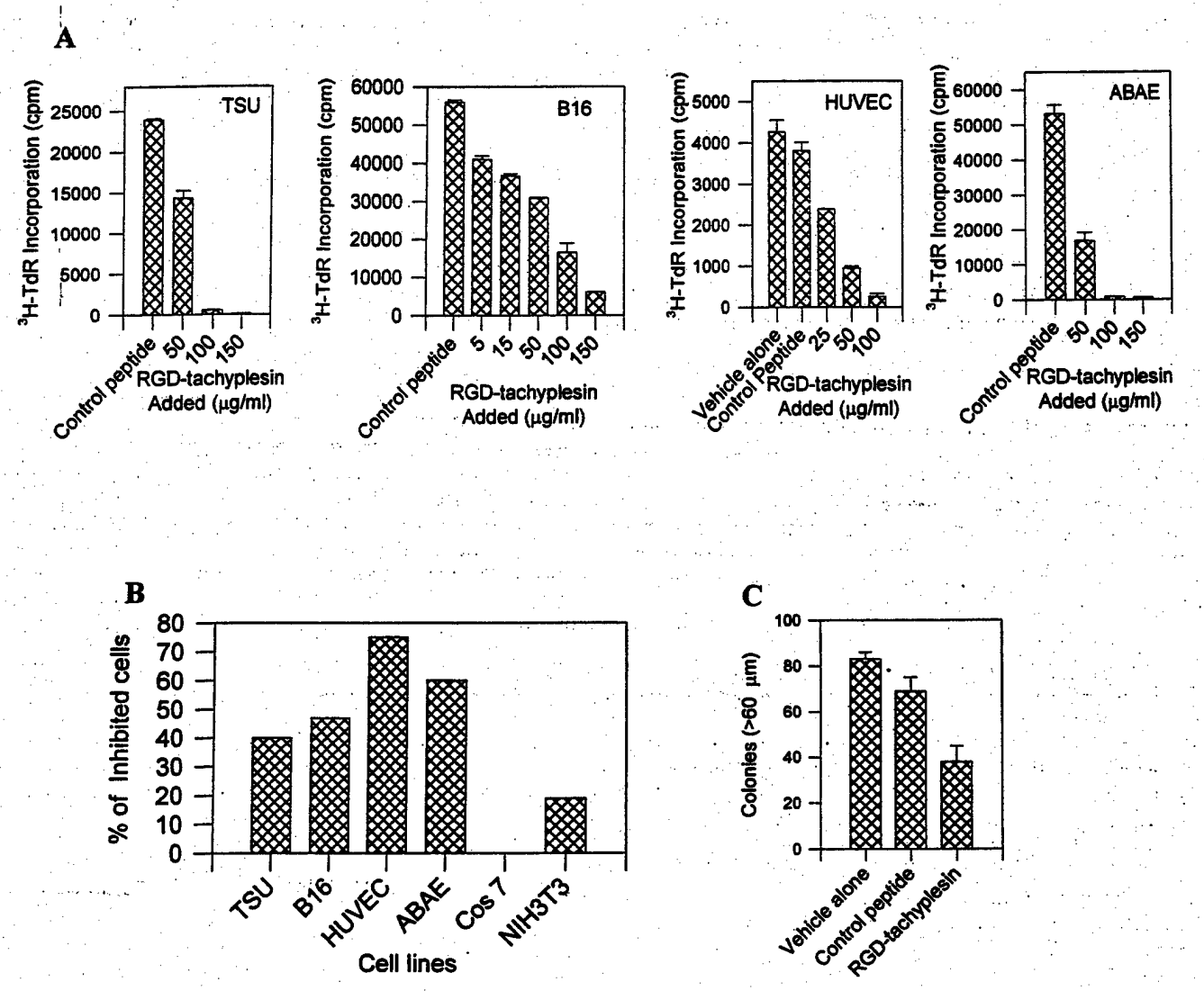

Fig. 1. Effects of RGD-tachyplesin and scrambled peptide on cell proliferation. *A*, effect of RGD-tachyplesin on cell proliferation. TSU cells were treated with vehicle alone, 100 μg/ml control peptide, or different doses of RGD-tachyplesin for 24 h, followed by a [^{3}H]thymidine incorporation assay. The proliferation of both the tumor and endothelial cells was greatly inhibited by RGD-tachyplesin in a dose-dependent manner ($P < 0.01$). *B*, effect of RGD-tachyplesin on different cell lines. The cells were treated overnight with 50 μg/ml control peptide or RGD-tachyplesin and then treated with [^{3}H]thymidine. The rate of inhibition was calculated as follows: (1 − cpm of cells treated with RGD-tachyplesin/cpm of cells treated with control peptide) × 100%. The nontumorigenic cell lines Cos-7 and NIH-3T3 were inhibited to a lesser degree than the tumor or endothelial cells ($P < 0.05$). *C*, effect of RGD-tachyplesin on colony formation of TSU cells. TSU cells were suspended in 0.36% agarose containing 100 μg/ml control peptide or RGD-tachyplesin and then placed on top of 0.6% agarose. Two weeks later, colonies larger than 60 μm were counted with the Omnicon Image Analysis system. The colony formation of TSU cells was inhibited by RGD-tachyplesin ($P < 0.01$). All of the experiments were repeated three times, and similar results were obtained.

RGD-Tachyplesin Inhibits the Growth of TSU and B16 Tumor *in Vivo*. In the final series of experiments, we examined the *in vivo* effects of RGD-tachyplesin on the growth of TSU or B16 tumor cells in CAM (14) or mouse models. As shown in Fig. 4, the TSU tumor xenografts growing in CAM in the group treated with RGD-tachyplesin (Fig. 4*B*) were smaller than those in the group treated with control peptide (Fig. 4*A*). In addition, the average weight of the xenografts in the RGD-tachyplesin-treated group was significantly less than that of xenografts in the control group (Fig. 4*C*). Similarly, in the B16 mouse model, the B16 tumor xenografts in the RGD-tachyplesin-treated group (Fig. 4*E*) were smaller than those in the control group (Fig. 4*D*), and this difference was statistically significant ($P < 0.05$; Fig. 4*F*). It should be noted that RGD-tachyplesin did not appear to be toxic to the mice, as judged by their weights and activity at the end of the experiment. Thus, the results from two models are consistent with each other, indicating that RGD-tachyplesin can inhibit tumor growth *in vivo*.

Discussion

The major conclusion of this study is that RGD-tachyplesin can inhibit tumor growth by inducing apoptosis in the tumor cells and the associated endothelial cells. This conclusion was supported by the following observations. First, RGD-tachyplesin was able to inhibit the growth of TSU tumor cells on the CAM of chicken embryos as well as the growth of B16 tumor cells in syngenic mice. Second, RGD-tachyplesin also blocked the proliferation of both tumor and endothelial cells in culture in a dose-dependent fashion, whereas proliferation was relatively unaffected in nontumorigenic cell lines Cos-7 and NIH-3T3. Third, RGD-tachyplesin induced apoptosis in cultured TSU cells, as indicated by staining with fluorescent markers for apoptosis including FITC-annexin V, which detects exposed phosphatidylserine, and JC-1, which tracks mitochondrial membrane potential. Finally, RGD-tachyplesin stimulated the activation and production of several molecules in the apoptotic cascade in both TSU and endothelial cells, as judged by Western blotting.

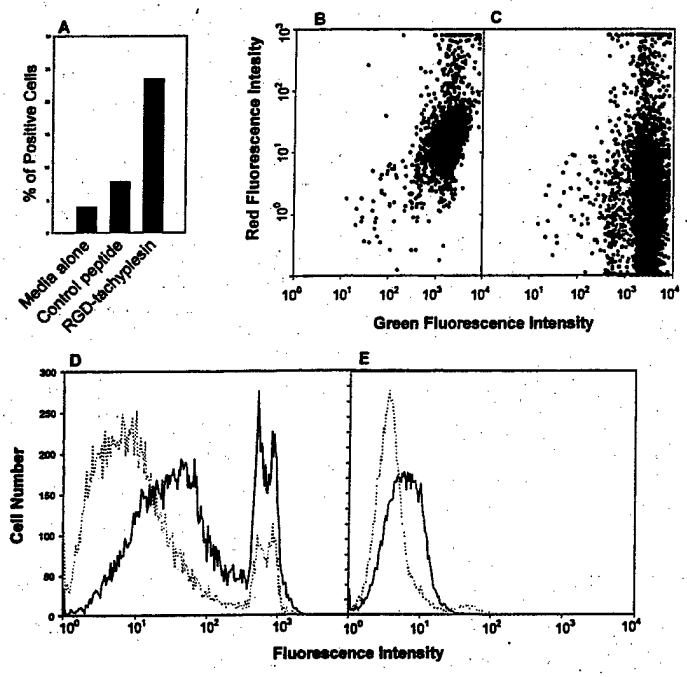

Fig. 2. The effect of RGD-tachyplesin on the function of TSU cells. TSU cells were treated overnight with 50 μg/ml control peptide or RGD-tachyplesin and then stained with different membrane probes. *A*, staining with annexin V and propidium iodide for apoptotic cells. The percentage of cells that were positive for FITC-annexin V and negative for propidium iodide was analyzed by flow cytometry. The RGD-tachyplesin-treated cells had a high percentage of apoptotic cells ($P < 0.01$). *B* and *C*, staining with JC-1 for mitochondrial membrane potential. The cells treated with the control peptide (*B*) and RGD-tachyplesin (*C*) were stained with 10 μg/ml JC-1 for 10 min and then analyzed by flow cytometry. The RGD-tachyplesin shifted the spectrum of the cells from high red (*B*, healthy) to high green and low red (*C*, loss mitochondrial potential). *D*, staining with YO-PRO-1 for integrity of nuclei membrane. The peptide-treated cells were stained with 0.1 μg/ml YO-PRO-1 dye, an indicator for damaged nuclei membranes (the *first peak* represents the dye-stained G_0-G_1-phase cells; the *second peak* represents the dye-stained S-M-phase cells). The RGD-tachyplesin treated cells shift from right to left, indicating the loss of integrity of the nuclei membrane. *E*, staining with FITC-dextran for integrity of plasma membrane. The peptide-treated cells were incubated with 50 μg/ml FITC-dextran (M_r 40,000) for 30 min and analyzed with flow cytometry. A higher proportion of RGD-tachyplesin-treated cells allowed FITC-dextran to pass through their plasma membrane as compared to the control.

Our results also suggest that RGD-tachyplesin up-regulates apoptosis related to both the mitochondrial and the death receptor pathways. The involvement of the mitochondrial pathway was suggested by the facts that staining with JC-1 indicated the membrane potential of mitochondria was decreased (Fig. 2, *B* and *C*) and that the caspase 9 was activated (Fig. 3) in cells treated with RGD-tachyplesin. Presumably, this resulted from the release of cytochrome *c*, which, in turn, bound to Apaf-1 and activated caspase 9 and then caspase 3, caspase 7, and caspase 6 (13, 15–17). This is the mechanism by which the peptide described by Ellerby *et al.* (10) induced apoptosis. In addition, we found that members of the death receptor pathway (Fas ligand, FADD, and caspase 8) were also up-regulated. Thus, RGD-tachyplesin may have multiple effects on the target cells. It is difficult at this point to determine what initial event is responsible for the RGD-tachyplesin-induced activation of apoptosis.

There appears to be considerable cross-talk between the mitochondrial apoptotic pathway and Fas-dependent pathway. The caspase 6 activated by the mitochondrial pathway (cytochrome *c*→Apaf-1→caspase 9→caspase 3) could act on FADD and then on caspase-8, which triggered the Fas-dependent pathway. On the other hand, the caspase 8-activated Fas-FADD pathway could act on BID that stimulates the mitochondrial pathway (15–17). This cross-talk creates positive feedback and enhances the apoptosis cascade.

RDG-tachyplesin also appeared to be relatively nontoxic to cells not associated with tumors. When RGD-tachyplesin was administered at a concentration that inhibited tumor growth, there was no notable side effects on either the chicken embryos or mice with regard to animal body weight and activity at the end of each experiment. In addition, studies on cultured cells indicated that the sensitivity to RGD-tachyplesin varied depending on cell type. In comparison to tumor cells and proliferating endothelial cells, immortalized cells such as Cos-7 (green monkey kidney cells) and NIH-3T3 (fibroblast cells) were less sensitive to RGD-tachyplesin. Taken together, these results suggest that RGD-tachyplesin is a well-tolerated peptide.

RGD-tachyplesin also appears to be more potent than similar cationic peptides. The unique cyclic structure of tachyplesin maintained by two disulfide bonds may make it more effective in targeting membranes than the linear antimicrobial peptides, such as KLAK-LAKKLAKLAK (a proapoptotic peptide; Ref. 10), which is suggested by its lower minimal inhibition concentration on both *Escherichia coli* and *Staphylococcus aureus* of 2 *versus* 6 μM (18, 19). Furthermore, tachyplesin interacts not only with anionic phospholipids of bacterial and mitochondria but also with neutral lipids of eukaryotic plasma membrane (4, 5, 18). Ellerby *et al.* (10) reported that their proapoptotic peptide inhibited proliferation with an EC_{50} of about 100 μg/ml for endothelial cells, whereas our results indicated that RGD-tachyplesin had a much stronger efficacy on proliferating

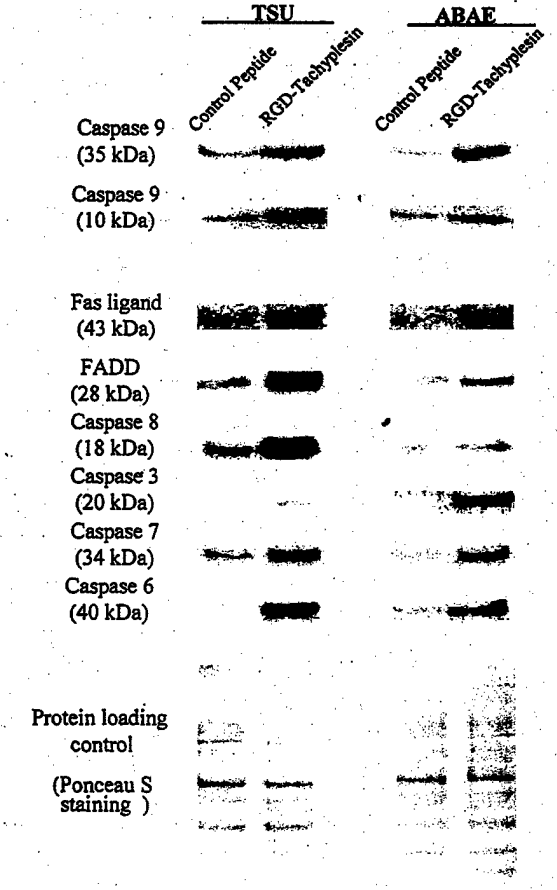

Fig. 3. Effect of RGD-tachyplesin on molecules involved in the apoptosis cascade. Twenty μg of lysate from TSU and ABAE cells treated with 100 μg/ml control peptide or RGD-tachyplesin were loaded onto a 4–12% BT NuPAGE gel, electrophoresed, and transferred to a nitrocellulose membrane. The loading and transfer of equal amounts of protein were confirmed by staining with a Ponceau S solution. After blocking with 5% nonfat milk, the membranes were incubated for 1 h with 1 μg/ml antibodies to caspase 9, Fas ligand, FADD, caspase 8, caspase 3, caspase 7, and caspase 6 followed by horseradish peroxidase-conjugated antirabbit IgG and enhanced chemiluminescence substrate and finally exposed to Hyperfilm MP.

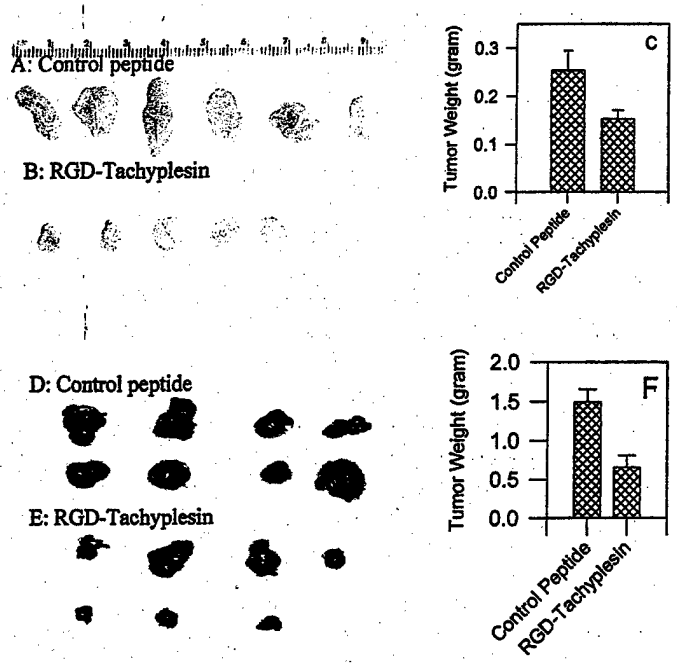

Fig. 4. Effect of RGD-tachyplesin on tumor growth *in vivo*. *A–C*, effect of RGD-tachyplesin on the TSU xenografts on CAM. TSU cells (2×10^6) were mixed with either control peptide or RGD-tachyplesin (100 μg) and immediately placed on top of the CAM of 10-day-old chicken embryos and incubated at 37.8°C. Every other day, additional peptides were applied tropically to the TSU xenografts. Five days later, the xenografts were removed from the CAM, photographed, and weighed. The TSU xenografts treated with RGD-tachyplesin were significantly smaller than those treated with the control peptide ($P < 0.01$). *D–F*, effect of RGD-tachyplesin on tumor growth in the mouse model. B16 melanoma cells (5×10^5) were injected s.c. into the flank of C57BL/6 mice and allowed to establish themselves for 2 days. Every other day after that, 250 μg of control peptide or RGD-tachyplesin were injected i.p. into the mice. At the end of 2 weeks, the mice were sacrificed, and the xenografts were removed, photographed, and weighed. The B16 xenografts from animals treated with RGD-tachyplesin were significantly smaller than those from animals treated with the control peptide ($P < 0.01$).

endothelial cells, with an EC_{50} of about 35 μg/ml. Furthermore, RGD-tachyplesin acts not only on proliferating endothelial cells but also on tumor cells. This dual effect of RGD-tachyplesin will enhance its antitumor function.

In conclusion, this study demonstrates that RGD-tachyplesin can be used as an antitumor agent. By disrupting vital membranes and inducing apoptosis, it inhibits all of the tumor cells tested. Further study of RGD-tachyplesin and its analogues may lead to finding a new category of antitumor drug.

Acknowledgments

The animal protocols were reviewed and approved by the Animal Care and Use Committee of Georgetown University.

References

1. Kokryakov, V. N., Harwig, S. S., Panyutich, E. A., Shevchenko, A. A., Aleshina, G. M., Shamova, O. V., Korneva, H. A., and Lehrer, R. I. Protegrins. Leukocyte anti-microbial peptides that combine features of corticostatic defensins and tachyplesins. FEBS Lett., *327:* 231–236, 1993.
2. Shigenaga, T., Muta, T., Toh, Y., Tokunaga, F., and Iwanaga, S. Anti-microbial tachyplesin peptide precursor. cDNA cloning and cellular localization in the horseshoe crab (*Tachypleus tridentatus*). J. Biol. Chem., *265:* 21350–21354, 1990.
3. Nakamura, T., Furunaka, H., Miyata, T., Tokunaga, F., Muta, T., Iwanaga, S., Niwa, M., Takao, T., and Shimonishi, Y. Tachyplesin, a class of anti-microbial peptide from the hemocytes of the horseshoe crab (*Tachypleus tridentatus*). Isolation and chemical structure. J. Biol. Chem., *263:* 16709–16713, 1988.
4. Park, N. G., Lee, S., Oishi, O., Aoyagi, H., Iwanaga, S., Yamashita, S., and Ohno, M. Conformation of tachyplesin I from *Tachypleus tridentatus* when interacting with lipid matrices. Biochemistry, *31:* 12241–12247, 1992.
5. Katsu, T., Nakao, S., and Iwanaga, S. Mode of action of an anti-microbial peptide, tachyplesin I, on biomembranes. Biol. Pharm. Bull., *16:* 178–181, 1993.
6. Gray, M. W., Burger, G., and Lang, B. F. Mitochondrial evolution. Science (Washington DC), *283:* 1476–1481, 1999.
7. Brenner, C., and Kroemer, G. Mitochondria: the death signal integrators. Science (Washington DC), *289:* 1150–1151, 2000.
8. Li, H., Kolluri, S. K., Gu, J., Dawson, M. I., Cao, X., Hobbs, P. D., Lin, B., Chen, G., Lu, J., Lin, F., Xie, Z., Fontana, J. A., Reed, J. C., and Zhang, X. Cytochrome *c* release and apoptosis induced by mitochondrial targeting of nuclear orphan receptor TR3. Science (Washington DC), *289:* 1159–1164, 2000.
9. Du, C., Fang, M., Li, Y., Li, L., and Wang, X. Smac, a mitochondrial protein that promotes cytochrome *c*-dependent caspase activation by eliminating IAP inhibition. Cell, *102:* 33–42, 2000.
10. Ellerby, H. M., Arap, W., Ellerby, L. M., Kain, R., Andrusiak, R., Rio, G. D., Krajewski, S., Lombardo, C. R., Rao, R., Ruoslahti, E., Bredesen, D. E., and Pasqualini, R. Anti-cancer activity of targeted pro-apoptotic peptides. Nat. Med., *5:* 1032–1038, 1999.
11. Arap, W., Pasqualini, R., and Ruoslahti, E. Cancer treatment by targeted drug delivery to tumor vasculature in a mouse model. Science (Washington DC), *279:* 377–380, 1998.
12. Brooks, P. C., Clark, R. A. F., and Cheresh, D. A. Requirement of vascular integrin $\alpha_v\beta_3$ for angiogenesis. Science (Washington DC), *264:* 569–571, 1994.
13. Kaufmann, S. H., and Earnshaw, W. C. Induction of apoptosis by cancer chemotherapy. Exp. Cell Res., *256:* 42–49, 2000.
14. Brooks, P. C., Silletti, S., von Schalscha, T. L., Friedlander, M., and Cheresh, D. A. Disruption of angiogenesis by PEX, a noncatalytic metalloproteinase fragment with integrin binding activity. Cell, *92:* 391–400, 1998.
15. Liu, X., Kim, C. N., Yang, J., Jemmerson, R., and Wang, X. Induction of apoptotic program in cell-free extracts: requirement for dATP and cytochrome *c*. Cell, *86:* 147–157, 1996.
16. Desagher, S., Osen-Sand, A., Nichols, A., Eskes, R., Montessuit, S., Lauper, S., Maundrell, K., Antonsson, A., and Martinou, J. C. Bid-induced conformational change of Bax is responsible for mitochondrial cytochrome *c* release during apoptosis. J. Cell Biol., *144:* 891–901, 1999.
17. Slee, E. A., Harte, M. T., Kluck, R. M., Wolf, B. B., Casiano, C. A., Newmeyer, D. D., Wang, H-G. Reed, J. C., Nicholson, D. W., Alnemri, E. S., Green, D. R., and Martin, S. J. Ordering the cytochrome *c*-initiated caspase cascade: hierarchical activation of caspases-2, -3, -7, -8, and -10 in a caspase-9-dependent manner. J. Cell Biol., *144:* 281–292, 1999.
18. Matsuzaki, K. Why and how are peptide-lipid interactions utilized for self-defense? Magainins and tachyplesins as archetypes. Biochim. Biophys. Acta, *1462:* 1–10, 1999.
19. Javadpour, M. M., Juban, M. M., Lo, W. C., Bishop, S. M., Alberty, J. B., Cowell, S. M., Becker, C. L., and McLaughlin, M. L. *De novo* anti-microbial peptides with low mammalian cell toxicity. J. Med. Chem., *39:* 3107–3113, 1996.

Extracellular matrix protein 1 (ECM1) has angiogenic properties and is expressed by breast tumor cells

ZEQIU HAN,*,[1] JIAN NI,†,[1] PATRICK SMITS,**,[1] CHARLES B. UNDERHILL,* BIN XIE,* YIXIN CHEN,§ NINGFEI LIU,* PRZEMKO TYLZANOWSKI,¶ DAVID PARMELEE,† PING FENG,† IVAN DING,‡ FENG GAO,* REINER GENTZ,† DANNY HUYLEBROECK,¶ JOZEF MERREGAERT,**,[2] AND LURONG ZHANG*,[2,3]

*Department of Oncology, Georgetown University Medical Center, Washington, D.C. 20007, USA; †Human Genome Sciences, Rockville, Maryland 20850, USA; ‡Department of Radiology, Rochester University Medical Center, Rochester, New York 14642, USA; §Department of Biology, Xiamen University, China; ¶Laboratory of Molecular Biology (Celgen) and Department of Cell Growth, Differentiation and Development, Flanders Interuniversity Institute of Biotechnology (VIB), University of Leuven, Leuven, Belgium; and **Laboratory of Molecular Biotechnology, Department of Biochemistry, Universiteitsplein 1, Wilrijk, Belgium

ABSTRACT **Tumor growth and metastasis are critically dependent on the formation of new blood vessels. The present study found that extracellular matrix protein 1 (ECM1), a newly described secretory glycoprotein, promotes angiogenesis. This was initially suggested by *in situ* hybridization studies of mouse embryos indicating that the ECM1 message was associated with blood vessels and its expression pattern was similar to that of flk-1, a recognized marker for endothelium. More direct evidence for the role of ECM1 in angiogenesis was provided by the fact that highly purified recombinant ECM1 stimulated the proliferation of cultured endothelial cells and promoted blood vessel formation in the chorioallantoic membrane of chicken embryos. Immunohistochemical staining with specific antibodies indicated that ECM1 was expressed by the human breast cancer cell lines MDA-435 and LCC15, both of which are highly tumorigenic. In addition, staining of tissue sections from patients with breast cancer revealed that ECM1 was present in a significant proportion of primary and secondary tumors. Collectively, the results of this study suggest that ECM1 possesses angiogenic properties that may promote tumor progression.—Han, Z., Ni, J., Smits, P., Underhill, C. B., Xie, B., Chen, Y., Liu, N., Tylzanowski, P., Parmelee, D., Feng, P., Ding, I., Gao, F., Gentz, R., Huylebroeck, D., Merregaert, J., Zhang, L. Extracellular matrix protein 1 (ECM1) has angiogenic properties and is expressed by breast tumor cells. *FASEB J.* 15, 988–994 (2001)**

Key Words: angiogenesis · breast cancer · ECM1 · endothelial cells

ANGIOGENESIS REPRESENTS A critical factor in tumor progression (1). Before the formation of blood vessels, most tumors are relatively small, remain localized, and grow slowly. However, with the advent of vascularization, the tumors become more malignant, as characterized by rapid growth, invasiveness, and metastasis. In many cases, tumor cells facilitate their own progression by directly producing angiogenic factors such as vascular endothelium growth factor (VEGF) and fibroblast growth factors (FGFs), to stimulate a persistent angiogenesis that leads to their uncontrolled growth and metastasis (1–3). Alternatively, some tumors act by inducing the adjacent normal cells to synthesize the angiogenic factors (4). In either case, the process of neovascularization is a common feature of malignant progression of solid tumors and as such represents a potential target for inhibition of tumor growth and metastasis.

In this study, we examined the angiogenic properties of extracellular matrix protein 1 (designated ECM1 in the human and Ecm1 in the mouse) that was initially isolated from an osteogenic stromal cell line (5). Although earlier sequencing studies indicated that ECM1 was not directly homologous to any other known proteins, it did contain six cysteine doublets having a CC-(X_{7-10})-C arrangement, similar to those in serum albumin (6–8). Such sequences can generate "double-loop" domains that are likely involved in ligand binding (9, 10). In humans, the ECM1 message is differentially spliced, giving rise to two forms of the protein: a long form (ECM1a) composed of 540 amino acids, and a short form (ECM1b) of 415 amino acids that lacks the amino acids derived from the central seventh exon (7). Northern analysis of different human tissues has indicated that the 1.8 kb transcript for ECM1a was expressed predominantly in the blood vessel-rich placenta and heart, whereas the 1.4 kb mRNA for ECM1b was present in the tonsils and skin (6, 7, 11).

[1] Zeqiu Han, Jian Ni, and Patrick Smits share first authorship.

[2] Jozef Merregaert and Lurong Zhang share senior authorship.

[3] Correspondence: Department of Oncology, Georgetown University Medical Center, 3970 Reservoir Road, NW, Washington, D.C. 20007, USA. E-mail: zhangl@georgetown.edu

0892-6638/01/0015-0988 © FASEB

Previous studies have suggested that mouse Ecm1a plays a regulatory role in the process of endochondral bone formation (12). When recombinant human ECM1a was added to organ cultures of metatarsals isolated from mouse embryos, it inhibited both alkaline phosphatase activity and mineralization in a dose-dependent fashion. In the mouse embryo, Ecm1a mRNA was expressed by perichondral connective tissue but not by the chondrocytes. Thus, Ecm1a produced by perichondral tissue appears to act in a paracrine fashion and can be considered a negative regulator of endochondral bone formation. However, beyond this, little was known about other possible functions of human ECM1.

Here, we report that ECM1 also possesses angiogenic-promoting properties as indicated by its ability to stimulate the formation of blood vessels in the chorioallantoic membrane (CAM) of chicken eggs. The angiogenic property of ECM1 was also suggested by its close association with embryonic endothelial cells and its ability to stimulate the proliferation of endothelial cells in tissue culture. Furthermore, the fact that ECM1 was up-regulated in some breast cancer cells suggests that it may play a role in tumor progression.

MATERIALS AND METHODS

In situ hybridization

The pUIA671 construct used for *in situ* hybridization was made by ligating a 512 bp *Pst*I fragment from the 5′-region of mouse Ecm1 cDNA into the *Pst*I cloning site of pSport (Life Technologies, Gaithersburg, Md.). *In situ* hybridization was done as described previously (13).

Purification of human ECM1

The human cDNA sequences encoding ECM1a and ECM1b proteins were amplified by polymerase chain reaction using a human fetal liver cDNA library as a template and the following primers: 5′-primer: 5′-CGGGATCCGCCATCATGGGGACCACAGCCAG-3′, consisting of a *Bam*HI restriction site, a "Kozak" sequence, and the first 17 bases of the open reading frame; 3′-primer: 5′-GCTCTAGATCCAAGAGGTGTTTAGTG-3′, containing an *Xba*I restriction site followed by 18 nucleotides complementary to the 3′-untranslated sequence. The amplified fragments were cloned into the baculovirus expression vector pA2. The generation of recombinant baculoviruses and expression of ECM1 were performed as described previously (14, 15).

For isolation of the ECM1a protein, conditioned medium from the virus-infected insect cells was directly applied to a strong cation exchange column (Poros HS, PerSeptive Biosystems, Framingham, Mass.) equilibrated with 0.05 M NaCl, 0.02 M Bis-Tris, pH 6.0, and 10% (v/v) glycerol (buffer A). The protein was eluted with a step gradient of a high ionic strength buffer consisting of 35% 1.0 M NaCl, 0.02 M Bis-Tris, pH 6.0, and 10% (v/v) glycerol (buffer B). The fractions containing protein were pooled and diluted with water to reduce the ionic strength. The sample was clarified by centrifugation and was then applied to a strong anion exchange column (Poros HQ) connected in tandem to a strong cation exchange column (Poros HS) pre-equilibrated with buffer A. The columns were eluted with a gradient from 0 to 70% buffer B. The fractions containing ECM1a, as determined by sodium dodecyl sulfate-polyacrylamide gel electrophoresis (SDS-PAGE), were pooled, diluted with water, and adjusted to pH 8.0 with 0.5 M Bis-Tris propane (pH 9.0). The resulting solution was then applied to a Poros HQ column equilibrated with buffer A at pH 8.0. The proteins were eluted using a gradient of from 0 to 100% buffer B at pH 8.0.

ECM1b was purified in a similar fashion with only slight modification of the buffers. For the first cation exchange column (Poros HS), the proteins were eluted with a step gradient of 35% 2.0 M NaCl, 0.02 M Bis-Tris, pH 6.0, and 10% (v/v) glycerol (buffer C). The ECM1b-containing peaks were pooled, diluted, and adjusted to pH 8.0. For the second columns (Poros HS and HQ connected in tandem), the proteins were eluted with a gradient of from 0 to 50% 2.0 M NaCl with 0.02 M Tris pH 8.0. For the final purification step, the fractions containing ECM1b, were pooled, diluted, and adjusted to pH 5.0; applied to an HS column; and eluted with a gradient of from 0 to 100% buffer C.

The fractions containing purified ECM1a or ECM1b were analyzed by SDS-PAGE, and those containing a single band were pooled. The purified proteins were stored as a stock solution of ~1.4 mg/ml in phosphate-buffered saline, pH 7.3. The identity of these preparations was verified by N-terminal amino acid sequencing, and the purity was greater than 98% as determined by reverse-phase high-pressure liquid chromatography. Endotoxin levels of the preparations were less than 5 EU/mg protein as determined by the Amebocyte Lysate Test (Bio-Whittaker, Walkersville, Md.).

Antibodies

Antiserum against human ECM1 was raised by injecting 0.2 mg of highly purified recombinant ECM1a or ECM1b in Freund's complete adjuvant (Difco Laboratories, Sparks, Md.) subcutaneously into rabbits. The injections were repeated after 3 weeks and the rabbits were bled every third week. Although the antisera generated by immunization with ECM1a cross-reacted with ECM1b and vice versa, they were specific for ECM1 as determined by ELISA and immunoelectrophoresis with the recombinant proteins. In some cases, the antibodies were further purified by affinity chromatography on ECM1 coupled to Sepharose 4B.

Cell culture

The human breast cancer cell lines (MCF-7, Hs578T, MDA-435, MDA-436, MDA-468, Sk-Br-3, ZR571, and T47D), TSU prostate cancer cells, and NIH-3T3 cells were purchased from the American Type Culture Collection (Rockville, Md.). The LCC-15 (derived from a bone metastasis of a breast cancer patient), the human umbilical vein endothelial cells (HUVEC), and the primary as well as metastatic breast cancer tissues were obtained from the Tumor Bank of the Lombardi Cancer Center, Georgetown University, Washington, D.C. Adult bovine aorta endothelial cells (ABAE) were kindly provided by Dr. Luyuan Li (Lombardi Cancer Center), and the bovine retinal endothelial cells (BREC) and bovine capillary endothelial cells (BCE) were the gift of Dr. Higger (Department of Pediatrics, Georgetown University Hospital). The tumor cells were maintained in 5% fetal bovine serum (FBS) plus 95% Dulbecco's modified Eagle's medium (DMEM), and the endothelial cells, in 10–20% FBS plus 90–80% DMEM containing 10 ng/ml basic FGF.

Proliferation assays

In the case of the endothelial cell lines (passage 4 of HUVEC, BCE, and ABAE), the cells were subcultured into 96-well

plates (2×10^3 cells/well) in 100 μl of endothelial cell culture media (20% FBS-DMEM containing 10 ng/ml of FGF-2 and VEGF). After 12 h, the medium was replaced with serum-free DMEM, and after 24 h the indicated amounts of ECM1a, heat-inactivated ECM1a (placed in a boiling water bath for 30 min), FGF-2, and VEGF were added. After 24 h, [^{3}H]TdR (0.3 μCi/well) was added to the medium, and the next day the cells were harvested and the amount of incorporated [^{3}H]TdR was determined with a β-counter. In the case of the other cell lines (MDA-435, MDA-468, TSU, and NIH-3T3), the protocol was the same as above except that ECM1 was added in medium containing 1% FBS plus 99% DMEM. In each case, all experiments were done in triplicate.

Histochemical staining

Cultured cells were grown overnight in 8-well chamber slides and then fixed with 3.7% formalin for 5 min. The staining of these cells as well as sections of human breast cancers was carried out by using the same procedure as follows. The samples were incubated with rabbit anti-ECM1b (1:400), followed by biotinylated goat anti-rabbit (1:250), peroxidase-labeled streptavidin, and the peroxidase substrate 3-amino-9-ethyl-carbazole, and H_2O_2, which gives a dark red reaction product. The cells were counterstained with hematoxylin (blue) and preserved with CrystalMount (Biomeda, Foster City, Calif.).

Western blotting

Cell lysates containing 30 μg of protein from different breast cancer cell lines were subjected to electrophoresis on a 10% SDS-polyacrylamide gel, transferred to a nitrocellulose membrane, and were incubated with rabbit anti-ECM1b (1:1000) and peroxidase labeled anti-rabbit antibodies (1:4,000) followed by enhanced chemiluminescence.

Angiogenesis assay

This assay was performed according to the methods of Brooks et al. with some modifications (16). The top air sac portions of 7-day-old chicken eggs were opened and the CAMs exposed. Two days later, filter disks (Whatman No. 1, 0.5 cm diameter) containing varying concentrations of ECM1 and VEGF (15 μl of 0, 0.5, 1, and 2 μg/ml solutions) were applied to the CAMs. Care was taken to place the filters on regions of the CAM that were relatively deficient in preexisting blood vessels. Each group consisted of 10 eggs. Additional ECM1 and VEGF were applied to the filter discs for each of 3 consecutive days. On day 4, the CAMs and associated discs were cut out and immersed immediately in 3.7% formaldehyde. For computer analysis, the discs were divided into four quarters with fine wires. The blood vessels in each quarter of the CAM were digitally photographed, and the results were analyzed by use of an *Optimas 5* program to calculate the vessel area and length in the viewing area. The total length and area of the vessels in the four quadrants of each disc were normalized to the total area measured and expressed as vessel length or area index. The means and the standard errors were calculated from all quadrants of all discs in each group, and the statistical significance was examined by Student's *t* test.

RESULTS

Expression of Ecm1 in mouse embryos

In initial experiments, we examined the expression of Ecm1 mRNA in embryonic mice, using *in situ* hybridization with antisense RNA. In early embryos (embryonic day 7.5), a strong Ecm1 signal was detected in the trophoblast but not in blood islands, and in the angiogenic extraembryonic tissue of the decidua where it formed a gradient, with the highest concentration on the mesometrial side (data not shown). In a 12.5-day-old mouse embryo that is shown in **Fig. 1**, a strong Ecm1 signal was detected in almost all of the newly formed blood vessels. The mRNA for Ecm1 was particularly prominent in the endothelial cells lining the heart, aortic arch, pulmonary trunk, thoracic aorta, and dorsal aorta (Fig. 1*A* and *E*). In the brain, the signal formed a striated pattern, indicative of new blood vessels (Fig. 1*C*). Additional studies indicated that this pattern of Ecm1 expression occurred only during spe-

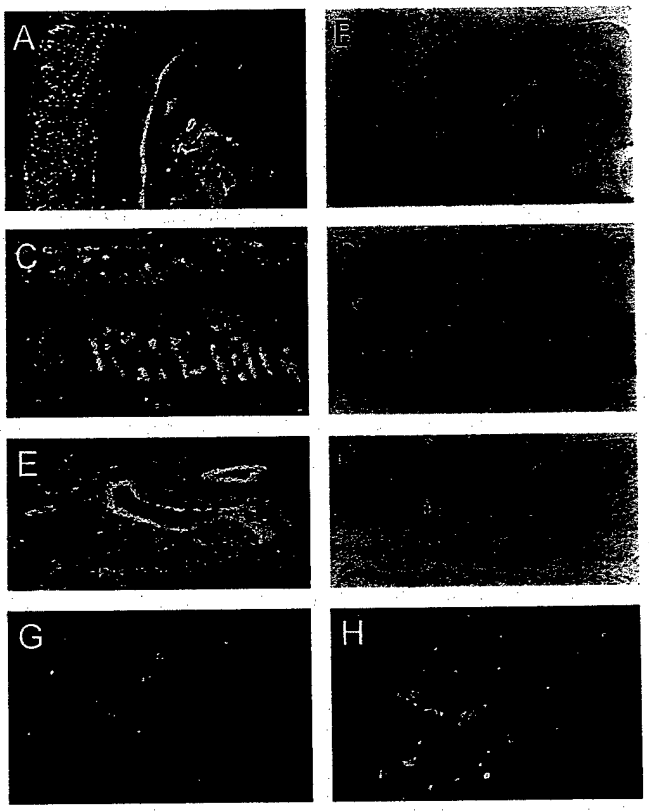

Figure 1. *In situ* hybridization of Ecm1 and flk-1 mRNA in midgestation mouse embryos. The mRNA transcript of Ecm1 in a 12.5-day-old mouse embryo was detected with a probe consisting of a ^{35}S-dATP-labeled, 512 bp antisense sequence of the 5′-region of mouse Ecm1. *A* and *B*) Dark- and light-field views of the Ecm1 message in a sagittal section through the embryo at low magnification. The following structures have been labeled: N, neural tube; H, heart; D, dorsal aorta; A, aortic arch; and P, pulmonary trunk. *C* and *D*) Dark- and light-field views of the Ecm1 message in a sagittal section of the neural tube at higher magnification. The label is associated with the newly forming blood vessels. The following structures have been labeled: C, central canal of spinal cord; B, blood vessel; N, neural tube. *E* and *F*) Dark- and light-field views of the Ecm1 message lining the blood vessels of the aortic arch (A) and the pulmonary trunk (P). *G* and *H*) Dark-field views of the developing brain showing the distribution of the Ecm1 and flk-1 messages, respectively. The pattern of Ecm1 is very similar to that of flk-1, which is a marker for endothelial cells.

cific stages of embryonic development. In older embryos (embryonic day 15.5), the signal dramatically decreased in the central nervous system and completely disappeared from the walls of arteries and the heart (data not shown). Thus, the expression of Ecm1 in blood vessels occurred during a specific window of embryonic development in the mouse.

As shown in Fig. 1*G* and *H*, the expression pattern of Ecm1 in the central nervous system was very similar to that of the VEGF receptor flk-1, a marker of endothelial cells (17). The most striking difference between flk-1 and Ecm1 was in the timing of their expression. As previously reported, flk-1 mRNA persists throughout postnatal development (17). In contrast, Ecm1 mRNA was dramatically down-regulated during later stages of gestation, coinciding with the establishment of the blood-brain barrier on embryonic day 14.5 (18). These results suggested that Ecm1 was closely associated with early stages of angiogenesis and prompted us to investigate its role in this process.

ECM1 stimulated endothelial cell proliferation

Next, we examined the effect of ECM1 on the proliferation of cultured endothelial cells. For this, varying concentrations of recombinant ECM1a were added to the cultures of HUVEC in serum-free medium, and the extent of proliferation was determined by the incorporation of radioactive thymidine. As shown in **Fig. 2*A***, ECM1a significantly stimulated the growth of these cells, with a maximal response at ~20 ng/ml. We then compared the stimulatory effects of ECM1a with those of both FGF-2 and VEGF, known stimulators of endothelial proliferation. As shown in Fig. 2*B*, the effects of ECM1a were significant but not as great as those of either FGF-2 or VEGF (in each case the optimal concentration was used). In addition, heat inactivation of the ECM1 preparation abolished the effects of ECM1a (Fig. 2*B*). Similar results were obtained with ECM1b (data not shown). ECM1 (both a and b forms) also stimulated the proliferation of other endothelial cell lines such as ABAE, BREC, and BCE (data not shown). In contrast, when ECM1a over a range of concentrations was added to cultures of MDA-435 and MDA-468 cells, no obvious effect on thymidine incorporation was apparent (Fig. 2*C* and *D*, respectively). There was a similar lack of effect on other nonendothelial cell lines tested (TSU and NIH-3T3). Thus, the biological activity of ECM1a appears to be at least partially selective in that it stimulates the proliferation of endothelial cells but not other cell types that we tested.

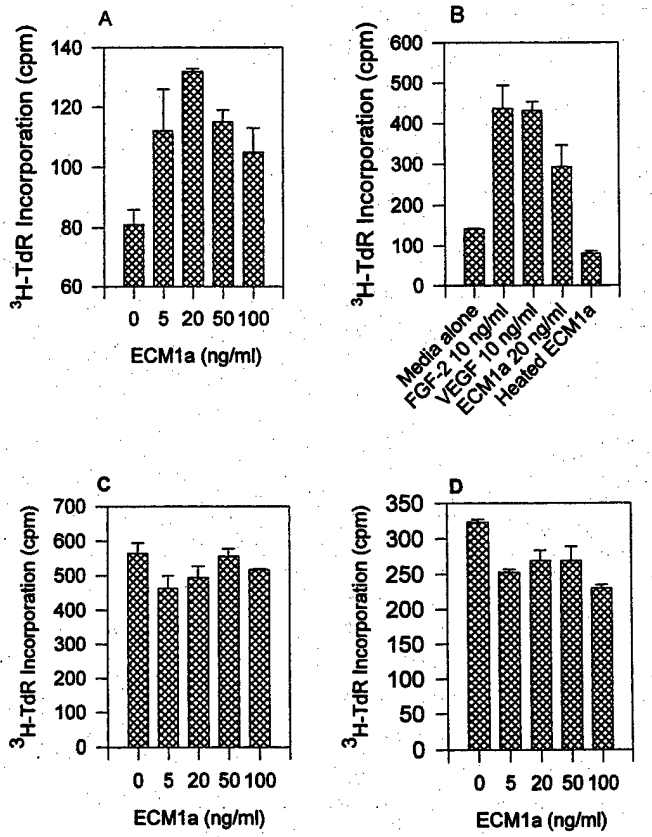

Figure 2. Effects of ECM1 and other factors on cell proliferation. *A*) Cells of the cell line HUVEC were cultured in the absence of serum, treated with varying amounts of ECM1a, and pulsed with [^{3}H]TdR. The cells were then harvested and the amount of labeled thymidine incorporated by the cells was determined. ECM1a stimulated the proliferation of HUVEC with a optimal effect at 20 ng/ml ($P < 0.01$). Similar results were also obtained with all of the other endothelial cell lines that we tested (ABAE, BREC, and BCE). *B*) To compare the effects of ECM1a with those of other angiogenic factors, HUVEC were treated with FGF-2, VEGF, and ECM1a (optimal doses of each factor). Although ECM1a stimulated the proliferation of HUVEC, the effect was less than that of either FGF-2 or VEGF. As a control, a heat-treated preparation of ECM1a (placed in a boiling water bath for 20 min) was tested and had no stimulatory activity on the proliferation of HUVEC. *C* and *D*) Varying concentrations of ECM1a were added to cultures of MDA-435 and MDA-468 cells, respectively, under conditions of reduced serum. No stimulation of proliferation was detected in either case. Four individual experiments yielded similar results.

ECM1 promoted angiogenesis

To determine whether ECM1 acts as an angiogenic factor *in vivo*, we examined its effect in the chick CAM assay. Recombinant ECM1a and ECM1b were adsorbed onto small pieces of filter paper that were then applied to the CAMs of chicken eggs. Two days later, the CAMs in direct contact with the filters were photographed and processed for image analysis. **Figure 3*B*** through *E* shows that ECM1a stimulated angiogenesis in a dose-dependent fashion and that a similar effect was obtained with ECM1b. The effects were comparable to that of VEGF, which was used as positive control (Fig. 3*F*). Image analysis of these tissues revealed that both the vessel length and area indices (Fig. 3*G* and *H*) were stimulated by application of ECM1a and ECM1b. These results suggest that ECM1 promotes angiogenesis either directly by stimulating endothelial cells or indirectly by induction of other factors.

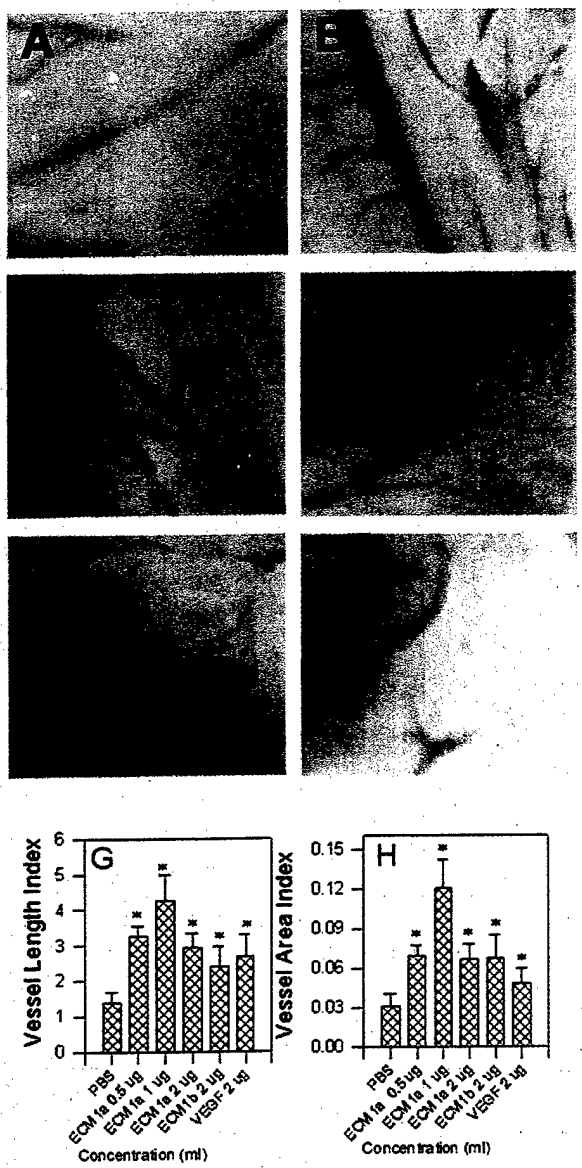

Figure 3. *In vivo* stimulation of angiogenesis by ECM1 on chicken CAM. Filter discs containing 15 μl of ECM1 solutions were placed on the CAMs of 9-day-old eggs and harvested on day 11. Photographs representative of each condition are shown. *A*) PBS control; *B*) ECM1a at 0.5 μg/ml; *C*) ECM1a at 1 μg/ml; *D*) ECM1a at 2 μg/ml; *E*) ECM1b at 2 μg/ml; and *F*) VEGF at 2 μg/ml as a positive control. *G* and *H*) Computerized image analysis of the digital photographs showed that the length and area indices were stimulated by the ECM1. The means and standard errors of the ratios from each group (with 40 individual samples) were calculated and analyzed statistically. $*P < 0.05$.

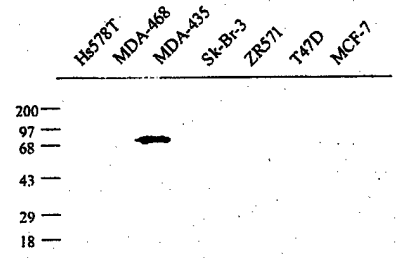

Figure 4. Detection of ECM1 in cell lysates of breast cancer cells by Western blotting. Lysates from different breast cancer cell lines were subjected to electrophoresis on 10% SDS-polyacrylamide gel, transferred to a nitrocellulose membrane, and incubated sequentially with rabbit anti-ECM1 antibodies, peroxidase-coupled anti-rabbit antibodies, and finally a chemoluminescent substrate (ECL). Similar results were obtained in three separate experiments.

ECM1 was expressed by human breast cancer cells

In many cases, tumor cells have been shown to secrete angiogenic factors that are associated with malignant progression (1–3). Furthermore, some tumor cells express proteins that are normally present only during embryonic development (19–21). Consequently, we decided to determine whether tumor cells also express ECM1 by Western blotting using antibodies specifically directed against ECM1. With such antibodies, we tested a panel of human breast cancer cell lines (Hs578T, MDA-468, MDA-435, Sk-Br-3, ZR571, T47D, and MCF-7) and found that only the MDA-435 cell line expressed high levels of ECM1 protein (**Fig. 4**). On the basis of its approximate size of 68 kDa, we believe that this protein corresponds to the ECM1a isoform, because purified recombinant ECM1a from CHO cells yielded a protein of similar molecular size (data not shown). Histochemical staining of cultured MDA-435 cells indicated that most of the ECM1 was located focally in the cytoplasm, where it was probably associated with organelles of the secretory pathway (**Fig. 5*D***). Interestingly, in our hands, the MDA-435 cells were also the most malignant cell line, as judged by their growth in nude mice (unpublished observations). Subsequently, we found that other cell lines, such as LCC15 that was derived from a bone metastasis of breast cancer, also express ECM1 (22). The expression of

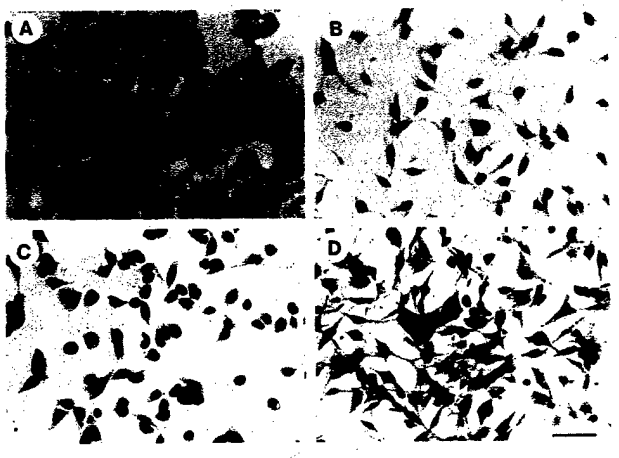

Figure 5. Expression of ECM1 in cultured breast cancer cells. MCF-7, MDA-436, MDA-468, and MDA-435 cells were cultured in an 8 well-chamber slide, fixed, and stained with antibodies to ECM1, which were detected using an immunoperoxidase reaction that gave rise to a dark red product. *A*, *B*, and *C*) Representative fields show that MCF-7, MDA-436, and MDA-468 cells were negative for staining with anti-ECM1; *D*) MDA-435 cells showed strong positive staining in the cytoplasm. Scale bar = 5 μm.

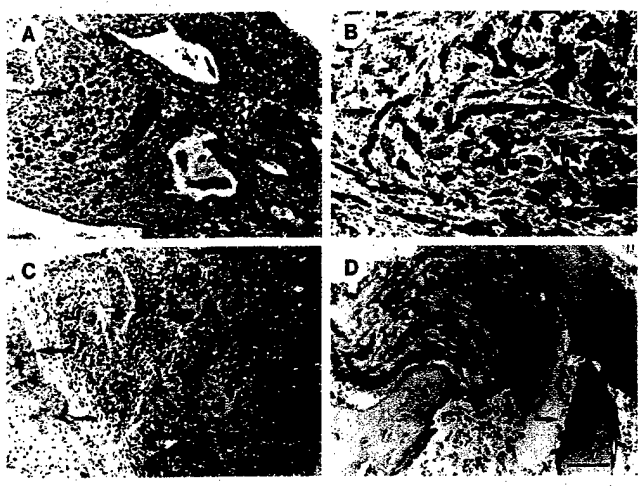

Figure 6. Expression of ECM1 in sections of primary and secondary breast cancers. Paraffin sections of human breast cancer tissues were stained for ECM1 by using specific antibodies with a peroxidase-coupled system (to produce a red reaction product) and then counterstained with hematoxylin (blue). *A* and *B*) Although the normal ductal epithelial and stromal cells (small arrow in *A*) showed little or no staining, the primary cancer cells (large arrows) stained positive (red). *C*) Metastatic breast cancer cells in the lymph node also showed positive staining (large arrow indicates tumor, small arrow indicates normal lymph node tissue). *D*) Metastatic breast cancer cells in the bone showed positive staining (large arrow indicates breast cancer cells; small arrows indicate normal cells in the tissues). Scale bar = 10 μm.

ECM1 in malignant tumor cells suggests that it may play a role in tumor progression.

To determine whether expression of ECM1 was associated with breast tumors, we used the antibody to stain a panel of sections of both primary and secondary tumors from human cancer patients. **Figure 6** shows examples in which ECM1 was detected in primary breast cancer cells (Fig. 6*A* and *B*) and secondary tumors formed in the lymph nodes (Fig. 6*C*) as well as in the bone marrow (Fig. 6*D*). In contrast, little or no staining was apparent in the normal breast ductal cells, stromal fibroblasts, and inflammatory cells (Fig. 6 small arrows). Of the definitive breast cancer biopsy samples that we tested, 68% (21 of 31) were positive for ECM1. Of these, 12 of 18 cases were metastatic tumors and 9 of 13 cases were primary tumors. Thus, expression of ECM1 is frequently associated with breast cancer cells.

DISCUSSION

In this study, we presented evidence that ECM1 has angiogenic properties. The most direct evidence for this came from experiments in which recombinant protein was applied to the CAMs of chicken embryos and resulted in an increase in both the length and the area of blood vessels, as determined by computer-assisted image analysis. Additional evidence for the angiogenic properties of ECM1 is that it stimulated the proliferation of cultured endothelial cells but not other tumor cell types (MDA-435, MDA-468, TSU, and NIH-3T3). In this regard, ECM1 appears to be similar to VEGF in that its mitogenic activity is at least partially restricted to endothelial cells (2, 3). However, the biological activity of ECM1 also extends to at least some other cell types, such as chondrocytes for which ECM1a has been shown to inhibit alkaline phosphatase activity and mineralization (12). To our knowledge, this is the first report suggesting that ECM1 plays a role in angiogenesis.

Our *in situ* hybridization studies have indicated that Ecm1 mRNA is closely associated with blood vessels at different stages of mouse embryogenesis, particularly during midgestation. The signal is present in newly formed vessels, and its distribution is very similar to that of flk-1 (one of the receptors for VEGF), which has been identified as a marker for endothelium (17). However, unlike flk-1, Ecm1 mRNA expression was down-regulated before birth. We propose that Ecm1 is a novel marker for embryonic angiogenesis. This could also account for the fact that high levels of ECM1 are present in the placenta, which contains numerous newly formed blood vessels.

Another organ system in which Ecm1 may be active is the skin. The mRNA of ECM1 is associated with the human epidermis but not the underlying dermis (11). It is tempting to speculate that epidermal keratinocytes secrete ECM1 into the adjacent dermis and stimulate the formation of blood vessels. Functionally, this area requires a high degree of vascularization so that the avascular epidermis can receive oxygen and other nutrients from underlying dermis for their proliferation.

ECM1 may also play a role in tumor angiogenesis, which is a prerequisite for rapid tumor growth and metastasis (1–3). In many cases, tumor cells facilitate their own progression by directly producing angiogenic factors or by inducing other cells to synthesize them (1–4). ECM1 may represent a new factor among those produced by tumor cells (such as MDA-435 and LCC-15) to promote their progression. In our hands, the MDA-435 line was also the most aggressive with respect to growth in nude mice (unpublished observations). More important, when both primary and secondary breast cancer tissues were tested for ECM1, a relatively high proportion of the tumor samples was positive. In contrast, we found little or no positive staining in normal breast ductal epithelial cells, fibroblasts, leukocytes, and other stromal cells. Thus, it appears that at least a proportion of tumor cells produce ECM1, which could stimulate vascularization and promote tumor cell progression.

In addition to stimulating the proliferation of endothelial cells, ECM1 proteins may have a number of other effects on these cells. This is suggested by the fact that during angiogenesis, endothelial cells must carry out a number of processes, including 1) the removal of the old basal lamina, 2) cell division, 3) migration to a new location, and 4) the synthesis of a new basal lamina (23). Indeed, other angiogenic factors such as FGFs and VEGF have been found to have multiple effects on

endothelial cells with regard to proliferation, migration, and production of proteases (1). Thus, it would be interesting to determine whether ECM1 has other effects on endothelial cells in addition to proliferation.

The association of ECM1 with tumor cells has a number of implications. First, the biological activity of ECM1 suggests that endothelial cells may have ECM1 receptors on their surface. In preliminary studies, we found that treatment of endothelial cells with ECM1a results in increased tyrosine phosphorylation, indicating the possible existence of a receptor for ECM1. Clearly, the identification of such a receptor would help in elucidating the signal transduction pathway. Second, ECM1 may represent an easily accessible marker for the presence of tumors. Because ECM1 is a secretory protein, the concentrations of this protein in the serum of patients may be correlated with the presence of certain types of tumors. Such a marker could prove to be very useful for assessing tumor load and may be of prognostic value in determining tumor recurrence after surgery.

In conclusion, the results of this study indicate that ECM1 has angiogenic properties and is produced by tumor cells, suggesting that it plays a role in tumor progression by stimulating tumor vascularization. If this is the case, it may be possible to slow or even reverse tumor progression by blocking the activity of ECM1 with competing factors or inhibitors. FJ

We thank Dr. Suette Mueller for her assistance with the computer imaging analysis. This work was supported in part by grants from the National Cancer Institute, National Institutes of Health (R29 CA71545), U.S. Army Medical Research and Material Command (DAMD 17-98-1-8099), and the Susan G. Komen Breast Cancer Foundation to L.Z., and U.S. Army Medical Research and Material Command (DAMD 17-94-J-4284 and PC970502) as well as Susan G. Komen Breast Cancer Foundation to C.B.U. J.M. and D.H. were supported by a grant from the Fonds voor Wetenschappelijk Onderzoek-Vlaanderen (No. G.0085.98).

REFERENCES

1. Folkman, J., and Shing, Y. (1992) Angiogenesis. *J. Biol. Chem.* **267,** 10931–10934
2. Thomas, K. A. (1996) Vascular endothelial growth factor, a potent and selective angiogenic agent. *J. Biol. Chem.* **271,** 603–606
3. Nguyen, M. (1997) Angiogenic factors as tumor markers. *Invest. New Drugs* **15,** 29–37
4. Polverini, P. J., and Leibovich, S. J. (1984) Induction of neovascularization *in vivo* and endothelial proliferation *in vitro* by tumor-associated macrophages. *Lab. Invest.* **51,** 635–642
5. Mathieu, E., Meheus, L., Raymackers, J., and Merregaert, J. (1994) Characterization of the osteogenic stromal cell line MN7: identification of secreted MN7 proteins using two-dimensional polyacrylamide gel electrophoresis, Western blotting, and microsequencing. *J. Bone Miner. Res.* **9,** 903–913
6. Bhalerao, J., Tylzanowski, P., Filie, J. D., Kozak, C. A., and Merregaert, J. (1995) Molecular cloning, characterization, and genetic mapping of the cDNA coding for a novel secretory protein of mouse. Demonstration of alternative splicing in skin and cartilage. *J. Biol. Chem.* **270,** 16385–16394
7. Smits, P., Ni, J., Feng, P., Wauters, J., Van Hul, W., Boutaibi, M. E., Dillon, P. J., and Merregaert, J. (1997) The human extracellular matrix gene 1 (ECM1): genomic structure, cDNA cloning, expression pattern, and chromosomal localization. *Genomics* **45,** 487–495
8. Johnson, M. R., Wilkin, D. J., Vos, H. L., Ortiz de Luna, R. I., Dehejia, A. M., Polymeropoulos, M. H., and Francomano, C. A. (1997) Characterization of the human extracellular matrix protein 1 gene on chromosome 1q21. *Matrix Biol.* **16,** 289–292
9. Yang, F., Brune, J. L., Naylor, S. L., Cupples, R. L., Naberhaus, K. H., and Bowman, B. H. (1985) Human group-specific component (Gc) is a member of the albumin family. *Proc. Natl. Acad. Sci. USA* **82,** 7994–7998
10. Kragh-Hansen, U. (1990) Structure and ligand binding properties of human serum albumin. *Dan. Med. Bull.* **37,** 57–84
11. Smits, P., Poumay, Y., Karperien, M., Tylzanowski, P., Wauters, J., Huylebroeck, D., Ponec, M., and Merregaert, J. (2000) Differentiation-dependent alternative splicing and expression of the extracellular matrix protein 1 gene in human keratinocytes. *J. Invest. Dermatol.* **114,** 718–724
12. Deckers, M. M. L., Smits, P., Karperien, M., Ni, J., Tylzanowski, P., Feng, P., Parmelee, D., Zhang, J., Bouffard, E., Gentz, R., Löwik, C. W. G. M., and Merregaert, J. Recombinant human extracellular matrix 1 (Ecm1) inhibits alkaline phosphatase activity and mineralization of mouse embryonic metatarsals *in vitro*. *Bone*. In press.
13. Dewulf, N., Verschueren, K., Lonnoy, O., Morén, A., Grimsby, S., Vande Spiegle, K., Miyazono, K., Huylebroeck, D., and Ten Dijke, P. (1995) Distinct spatial and temporal expression patterns of two type I receptors for bone morphogenetic proteins during mouse embryogenesis. *Endocrinology* **136,** 2652–2663
14. Ni, J., Abrahamson. M., Zhang, M., Fernandez, M. A., Grubb, A., Su, J., Yu, G-L., Li, Y., Parmelee, D., Xing, L., Coleman, T. A., Gentz, S., Thotakura, R., Nguyen, N., Hesselberg, M., and Gentz, R. (1997) Cystatin E is a novel human cysteine proteinase inhibitor with structural resemblance to family 2 cystatins. *J. Biol. Chem.* **272,** 10853–10858
15. Ni, J., Fernandez, M. A., Danielsson, L., Chillakuru, R. A., Zhang, J., Grubb, A., Su, J., Gentz, R., and Abrahamson, M. (1998) Cystatin F is a novel glycosylated cysteine proteinase inhibitor of human lymphoid cells. *J. Biol. Chem.* **273,** 24797–24804
16. Brooks, P. C., Silletti, S., von Schalscha, T. L., Friedlander, M., and Cheresh, D. A. (1998) Disruption of angiogenesis by PEX, a noncatalytic metalloproteinase fragment with integrin binding activity. *Cell* **92,** 391–400
17. Millauer, B., Wizigmann-Voos, S., Schnurch, H., Martinez, R., Moller, N. P., Risau, W., and Ullrich, A. (1993) High affinity VEGF binding and developmental expression suggest Flk-1 as a major regulator of vasculogenesis and angiogenesis. *Cell* **72,** 835–846
18. Hoffmann, A., Bachner, D., Betat, N., Lauber, J., and Gross, G. (1996) Developmental expression of murine Beta-trace in embryos and adult animals suggests a function in maturation and maintenance of blood-tissue barriers. *Dev. Dyn.* **207,** 332–343
19. Kew, M. (1974) Alpha-fetoprotein in primary liver cancer and other diseases. *Gut* **15,** 814–821
20. Jacob, F. (1983) Expression of embryonic characters by malignant cells. *Ciba Found. Symp.* **96,** 4–27
21. Yachnin, S. (1978) The clinical significance of human alpha-fetoprotein. *Ann. Clin. Lab. Sci.* **8,** 84–90
22. Sung, V., Gilles, C., Murray, A., Clarke, R., Aaron, A. D., Azumi, N., and Thompson, E. W. (1998) The LCC15-MB human breast cancer cell line expresses osteopontin and exhibits an invasive and metastatic phenotype. *Exp. Cell Res.* **241,** 273–284
23. Ausprunk, D. H., and Folkman, J. (1977) Migration and proliferation of endothelial cells in preformed and newly formed blood vessels during tumor angiogenesis. *Microvasc. Res.* **14,** 53–65

Received for publication October 28, 1999.
Revised for publication September 27, 2000.